SYNTHESIS, CHARACTERIZATION, ELECTROCHEMICAL PROPERTIES OF HALF-SANDWICH N, N'-BIDENTATE RUTHENIUM(II) COMPLEXES AND THEIR ANTIMICROBIAL ACTIVITY

MARGARET CHEPKEMOI KOSKE

A thesis submitted to the Graduate School in partial fulfillment for the requirements of the Master of Science Degree in Chemistry of Egerton University

EGERTON UNIVERSITY

NOVEMBER, 2018

DECLARATION AND RECOMMENDATION

DECLARATION

This thesis is my original work and has not been submitted or presented, for examination in any institution.

Signature……..... Date…….…….

Margaret C. Koske

SM11/14461/15

RECOMMENDATION

We wish to confirm that this thesis has been prepared under our supervision and is presented for examination as per the Egerton University regulations with our approval.

Signature……..... Date…….…….

Prof. S. M. Kagwanja , PhD

Egerton University

Signature……..... Date…….…….

Dr. J .M Gichumbi, PhD

Chuka University

COPYRIGHT

DEDICATION

To my husband Jonah and my children, Collins, Faith, Allan and Ephraim for their love and patience during my studies.

ACKNOWLEDGEMENT

First and foremost my sincere gratitude's is to God almighty for giving me good health and life throughout my research. I acknowledge Egerton University and Chemistry department for the opportunity given to me to pursue this course, special thanks goes to Dr P. Ongoma, Dr Alice Njue and S.M Kariuki . Special thanks goes to my supervisors, Prof S.M.Kagwanja and Dr. J. M. Gichumbi, for their guidance, advice and positive criticism during the entire research and write up of thesis. Thanks goes to Chuka University, Chemistry Department and their staff, for allowing me to pursue my research in their laboratories .Special thanks to Muraya and Bulemi of Chuka University. I wish to convey my sincere gratitude to Chemistry Department, Kenyatta University and their staff for allowing me to pursue my research in their laboratories. Special thanks to Jane and Sarah. Thanks goes to Dairy Department, Egerton University and their staff for allowing me to use their Microbiology laboratory. Thanks goes to University of KwaZulu Natal for facilitating some analysis. Last but not least, my family for their love, inspiration, encouragement and financial support throughout my education endeavours.

ABSTRACT

The emergence of bacterial resistance to existing antibiotics and other drugs is a worldwide problem. New classes of antimicrobial compounds with complete new mode of action are therefore urgently needed to control the rise of the multidrug resistant pathogens. The objective of this study was to synthesize and characterize half-sandwich organometallic compounds of ruthenium(II) containing bipyridine and pyridine- imine ligands and to test their biological activities against one Gram positive and Gram negative bacteria. The reaction of $[(\eta^6\text{-}C_6H_5CH_3)Ru(\mu\text{-}Cl)Cl]_2$ dimer and the N,N′- bidentate ligands in a 1 : 2 ratio in dry acetonitrile at ambient temperatures resulted in the formation of four versatile, half-sandwich, complexes, $[(\eta^6\text{-}C_6H_5CH_3)\ RuCl\ (N\text{-}N)]^+[PF_6]^-$, $[(\eta^6\text{-}C_6H_5CH_3)RuCl\ (C_5H_4N\text{-}2\text{-}CH{=}N\text{-}X]\ [PF_6]^-$, [(where (N-N) = 5,5'-dimethyl-2,2'-bipyridine , 4,4'-Di-*tert*-butyl-2,2'-bipyridine , 2,2'-bipyridine and X = *p*-fluorophenyl. The complexes were isolated as their hexafluorophosphate salts. Characterization of the complexes was accomplished using ^{1}H NMR, (some were subjected to ^{13}C NMR), elemental analyses, melting points determination, UV/VIS and FTIR spectroscopy which was used to confirm the formation of the imine functional group and the disappearance of the carbonyl band of the starting material containing 2-pyridinecarboxaldehyde in the formation of pyridine-imine Schiff base and also used to monitor the C=N moiety of the pyridine upon the complexation of the precursor complex and bipyridine ligands. Electrochemical properties of the complexes were determined by cyclic voltammetry. The synthesized and characterized complexes were subjected to *in vitro* bioassays to determine their antibacterial activity by agar disc diffusion method. They were also tested against an antimicrobial-susceptible and resistant Gram-negative *Escherichia coli* ATCC 11775 and Gram-positive *Staphylococcus aureus* ATCC 12600. Streptomycin was used as the positive control and Dimethyl sulfoxide as the negative control. Some of the synthesized mononuclear ruthenium complexes demonstrated potential antimicrobial activity against the selected bacteria with some showing better activity than well-known antibiotics such as streptomycin (S-10). The findings reported in this work including cyclic voltammetry and antimicrobial activities are reported for the first time since the synthesized ruthenium(II) bipyridine and pyridine-imine Schiff base complexes containing toluene as the cyclic polyhapto aromatic ligand has never been synthesized before.

TABLE OF CONTENTS

LIST OF SCHEMES

LIST OF FIGURES

LIST OF TABLES

LIST OF APPENDICES

LIST OF ABBREVIATIONS AND ACRONYMS

BINAP	(2,2’-bis(diphenylphosphino)-1,1’-binaphthyl)
C_P	Cyclopentadienyl
CV	Cyclic voltammetry
DCT	Decomposition temperature
DMPZ	3,5-dimethylpyrazolyl
DMSO	Dimethyl sulfoxide
DNA	Deoxyribonucleic acid
DPA	Dipyridylamine
ES-MS	Electro spray mass spectra
Fc	Ferrocene
FTIR	Fourier transform infrared
HOMO	Highest Occupied Molecular Orbital
LUMO	Lowest unoccupied molecular orbital
MPT	Melting point
M/Z	Mass charge
MLCT	Metal to ligand charge transfer
NMR	Nuclear Magnetic Resonance
TH	Transfer hydrogenation
UV/VIS	Ultra Violet/ Visible spectroscopy

CHAPTER ONE
INTRODUCTION

1.1 Background information

In the past couple of decades, synthesis and characterization of transition metal complexes in the area of organometallic chemistry have witnessed a large surge in research (Kumar *et al.*, 2014). It is notable that transition metal complexes in particular have found wide use in catalysis and in majority of chemical reactions resulting in the production of noble materials of high purity (De *et al.*, 2016).

When metals are sandwiched between two organic *pi* systems which are aromatic or anti aromatic such as cyclopentadiene, the complexes are referred to as sandwich complexes. Where this sandwich is not complete, they are referred to as half, bent or open sandwich complexes. In this perspective “half-sandwich" ruthenium organometallic complexes containing one facially bound cyclic arene conjugate polyhapto carbon ligand along with other ligands have drawn special attention (Gichumbi *et al.*, 2016a). Their structure looks like a piano stool in which the metal center in the complexes is surrounded by three monodentate or one monodentate and bidentate ligands besides the cyclic polyhapto hydrocarbon ligand. These three legged, piano-stool complexes have a pseudo-octahedral geometry around the Ruthenium(II), the arene ligand occupying three coordinating sites (the seat) with three other ligands (the legs) (Gichumbi *et al.*, 2016d).

The organometallic chemistry of half-sandwich arene ruthenium(II) complexes has been widely explored in the recent past due to their wide range of potential applications in catalysis as precursors for hydrogen transfer, alkene polymerization, ring opening metathesis polymerization and olefin oxidation (Gichumbi *et al.*, 2016b). These compounds have also been extensively investigated for their potential antibacterial and anticancer activity (Gichumbi *et al.*, 2016e). These complexes belong to a well-established family of robust metal-organic molecules which includes Ru(II), Rh(III), and Ir(III).

The complexes are soluble and stable in water and have many potential advantages such as; alleviation of environmental problems associated with the use of organic solvents and also

for industrial applications with the introduction of new biphasic processes and metal-mediated organic syntheses in water (Marchetti *et al.*, 2008).

Catalytic asymmetric hydrogenation using a chiral ruthenium complex is a powerful method for producing chiral alcohols and chiral amines with excellent enantioselectivity (Rhyoo *et al.*, 2002).

Studies of a series of water-soluble arene ruthenium complexes containing an N,N-chelating 2,2'-dipyridylamine ligand, have been undertaken describing the catalytic activity and in the transfer hydrogenation of aromatic ketones (Romain *et al.*, 2010). It has been observed that ruthenium complexes show unique properties such as mild reaction conditions required in their synthesis, high yields and a wide range of stability and solubility under aqueous conditions. These properties have enabled them to occupy an esteemed position in the organometallic chemistry (Kumar *et al.*, 2014).

Research has shown that the coordination of a metal fragment (ML_n) to an arene ring radically increases its electrophilic character. Consequently, because of the increased acidity, reactions like nucleophilic aromatic addition, substitution, arene and benzylic deprotonation becomes much more easily achieved (Clarke, 2003) .

The coordinated η^n-bonded hydrocarbon ligands in the complexes containing (η^6-arene) Ru- and (η^5-cyclopentadienyl)-Ru-moieties are relatively inert towards substitution and act as spectator ligands that stabilize and protect the metal center thereby preventing rapid oxidation of the Ru(II) to Ru(III). The sites opposite the η^n-bonded hydrocarbon ligand in these complexes may be occupied by various ligands having N-, O-, S or P-donor atoms (Gichumbi *et al.*, 2016a).

Ligands with nitrogen donor atoms such as diamines, pyridines and bipyridine are able to bind strongly to a large variety of metal centres and can therefore stabilize both low and high oxidation states (Zheng *et al.*, 2008). The nitrogen donor ligands when coordinated to ruthenium complexes are versatile because the steric and electronic properties around the metal centre can be easily changed with these ligands in place (Gichumbi *et al.*, 2016a). One such a ligand with nitrogen donor atoms is substituted bidentate pyridine–imine Schiff base

shown in Figure 1.1 which forms, half- sandwich (η^6-arene) Ru- complexes (Gichumbi *et al.*, 2016c).

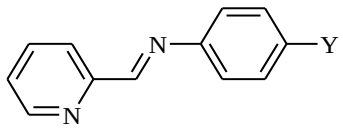

Where Y = *para* and *meta* halo substituents

Figure 1.1: Substituted bidentate Pyridine-imine Schiff base ligand

The chemistry of piano stool half-sandwich arene ruthenium(II) complexes continues to be explored (Linares *et al.*, 2009). The π-ligated arene confers great stability to Ru in the +2 oxidation state and the characteristic" piano stool" structure offers the possibility to vary additional donor ligands via substitution of halide(s) and a variety of σ donors ranging from phosphines to β diketones to aliphatic as well as aromatic amines (Marchetti *et al.*, 2008; Mohan *et al.*, 2018). Half-sandwich ruthenium complexes containing nitrogen ligands have been reported to be useful in olefin oxidation (Horn and Albrecht, 2011; Gichumbi *et al.*, 2016d). The redox and luminescent properties of Ru(II) metal centres using bipyridines have been reported (Horn and Albrecht, 2011) analogues' are huge and the topic of considerable current research (Shavaleev *et al.*, 2004). The interest in developing η^5-cyclopentadienyldicarbonylruthenium(II) metal complexes as antimicrobial agents is encouraged by the fact that bacteria are rapidly becoming resistant to new drugs (Nyawade *et al.*, 2015a). With such great interest in ruthenium(II) complexes ongoing this research was motivated to expand the chemistry of piano-stool ruthenium(II) complexes by synthesizing the ruthenium(II) bipyridine and pyridine-imine Schiff base complexes and to determine their electrochemical and antimicrobial activity.

The purpose of this study was to customize the N, N' bidentate ligand substituent (which would modify and fine tune the properties of the arene ruthenium complexes) and react them with $[(\eta^6\text{-arene})Ru(\mu\text{-}Cl)Cl]_2$, precursor complex to form noble half-sandwich ruthenium complexes [where arene = $C_6H_5CH_3$]. The ligands and complexes synthesized are shown in Figure 1.2 below.

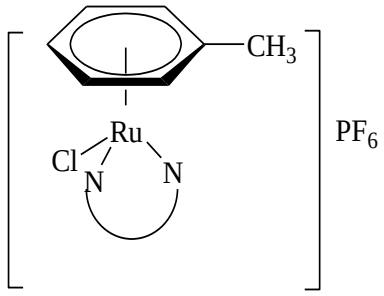

Where N N = 5,5'-dimethyl-2,2'-bipyridine **(L1)**
4,4'-Di-tert-butyl-2,2'-bipyridine (**L2**)
2,2'-bipyridine (**L3**)

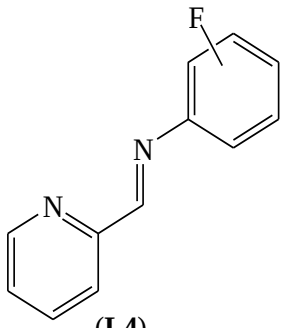

(**L4**)

Ligands	Complexes formed
5,5'-dimethyl-2,2'-bipyridine	$[(\eta^6\text{-}C_6H_5CH_3)RuCl(C_{12}H_{12}N_2)]PF_6$
4,4'-di- -butyl-2,2'-bipyridine	$[(\eta^6\text{-}C_6H_5CH_3)RuCl(C_{18}H_{24}N_2)]PF_6$
2,2'-bipyridine	$[(\eta^6\text{-}C_6H_5CH_3)RuCl(C_{10}H_8N_2)]PF_6$
4-fluoro-N-(2-pyridylmethylene)-aniline	$[(\eta^6\text{-}C_6H_5CH_3)RuCl(C_{12}H_9N_2F)]PF_6$

Figure 1.2 : N, N'-bidentate ligands and their respective Ru(II) complexes

1.2 Statement of the problem

Previous studies on arene ruthenium(II) complexes has established that the type of arene, the nature of the chelating ligands and leaving group in these compounds can significantly influence their chemical and biological activity and as such exhibit structure and activity relationships. While significant studies of these types of complexes have been reported where the arene ligand is benzene and *p*-cymene, little work has been done where the arene is toluene. With an objective of expanding the chemistry of piano-stool ruthenium(II) complexes and to develop alternative antimicrobial agents, synthesis and characterization of a series of piano stool ruthenium(II) complexes containing toluene as the arene ligand were synthesized and investigated.

1.3 Objectives

1.3.1 General objective

To synthesize, characterize and determination of electrochemical properties and antimicrobial activity of half-sandwich η^6- arene ruthenium(II) complexes with N, N'-bidentate ligands. [arene = $C_6H_5CH_3$]

1.3.2 Specific objectives

1. To synthesize, characterize and investigate electrochemical properties of half-sandwich η^6-arene ruthenium(II) complexes containing fluoro substituted pyridine-imine Schiff base ligand.
2. To synthesize, characterize and investigate electrochemical properties of half-sandwich η^6-arene ruthenium(II) complexes containing substituted bipyridine ligands.
3. To investigate the antimicrobial activities of the η^6-arene ruthenium(II) complexes synthesized with pyridine-imine Schiff base and bipyridine ligands.

1.4 Justification

Reactions of the dimeric $[(\eta^6\text{-arene})Ru(\mu\text{-}Cl)Cl]_2$ precursor complex occur through the cleavage of the chloro bridge giving rise to a mononuclear neutral and cationic half – sandwich complexes. The arene moiety which is strongly coordinated to the ruthenium can be varied by attaching different substituents of interest. Realizing that changes in the ligand composition could influence its properties significantly, this study therefore customized the bipyridine and an iminopyridyl substituents with an aim of modifying and fine tuning the properties of the η^6- arene ruthenium(II) iminopyridyl complexes and the η^6- arene ruthenium(II) bipyridine complexes. Furthermore, due to the resistance of microbes against the commonly used antimicrobial agents and the need for development and testing of new types of antimicrobial agents which can serve as alternatives or complementary antimicrobial agents, the newly synthesized complexes were tested for antimicrobial properties.

CHAPTER TWO
LITERATURE REVIEW

2.1 Chemistry of ruthenium

Ruthenium is a rare transition metal with electronic configuration ($[Kr]4d^7 5s^1$). It belongs to the platinum group of the periodic table. Like the other metals of the platinum group, ruthenium is inert to most other chemicals. Ruthenium is usually found as a minor component of platinum ores, most of the ruthenium produced is used in wear-resistant electrical contacts and thick-film resistors. A minor application for ruthenium is in platinum alloys and as a chemistry catalyst, ruthenium also exhibits characteristics universal to both early and late-transition metals giving it properties sufficient for catalysis and other applications (Cotton *et al.*, 1980). Ruthenium, rhodium and iridium have occupied an important position in transfer hydrogenation (Gichumbi *et al.*, 2016a).

Ruthenium is preferable in synthesis because of its good performance and it is cheaper when compared to the other platinum metals; rhodium and iridium (Gichumbi *et al.*, 2016a). The elements to its left in the periodic table are highly reactive while the ones to its right are Lewis acidic in nature. Whereas, all other group 8 elements have 2 electrons in the outermost shell, in ruthenium, the outermost shell has only one electron (the final electron is in a lower shell), this anomaly is observed in the neighboring metals, niobium, rhodium (Schutz, 1996). Ruthenium exhibits variable oxidation states; from Ru(VIII) (d^0) as the case of RuO_4 and Ru(VII) as is the case of RuO_4^- (d^1) to Ru(II) as is the case of $[RuCl(PPh_3)_3$ (d^6) (Cotton *et al.*, 1980). Higher oxidation states are stabilized by weak or poor σ-donors such as F^-, O^{2-} and N^{3-} while low oxidation states are stabilized by effective π-acceptors such as CO and NO^+. Ruthenium also displays various coordination geometries in each electron configuration, for instance, its complexes adopt the trigonal-bipyramidal and octahedral geometries in the primary lower oxidation states of 0, II and III. Derivatives of bipyridine and terpyridine are numerous, best known being the luminescent tris (bipyridine) ruthenium(II) chloride. Ruthenium forms a wide range of compounds with carbon-ruthenium bond, an example being Grubbs' catalyst which is used for alkene metathesis (Grubbs, 2006). Ruthenocenes are also analogous to ferrocene structurally but exhibits

distinctive redox properties they also possess some stoichiometric similarities, as iron is directly above ruthenium in group 8 of the periodic table. The chemistry of ruthenium is of great interest, mainly because its complexes have a range of valuable features; which include high Lewis acidity, high electron transfer ability, low redox potentials and ability to form stable reactive metallic species such as metallacycles, oxometals, and metal carbene complexes (Crutchley, 1994). Thus, such a variety of ruthenium complexes may possibly be utilized in new catalytic reactions, synthetic methods and in pharmaceuticals.

2.2 Ruthenium(II) complexes

A metal complex or a coordination complex is a species which has a central metal atom or ion to which a number of other molecules or ions, referred to as ligands, are bonded by co-ordinate bonds (Nyawade *et al.*, 2015b). The Ru(II) cation ([Kr] $4d^6$) has empty molecular orbital's into which ligands can donate their lone pairs of electrons and form coordinate bonds. The most common precursor in the synthesis of ruthenium complexes is the synthetically versatile ruthenium trichloride (Cotton, 1997). Ruthenium(II) complexes have gotten a good deal of attention in the recent past for catalytic transfer hydrogenation reactions (Gichumbi *et al.*, 2016b). A study of ruthenium(II) complexes designed with several ligands, including 2,2'-bis(diphenylphosphino)-1,1'-binaphthyl (BINAP), ethylene diamine, or other 1,2-diamines and Tertiary Phosphines(PR_3) for catalytic transfer hydrogenation (including asymmetric) and ruthenium half-sandwich complexes explored for catalytic transfer hydrogenation generally have benzene or *p*-cymene arene ligands (Sharma *et al.*, 2014). The ruthenium(II) arene complexes displays a three-legged piano stool structure (Figure 2.2) whereby the metal centre is in octahedral geometry and the arene ligand occupies three coordination sites (Gichumbi *et al.*, 2017a). This allows the possibility to introduce in the molecule two types of centres; the metal and the ligand. It has been found in the literature that the arylazophenol ligand is known to coordinate metal ions usually in a bidentate fashion with N, O donor atoms forming a five-membered chelate ring, the azo (-N=N-) group particularly due to its strong acid character stabilizes ruthenium in lower oxidation states while phenolate oxygen being a hard base stabilizes the higher oxidation state of the metal ion (Raja *et al.*, 2010).

A series of neutral and cationic Ru(II)complexes bearing pyridine-based tridentate ('N,N,N') and pyridine based bidentate (N,N') ligands, have been synthesized from $[RuCl_2(DMSO)_4]$ and $[RuCl_2(p\text{-cymene})]_2$ precursors shown in Figure 2.1 (Günnaz *et al.*, 2011).

Figure 2.1: Pyridine based Ru(II) complexes bearing ('N,N,N') and (N.N') ligands (Günnaz *et al.*, 2011).

2.3 Half-sandwich complexes

Half-sandwich complexes are some of the most studied class of organometallic compounds because of their potential applications in many areas of chemistry (Gichumbi *et al.*, 2017b). These compounds are organometallic complexes that feature a cyclic polyhapto ligand bound to an ML_n center, where M is a metal centre and L is a ligand (Elschenbroich, 2006). Half-sandwich compounds employing Ru(II) such as (cymene)ruthenium dichloride dimer have been mainly investigated as catalysts for transfer hydrogenation (Ikariya and Blacker, 2007). These complexes feature three coordination sites that are susceptible to substitution, while the arene ligand is tightly bonded and protects the metal against oxidation to Ru(III) (Bennett *et al.*, 1982). Piano stool complexes, a typical example shown in Figure 2.2 are stable 18-electron coordination compounds with a variety of chemical and material applications. Many studies of cyclopentadienyl ruthenium(II) complexes with bidentate ligands have shown that substitution reactions occur predominantly with retention of configuration at the metal centre (Davies *et al.*, 1997).

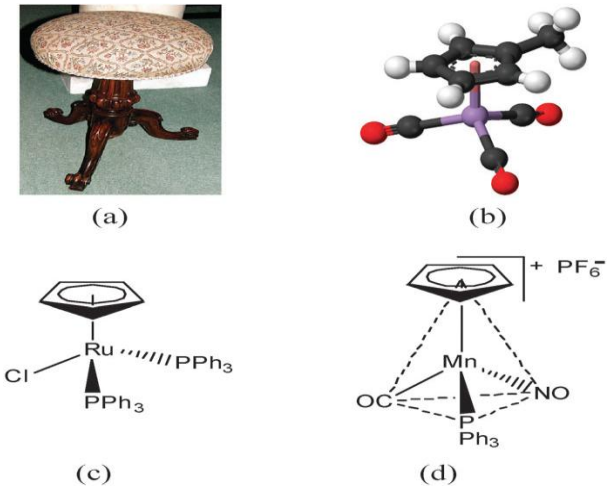

Figure 2.2: Examples of the piano stool complexes: (a) piano stool, (b)[(η^5-$C_5H_4CH_3$)$Mn(CO)_3$], (c) [(η^5-C_5H_5)$Ru(PPh_3)_2Cl$], (d) [(η^5-C_5H_5)Mn(CO)-(NO)PPh_3]PF_6 (Kumar *et al.*, 2014).

In organometallic compounds containing ruthenium, the metal adopts oxidation states from -2 ($[Ru(CO)_4]^{2-}$) to +6 ($[RuN(Me)_4]^-$). However the most common compounds are those in which the metal is in the +2 oxidation state, 1st generation Grubbs catalyst is a suitable example, illustrated in Figure 2.3 below. This is a five-coordinate, 16-electron, ruthenium complex exhibiting a distorted square pyramidal geometry with an alkylidene moiety in the apical site (Grubbs, 2006).

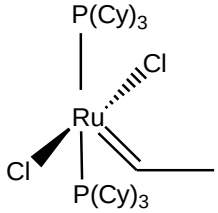

Cy = cyclohexyl

Figure 2.3: 1st Generation Grubbs catalyst.

Several half sandwich complexes have been reported; ruthenium(II) complexes have been synthesized whereby the labile chloride from the precursor compounds has been replaced by CN^- or NCS^- group shown in Figure 2.4 exhibiting several catalytic activity and used in

the reduction of ketones into corresponding alcohol in the absence of a base (Kumar *et al.*, 2010).

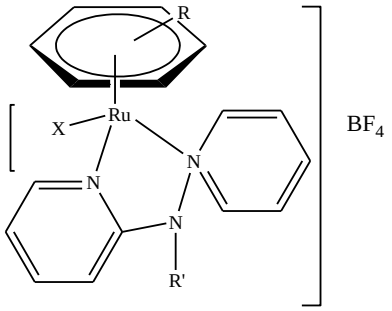

X = CN^- or NCS^- , Ar-R = *p*-iPrC6H4Me, R' = benzyl

Figure 2.4: Half-sandwich cationic ruthenium compound (Kumar *et al.*, 2010) .

2.3.1 Synthesis of half-sandwich complexes with N,N' -bidentate ligands

Several half-sandwich complexes have been synthesized and reported. A typical example is synthesis involving **[(**(η^6-$C_{10}H_{14}$)RuCl(μ-Cl)]$_2$ (η^6-$C_{10}H_{14}$ = η^6-*p*-cymene) dimer subjected to a bridge-splitting reaction with *N,N′,N″*-triarylguanidines) to afford [(η^6-$C_{10}H1_4$)RuCl(N,N')$(ArN)_2$C-N(H)Ar)] half-sandwich, where Ar = C_6H_4Me (Singh *et al.*, 2011) they were synthesized in high yield and subjected to a reaction with an aim of understanding the influence of substituent(s) on the aryl rings of the guanidine . Studies on the solid-state structure, solution behavior, and reactivity pattern of the products of the ruthenium atom in the aforementioned complexes revealed pseudo octahedral "three legged piano stool" geometry (Singh *et al.*, 2011). Among many other synthetic studies, half-sandwich ruthenium(II) complexes **(**η^6-*p*-cymene RuCl(C_5H_4-N-2-CH=N-R)] PF_6 where R is 4-iodophenyl and 4- bromophenyl have also been synthesized and reported to be useful in styrene oxidation (Gichumbi *et al.*, 2016d).

2.4 Chloro bridged arene ruthenium complexes

An [(arene)$RuCl_2$]$_2$ complex provides easy access to immobilized (arene)Ru complexes with rich chemistry via intermediary chloro bridge cleavage reaction, leading to the formation of a series of interesting neutral and cationic mononuclear complexes (Prakash *et*

al., 2013). The source of ruthenium in these half-sandwich complexes is (arene) ruthenium dichloride dimer $[(\eta^6\text{-}p\text{-cymene})RuCl_2]_2$ shown in Figure 2.5 below.

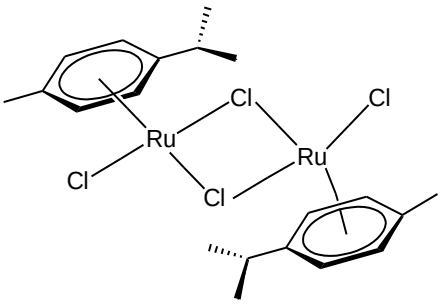

Figure 2.5: (p-cymene) Ruthenium dichloride dimer.

Dimeric chloro-bridged arene ruthenium complexes $[(\eta^6\text{-arene})Ru(\mu\text{-}Cl)Cl]_2$ (arene is benzene, *p*-cymene) and structurally analogous rhodium and iridium complexes $[(\eta^5\text{-}C_5Me_5)M(\mu\text{-}Cl)Cl]_2$ (M = Rh or Ir) containing η^6-/ η^5-cyclic hydrocarbon ligands are versatile and valuable synthetic intermediates that have seen many applications in the coordination/organometallic chemistry, catalysis, polymeric materials, chiral supramolecular hosts, nano-cages and nano-particle precursors (Singh *et al.*, 2010).

2.5 Schiff base ligands.

Schiff base ligands are compounds containing azomethine group RR'C=N- where R' is an alkyl or aryl substituent or a hydrogen. Schiff bases are moderate electron donors with chelating structure and form complexes with special and manipulable properties; they are easily prepared by condensation of aldehydes or ketones with amines (El-Aziz *et al.*, 2013). The formation of a Schiff base from aldehydes or ketones is a reversible reaction and generally takes place under acid or base catalysis, or upon heating according to the following mechanism (Scheme 2.1).

The ease of synthesis of these ligands and their wide applications such as dyes and pigments has given rise to the synthesis of many such ligands with diverse structural orientations. Complexes of Schiff base ligands are of great interest especially in inorganic and bioinorganic chemistry, because complexes obtained from transition and non-transition metals have high potential of being developed into new materials such as catalysts, optical materials, biological sensors, antibacterial, antifungal, antiviral, herbicidal and also as

anticancer agents. Schiff base complexes play a vital role in designing metal complexes related to synthetic and natural oxygen carriers (Al-Amiery *et al.*, 2012). Benzothiazole derivatives have been studied extensively and found to have diverse chemical reactivity and broad spectrum of biological activity (Shafi *et al.*, 2012).

Scheme 2.1: Mechanism for the formation of a Schiff base

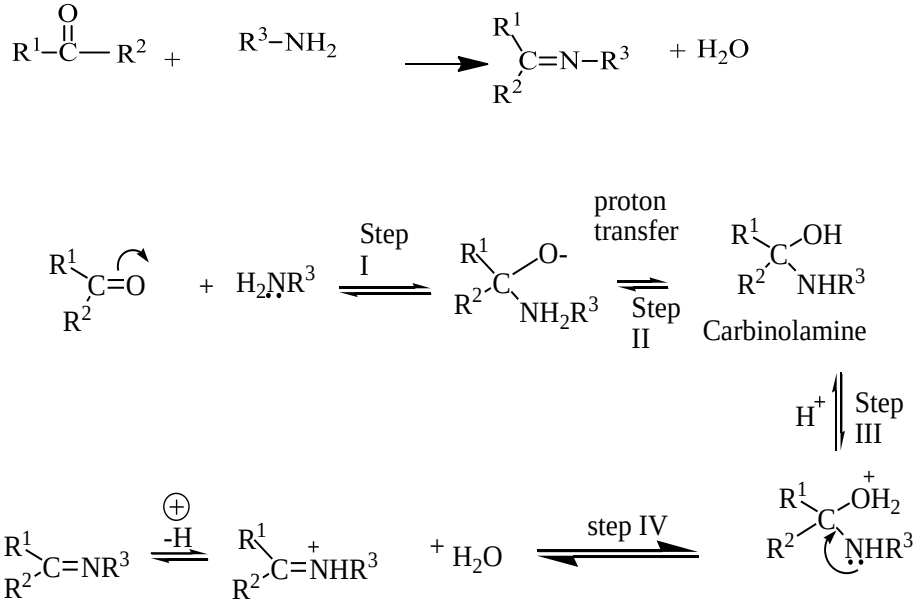

Although they have been known from long ago to be biologically active (Prabhu *et al.*, 2011). They have been pointed out as promising antibacterial agents. For example, N-(salicylidene)-2-hydroxyaniline, Figure 2.6, is effective against *Mycobacterium tuberculosis* H37rv (da Silva *et al.*, 2011).

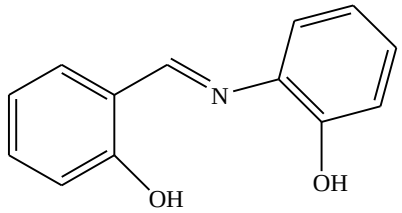

Figure 2.6: N-(salicylidene)-2-hydroxyaniline (da Silva *et al.*, 2011).

2.5.1 Pyridine-imine Schiff base complexes

Pyridine-imines belong to the diimine class of nitrogen based ligands which are known to bind metal ions as N, N'-donors forming stable five membered chelate rings. In these N,N-

donor ligands both the nitrogen donating fragments, i.e. the pyridyl fragments and the imine fragments, have considerable π acid character and hence complexation to the ruthenium centre stabilize the bivalent state of the ruthenium to a significant extent and thereby enhance the reactivity of the arene (Gichumbi *et al.*, 2016a). The coordination chemistry of Schiff bases, derived from 2-pyridine carboxaldehyde and their enhanced biological activities, has also received much attention for their role in inorganic chemistry (El-Aziz *et al.*, 2013).

It is well established that the biological activity associated with the hydrazone compound is attributed to the presence of the active pharmacophore (-CONH-N=C-) (Kumar *et al.*, 2014). Good biological activities according to the many products which contain a pyridine subunit exhibit biological activity such as antimicrobial and antituberculosis activities (Nyawade *et al.*, 2015a). An example being a pyridine-imine Schiff base derived from 2-aminobenzothiazole and 2-pyridine carboxaldehyde as shown in Figure 2.6 above and Figure 2.7 below.

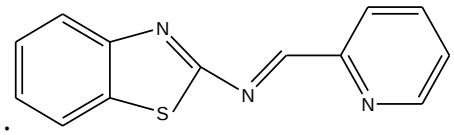

Figure 2.7: N-(pyridine-2-ylmethylene)benzo[d] thiazol-2-amine (El-Aziz *et al.*, 2013).

2.5.2 Metal Schiff base complexes

Metal complexes of Schiff base ligands represent an important and interesting class of co-ordination compounds (Syamal and Maurya, 1989). This fact is manifested by the large number of publications which ranges from purely synthetic to modern physiochemical and biochemical relevant studies of Schiff base complexes (Syamal and Maurya, 1989). A tremendous variety of stable chemical species containing transition, non-transition, inner transition, actinide metal ions and Schiff base ligands have been synthesized (Holm *et al.*, 1966). The doubly bonded nitrogen atom causes rather strong ligand field which leads to a large splitting of d-d orbital energies and consequently, a preferential occurrence of low spin configuration in such complexes (Daul *et al.*, 1979). They are able to stabilize different metals in various oxidation states.

2.5.3 Bipyridine ligands

Bipyridines also known as bipyridyls, dipyridyls, and dipyridines, are a family of chemical compounds with the formula $(C_5H_4N)_2$ shown in Figure 2.8. They are formed by the coupling of two pyridine rings. They are aromatic nitrogen heterocycles that form complexes with most transition metals via both σ-donating nitrogen atoms and π-accepting property of pyridine ligands or by accepting electron density from metal d - orbitals into the π^* molecular orbitals of the pyridine ligands. Bipyridine are neutral N, N' donor bidentate ligand. They are useful in studies of electron and energy transfer, supramolecular and materials chemistry, and catalysis (McCleverty and Meyer, 2004). It is known that $[Ru(II)(bpy)_3]^{2+}$complexes have a unique combination of chemical stability, redox properties, excited state reactivity, luminescence emission and long excited state lifetimes. There is a possibility of making this process more selective and effective by tailoring the bi-or terpyridines with appropriate functional groups or attachments at either *meta* or *para* positions leading to increased luminescence intensities and increase lifetime of excited state (Nurkkala, 2007).

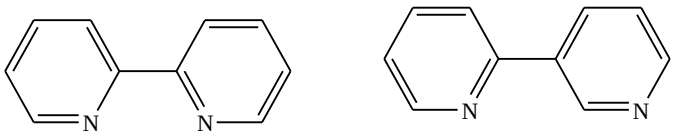

2,2'-bipyridine 2,3'-bipyridine

Figure 2.8: Examples of bipyridine ligands

2.6 Phosphine Ligands

In general, phosphines and its derivatives are usually preferable in synthesis as the ligand of choice, due to the ligands being good stabilizers of the ruthenium in its low oxidation state and accelerating the oxidative addition of the catalyst to the substrate by increasing electron density around the metal centre (Swartz, 2015).

2.7 Electrochemistry of ruthenium arene complexes

Cyclic voltammogram for $[Ru(\eta^6\text{-}p\text{-cymene})(Cl)(CH_3)]$ recorded in dichloromethane at glassy carbon electrode showed two metal centered voltammetric responses. A quasi-reversible oxidation due to Ru(II) ↔ Ru(III) + e^- and an irreversible reduction peak due to

reduction of a ligand at a scan rate of 100 mV/s with respect to Ag/AgCl. Showing that the changes in oxidation and reduction potentials are probably due to relative stabilization of the ruthenium(II) state over ruthenium(III) by a combination of both σ and π effects characteristic of the ligands as shown in Figure 2.9 below (Kumar *et al.*, 2008).

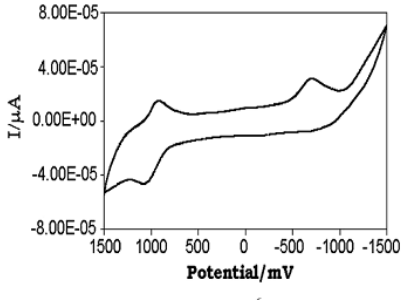

Figure 2.9: Cyclic Voltammogram of [Ru (η^6-p-cymene)(Cl)(CH_3)] (Kumar *et al.*, 2008).

2.8 Applications of ruthenium complexes

Organometallic complexes of Ruthenium(II) are mainly homogeneous catalysts and because of that, arene ruthenium(II) complexes constitute an important group of derivatives that have applications in numerous catalytic activities and processes (Clarke, 2003).

2.8.1 Ruthenium complexes in catalysis

Half-sandwich organoruthenium(II) complexes have of late gained interest in catalytic organic transformations including transfer hydrogenation (Gichumbi *et al.*, 2016b). Many transition metal complexes, including half-sandwich ruthenium(II) complexes, have been studied for these transformations (Saleem *et al.*, 2013). The half-sandwich complexes of Ru have been used in a biomimetic coupled catalytic system for alcohol oxidation (Singh *et al.*, 2010). And also in transfer hydrogenation where hydrogen is added to a molecule from a non-H_2 source making it a convenient and powerful method to access various hydrogenated compounds (Romain *et al.*, 2010). Transfer hydrogenation has several advantages over direct hydrogenation in that it does not require hazardous pressurized H_2 gas nor elaborate equipment setup. Transition metal-catalyzed transfer hydrogenation of ketones is preferred because it requires mild conditions. In particular ruthenium complexes with nitrogen and phosphorus donor ligands have been reported to be good catalysts for catalytic transfer

hydrogenation of ketones. Ruthenium(II) complexes ability to dehydrogenate alcohols and deliver the hydrides to a ketone or an $\propto, \beta$ −unsaturated ketone has made them useful as transfer hydrogenation catalysts (Raja *et al.,* 2010). The complex shown in Figure 2.10 designed by Shvo and mechanistically studied by Casey and coworkers shows a type of catalysis, where, Ru−H donates a hydride and OH of the modified Cp ligand donates a proton to substrate and therefore over the course of each catalytic cycle the nature of the η^5-C_5Ph_4OH ligand

changes in terms of both the charge and number of electrons donated to the metal (Nieto *et al.*, 2011).

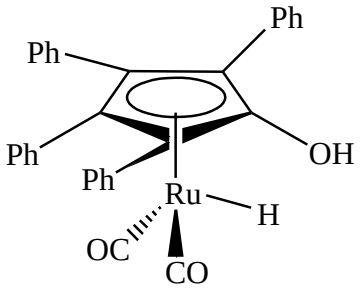

Figure 2.10: Metal−ligand bifunctional catalysts (Casey/Shvo) (Nieto *et al.*, 2011).

Synthesis and catalytic activity of cationic arene ruthenium complexes containing 1,10-phenanthroline and its derivatives as chelating N,N-donor ligands, have also been isolated as chloride or tetrafluoroborate salts (Canivet *et al.*, 2005). Water-soluble Ru(II)-catalyst system that can catalyze an asymmetric hydrogen-transfer reduction of aromatic ketones in aqueous solution, have been found to possess high conversion rates and enantioselectivities, the catalytic system can be recycled at least six times without loss of performance (Rhyoo *et al.*, 2001).

Also, it has been established that cationic chiral half-sandwich ruthenium complexes having a labile group act as a chiral Lewis-acid in organic transformations (Kumar *et al.*, 2014). Cleavage reactions of the [(η^6-*p*-cymene)Ru(μ-Cl)Cl_2] dimer with bipyridyl-based ligands were reported to give water-soluble half-sandwich Ru(II) complexes, which show good catalytic activity for transfer hydrogenation (TH) of aryl ketones (Türkmen *et al.*, 2012). Ruthenium phenanthroline complexes shown in Figure 2.11 have been found and reported

to be good catalysts in transfer hydrogenation of ketones in aqueous solution (Canivet *et al.*, 2005).

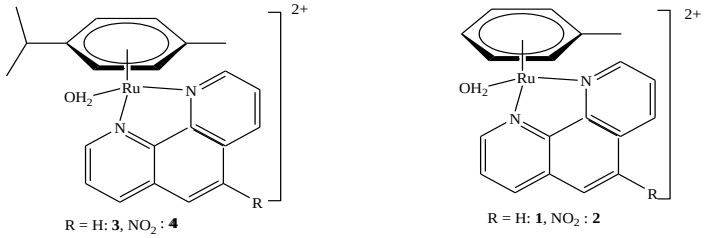

Figure 2.11: Ruthenium phenanthroline complexes (Canivet *et al.*, 2005).

The above complexes, Figure 2.11 have been isolated as chloride or hexafluorophosphate salts and they have been found to be water soluble (Canivet *et al.*, 2005).

2.8.2 Ruthenium in medicine

The success of cisplatin and related platinum complexes as anticancer agents has stimulated a search for other active transition metal anticancer complexes, and ruthenium in particular has attracted recent attention. The activity of *fac*-[$Ru^{III}Cl_3(NH_3)_3$] was discovered early, but its poor aqueous solubility prevented further use (Morris *et al.*, 2001). The synthetic chemistry of ruthenium(II) is well developed, particularly with amine, ammine and imine ligands, and provides for many approaches to innovative new metallopharmaceuticals. Due to strong ligand-field stabilization energy, the more common oxidation states Ru(II), Ru(III) and Ru(IV) in aqueous solution are usually octahedral and are often fairly inert to ligand substitution. The drug-like effects of ruthenium red, which has been used as a cytological stain for over a century, have long been known (Allardyce and Dyson, 2001). Ruthenium's properties are well suited toward pharmacological applications. It's wide range of oxidation states (II, III and IV) under physiologically relevant conditions can be accessed and generally the rates of ligand exchange processes in ruthenium complexes are much faster than in square planar Pt(II) complexes (Gichumbi *et al.*, 2016e). The advantage of utilizing ruthenium amine and ammine complexes in drug development, is that there are reliable methods of synthesizing stable complexes with predictable structures; they have the ability to tune ligand affinities, electron transfer, substitution rates and reduction potentials.

Furthermore, many am(m)ine complexes of Ru(II) and Ru(III) tend to selectively bind to imine sites in biomolecules, because they do not protonate at neutral pH, thereby leaving their nitrogen lone pairs available for metal ion coordination (Clarke, 2003).

2.8.3 Antimicrobial activity

Ruthenium complexes have attracted interest as antimicrobial agents (Li *et al.*, 2015). Multidrug resistance (MDR) has posed a major problem in health and there is a clear need for the development of new types of antimicrobial agents, which can overcome the bacterial mechanisms of resistance developed against the current range of drugs. The increase in the mortality rate associated with infectious diseases is directly related to bacteria that exhibit multiple resistances to antibiotics (da Silva *et al.*, 2011). Resistance against antimicrobial agents develops quickly, even against synthetic compounds that bacteria have never encountered previously. This has triggered interest in new classes of antimicrobial agents and several avenues are being pursued to find new compounds that inhibit the growth or virulence of pathogenic bacteria (Gichumbi *et al.*, 2016e).

The activity of organic antimicrobial drugs has been enhanced by binding the organic molecule to a ruthenium centre (Allardyce and Dyson, 2001). Ruthenium complexes in particular are of interest due to the ability of ruthenium to mimic iron when bound to biological molecules (Gichumbi *et al.*, 2016e). Success depends on complex geometries and ligand modification in these applications (Dayan *et al.*, 2015). Benzothiazole derivatives though known for long to be biologically active have been studied extensively and found to have diverse chemical reactivity and broad spectrum of biological activity.

2.8.4 Anticancer activity of Ruthenium complexes

Despite the success of platinum-based anticancer compounds in the clinic, there is still need for new and improved metal-based anticancer drugs fueled by the inability of platinum compounds to tackle some high social incidence types of cancer (Allardyce and Dyson, 2001). There are also associated toxic side effects of the current platinum compounds in clinical use (Florea and Büsselberg, 2011). Platinum anticancer drugs bind DNA, causing damage that prevents protein synthesis and replication thus causing cell death. The success

of platinum anticancer drugs has biased the screening of new metal-based anticancer compounds. Many Ru(II), Ru(III) and Ru(IV) complexes with amine, dimethylsulfoxide, imine, polyaminopolycarboxylate and N-heterocyclic ligands have been found to bind to DNA (Clarke, 2003). The success of cisplatin and related platinum complexes as anticancer agents has stimulated a search for other active transition metal anticancer complexes and ruthenium in particular has attracted recent attention. The complex-[$Ru^{III}Cl_4$(DMSO)(Im)] NAMI-A has a low cytotoxicity but is active against tumors and has recently entered clinical trials (Morris *et al.*, 2001).

Alternative metal compounds are presently being evaluated for anticancer applications to overcome these limitations, ruthenium complexes with N, N'-bidentate ligands being studied as one of the anticancer drugs. Ruthenium based compounds are regarded as the most promising alternatives to platinum complexes (Ang *et al.*, 2011). This is because these compounds have also shown antiproliferative activity *in vitro* and *in vivo* (Gichumbi et al., 2016e). The promising anticancer properties of ruthenium complexes have prompted other researchers to synthesize a series of organometallic ruthenium(II) complexes (Gichumbi *et al.*, 2017b). Some Ru(III) complexes are known to bind to Fe(III) sites of the proteins lactoferrin and transferrin which is thought to be responsible for the delivery of Ru(III) to cancer cells where it is taken up via receptor-mediated endocytes (Allardyce and Dyson, 2001). Transferrin normally transports Fe(III) in the blood but is only about one third occupied by Fe(III) and so there are vacant sites available for Ru(III) binding (Morris *et al.*, 2001).

Several half-sandwich Ru(II) compounds have shown promising anticancer activity. Consequently related chemistry has also gotten attention. The (η^6-arene)Ru(II) complexes with pyrone-derived ligands are rendered active against cancer (Singh and Singh, 2010). The water-soluble (η^6-arene)ruthenium(II) complexes containing pyridinethiolato ligands show cytotoxicity toward ovarian cancer cells (Singh and Singh, 2010).

CHAPTER THREE
MATERIALS AND METHODS

3.1 Materials and Apparatus

All manipulations were carried out using modified Schlenk techniques under an inert atmosphere of nitrogen gas. Chemical reagents and solvents were obtained from the suppliers. Analytical reagent grade diethyl ether (Sigma-Aldrich), acetonitrile, ethanol, ruthenium trichloride hydrate, 1-Methyl-1,4-cyclohexadiene, pyridine-2-carboxaldehyde, 5,5'-dimethyl-2,2'-bipyridine ,4,4'-di-*tert*-butyl-2,2'-bipyridine and 2,2'-bipyridine, (Aldrich), were used without further purification.

Melting points were measured using a Gallenkamp Melting point apparatus. Elemental analyses were performed on a Vario EL III elementar CHNS/O analyzer. Infrared spectra were recorded using an ATR Perkin Elmer Spectrum 100 spectrophotometer with a range of 4000 and 380 cm^{-1}. Electronic spectra were recorded in acetonitrile with a Perkin-Elmer Lamba 35 UV–visible spectrophotometer. ^{1}H NMR and ^{13}C NMR spectra were recorded on a Bruker Top Spin 400 and 600 MHz spectrometers respectively using deuterated DMSO, however ^{13}C NMR was performed for complex **3** ($[(\eta^6\text{-}C_6H_5CH_3)RuCl(C_{10}H_8N_2)]$ only . Electrochemical measurements were performed using BASi Epsilon E2 1177 model potentiostat, using a conventional three-electrode cell with platinum working electrode, platinum wire counter electrodes and a Ag/AgCl reference electrode.

3.2 Characterization of the complexes

The complexes were characterized using the methods given below.

3.2.1 Melting points determination

Melting point of the precursor molecule $[(\eta^6\text{-}C_6H_5CH_3)Ru(\mu\text{-}Cl)Cl]_2$, pyridine-imine Schiff base ligand and synthesized ruthenium complexes were determined using the Gallenkamp Melting point apparatus (MPD350.BM3.5).This was done to provide information about the purity of the compounds. Pure compounds are known to have sharp melting points (less than 2 ^{0}C). A glass capillary tube containing the sample was inserted into the heating block. Preliminary melting points determinations were done rapidly but the actual melting points

were determined by heating the samples rapidly to temperatures about 10 ºC below their expected melting points guided by preliminary determinations, then slowly the rate of temperature was allowed to increase to about 1 ºC per minute. This ensured that the sample and the block were at thermal equilibrium, guaranteeing accuracy of results.

3.2.2 Elemental analysis

Elemental analysis was done using Vario EL III CHNS/O analyzer. The samples were encapsulated in tin vials and inserted automatically into the machine. In the combustion process (furnace at 1150 ℃), in the presence of oxygen, carbon present in the sample was converted to CO_2, hydrogen to H_2O and nitrogen to oxides of nitrogen. Combustion products were swept out of combustion chamber by inert carrier gas (helium) and passed over heated copper (to remove any oxygen present) the gases were then passed through absorbent traps and CO_2, H_2O and N_2O were only left. Detector used was a thermal conductivity detector, quantification of elements, was done by calibrating each element using Sulphanilic acid as the reference material (Fadeeva *et al.*, 2001).

3.2.3 Infra-red spectroscopy (IR)

The IR spectra of the synthesized complexes and the ligands were done using an FTIR Perkin Elmer 100 spectrophotometer in the range of 4000 and 380 cm^{-1}. This was done on solid samples as a KBr pellets. 2 mg of the sample were mixed with 100 mg of KBr and ground together in an agate mortar into fine powder that was hard pressed to form pellet disks in a hard press. The disks were mounted to the IR spectrophotometer and the spectra read and recorded directly.

3.2.4 UV/VIS spectroscopy

The electronic spectra of the ligands and their respective complexes were obtained in acetonitrile, using the PerkinElmerLamba 35 UV/VIS Spectrophotometer. Blank sample solution was prepared by filling a cuvette with the appropriate solvent (acetonitrile). The spectrophotometer was then set to scan the region from 200 nm to 800 nm. A blank was run followed by each sample as per the laid down instructions and the changes in absorbance were recorded.

3.2.5 ^{1}H NMR spectroscopy

^{1}H NMR was done to confirm the molecular structure of the complexes by determining the protons present and the environment in which they exist. The chemical shifts were recorded in ppm.

3.2.6 Cyclic voltammetry

Cyclic voltammetry measurements were carried out using BASi Epsilon E2 1177 model potentiostat, using a conventional three-electrode cell with platinum working electrode, platinum wire counter electrodes and a Ag/AgCl reference electrode (RE) using acetonitrile solvent containing 0.1 M tetrabutylammonium hexafluorophosphate ($[NBu_4][PF_6]$) supporting electrolyte which was prepared according to a literature method (Martin *et al.*, 1996). Acetonitrile was a suitable solvent for performing the experiment since it: (1) provides better solubility to the Ru(II)-arene complexes, (2) prevents the ligand-exchange of the complexes with solvent molecules that would be observed in aqueous solutions, and (3) displays a better reversibility for RuIII/II redox couples as compared to other solvents. Ferrocene was used as an internal standard.

3.3 Evaluation of antimicrobial activity

Antimicrobial activity was performed on both ligands and synthesized ruthenium complexes as explained below.

3.3.1 Preparation of Liquid media

The Nutrient broth (1.3 g) was weighed and dissolved in 100 ml of distilled water and transferred into a 250 ml reagent bottle. Four vials were filled with distilled water and all placed in an autoclave and allowed to rise to a pressure of 1.5 Kpa then cooled to zero temperature.

After removing from the autoclave, they were allowed to cool to room temperature. The nutrient broth was then divided into four portions (15 ml) per sterile vial under sterile conditions in a lamina flow hood. The microorganisms were swabbed into the vials in duplicate and transferred to the incubator and left at 37 ^{0}C for 24 h.

3.3.2 Preparation of Test plates

Mueller Hinton agar (19 g) was dissolved in 500 ml distilled water and placed in an autoclave at 121 ^{0}C at 1.5 Kpa /cm^3 for 15 minutes then cooled to 40 ^{0}C.15 ml of agar was dispensed to sterile petri dishes under sterile conditions in a lamina flow hood. The plates were used to grow the strains (*E.coli* and *S. aureus)* by inoculating 1 ml of microbial suspension in the petri dishes. Stock solutions of the synthesized ruthenium complexes were made by dissolving 20 mg of the complexes in 1 mL DMSO, followed by serial dilutions into (0.2,0.4,0.8 mg/mL)with the same solvent. Sterile blank disks (6 mm) were impregnated with 10 µL (0.2 mg), 20 µL (0.4 mg), and 40 µL (0.8 mg) of the stock solution, respectively and allowed to dry for 1 h. Gram-negative (*E. coli* ATCC 11775) and Gram - positive (*S. aureus* ATCC 12600) bacterial strains were grown overnight on agar plate then re-suspended in sterile distilled water and the turbidity of cell suspensions adjusted equivalent to that of a 0.5 McFarland (Gichumbi *et al.*, 2016e). Plates were then incubated for 24 h at 37 °C. Testing was done in duplicate and Streptomycin (S-10) was used as standard antimicrobial agent controls, while DMSO-impregnated discs were used as negative controls.

Zones of inhibition were measured using a ruler (Wilkins and Thiel, 1973; Dickert *et al.*, 1981). The bacterial response to the complexes was evaluated as indicated in Table 3.1 (Johnson and Case, 1995).

Table 3.1 : Sensitivity evaluation table

	Diameter of zone of inhibition (mm)
Resistant	≤ 11
Intermediate	12-14
Susceptible	≥ 15

3.4 Synthesis of Precursor complex

The precursor complex $[(\eta^6\text{-}C_6H_5CH_3)Ru(\mu\text{-}Cl)Cl]_2$ used in this study was prepared following a reported method (Bennett and Smith, 1974) . To ethanolic solution of hydrated ruthenium (III) trichloride (2 g,7.7 mmol) in a 150 cm^3 round bottomed flask, purged with nitrogen gas for 10 minutes were added 10 cm^3 of 1-methyl-cyclohexa-1,4-diene.The

mixture was refluxed for 4 h under nitrogen blanket. $[(\eta^6\text{-}C_6H_5CH_3)Ru(\mu\text{-}Cl)Cl]_2$ mixture turned brown and subsequently a red precipitate was formed. The red precipitate was allowed to cool to room temperature. The mixture was filtered under reduced pressure and the residue washed with two portions of ethanol (10 ml). The red solid was then dried in vacuo; Yield: 1.56 g, 78 %.

3.5 Synthesis of monometallic half-sandwich N,N '-bidentate Ruthenium complexes $[(\eta^6\text{-}C_6H_5CH_3)RuCl(N,N]PF_6$

The ruthenium bipyridine complexes and ruthenium pyridine-imine complex were synthesized as illustrated in Scheme 3.1 below.

Scheme 3.1: Schematic representation of the formation of the ruthenium complexes

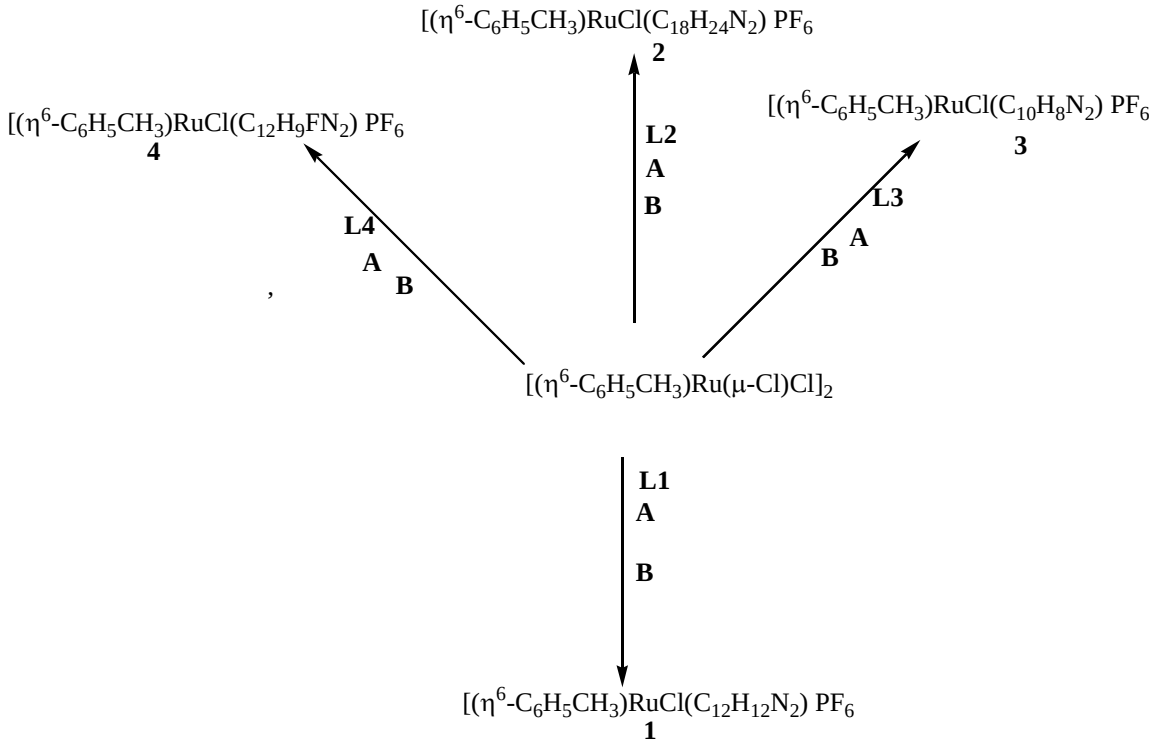

Where;

L1 = 5,5'-dimethyl-2,2'-bipyridine
L2 = 4,4'-di-tert-butyl-2,2'-bipyridine
L3 = 2,2'-bipyridine
L4 = 4-Fluoro-N-(2-pyridylmethylene)-aniline
A = CH_3CN
B = Excess NH_4PF_6 in C_2H_5OH

3.5.1 Synthesis of $[(\eta^6\text{-}C_6H_5CH_3)RuCl(C_{12}H_{12}N_2)]PF_6$

To a solution of the precursor complex $[(\eta^6\text{-}C_6H_5CH_3)Ru(\mu\text{-}Cl)Cl]_2$ (106 mg, 0.20 mmol) dissolved in acetonitrile (10 cm^3) and contained in a 100 mL volumetric flask was added to a slightly excess 5,5'-dimethyl-2,2'-bipyridine (0.43 mmol,79.22 mg) of the ligand dissolved in 15 mL acetonitrile. The mixture was stirred for 3 h under inert nitrogen atmosphere on a magnetic stirrer. The mixture changed colour from dark brown to yellow. The volume of the mixture was reduced in vacuo to 10 mls and yellow residue settled at the bottom of the flask. Excess ammonium hexafluorophosphate (70.09 mg, 0.43 mmol) dissolved in ethanol (15 ml) was added to the yellow residue and the mixture cooled in an ice bath while stirring for 30 minutes. The formed yellow residue was filtered by vacuum filtration and washed twice with diethyl ether (10 ml) and dried in vacuo for 4 h. Yield: (94.7 mg, 89 %). The yield was calculated using the precursor complex $[(\eta^6\text{-arene})Ru(\mu\text{-}Cl)Cl]_2$ as the limiting reagent.

3.5.2 Synthesis of $[(\eta^6\text{-}C_6H_5CH_3)RuCl(C_{18}H_{24}N_2)]PF_6$

To a solution of the precursor complex $[(\eta^6\text{-}C_6H_5CH_3)Ru(\mu\text{-}Cl)Cl]_2$ (106 mg, 0.20 mmol,) dissolved in acetonitrile (10 cm^3) and contained in a 100 mL volumetric flask was added to a slightly excess 4,4'-di-tert-butyl-2,2'-bipyridine (115.24 mg, 0.43mmol,) of the ligand dissolved in 15 mL acetonitrile. The mixture was stirred for 3 h under inert nitrogen atmosphere on a magnetic stirrer. The mixture changed colour from dark brown to yellow. The volume of the mixture was reduced in vacuo to 10 mls and yellow residue settled at the bottom of the flask. Excess ammonium hexafluorophosphate (70.09 mg, 0.43 mmol) dissolved in ethanol (15 ml) was added to the yellow residue and the mixture cooled in an ice bath while stirring for 30 minutes. The formed yellow residue was filtered by vacuum filtration and washed twice with diethyl ether (10 ml) and dried in vacuo for 4 h. Yield (96.5 mg, 90 %)

3.5.3 Synthesis of $[(\eta^6\text{-}C_6H_5CH_3)RuCl(C_{10}H_8N_2)]PF_6$

To a solution of the precursor complex $[(\eta^6\text{-}C_6H_5CH_3)Ru(\mu\text{-}Cl)Cl]_2$ (106 mg, 0.20 mmol,) dissolved in acetonitrile (10 cm^3) and contained in a 100 mL volumetric flask was added to a slightly excess 2,2'-bipyridine (67.16 mg, 0.43mmol,) of the ligand dissolved in 15 mL

acetonitrile. The mixture was stirred for 3 h under inert nitrogen atmosphere on a magnetic stirrer. The mixture changed colour from dark brown to yellow. The volume of the mixture was reduced in vacuo to 10 mls and yellow residue settled at the bottom of the flask. Excess ammonium hexafluorophosphate (70.09 mg, 0.43 mmol) dissolved in ethanol (15 ml) was added to the yellow residue and the mixture cooled in an ice bath while stirring for 30 minutes. The formed yellow residue was filtered by vacuum filtration and washed twice with diethyl ether (10 ml) and dried in vacuo for 4 h. (Yield 95.8 mg, 90 %).

3.6 Synthesis of 4-fluoro-N-(2-pyridylmethylene)-aniline

The fluoro substituted pyridine-imine Schiff base ligand was synthesized by condensation reaction of 2-pyridinecarboxaldehyde and halo substituted anilines to give; [(C_5H_4N-2-CH=N-X)] where (X = 4- Fluorophenyl) following a general method for the preparation of Schiff bases shown in Scheme 3.2 below (Dehghanpour and Mahmoudi, 2007).

Scheme 3.2: Mechanism for the formation of a Schiff base

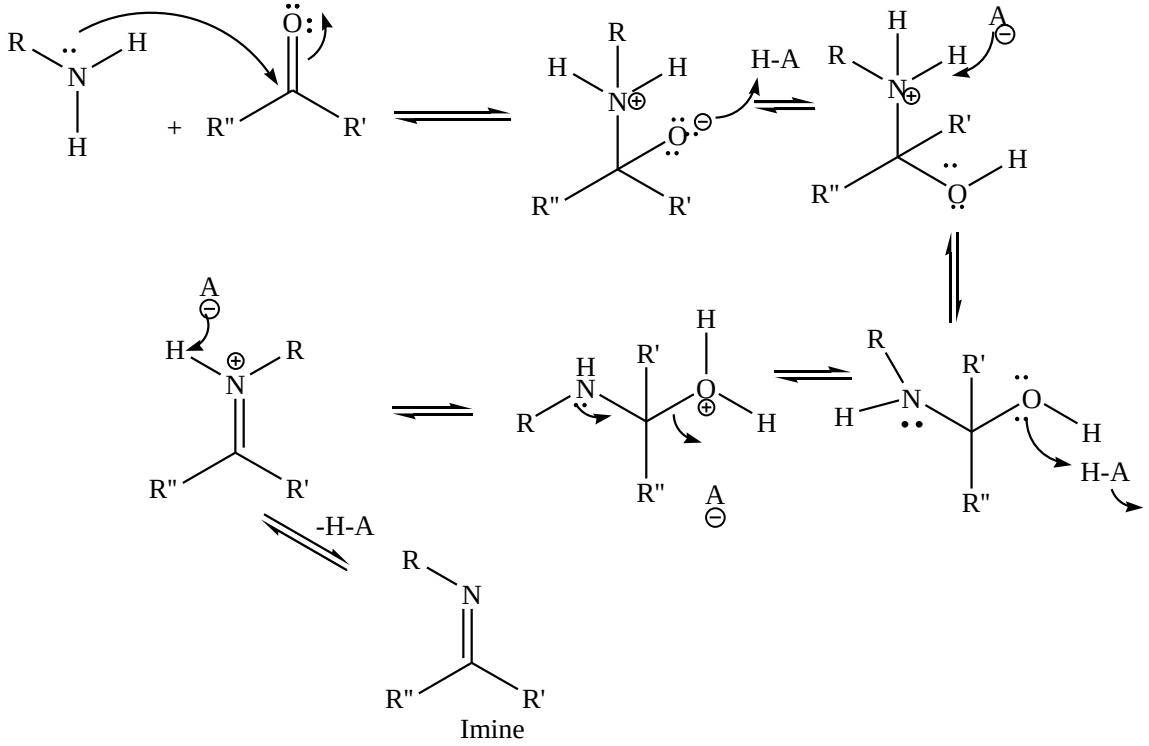

To a solution of 2-pyridinecarboxaldehyde (107 mg,1mmol) in diethyl ether was added a solution of 4-fluoroaniline (111.02 mg,1 mmol) dissolved in 10 ml diethyl ether and the

resultant mixture was stirred for 2h.The ligand 4-fluoro-N-(2-pyridylmethylene)-aniline was formed as a precipitate which was then filtered, washed with diethyl ether and dried in air. The obtained precipitate was yellowish grey microcrystalline precipitate, yield; 170.03 mg, 90 %.The mechanism for the formation of the 4-fluoro-N-(2-pyridylmethylene)-aniline from pyridine-2-carboxaldehyde and fluoro substituted aniline is depicted in Scheme 3.3 below.

Scheme 3.3: Mechanism of formation of 4-fluoro-N-(2-pyridylmethylene)-aniline

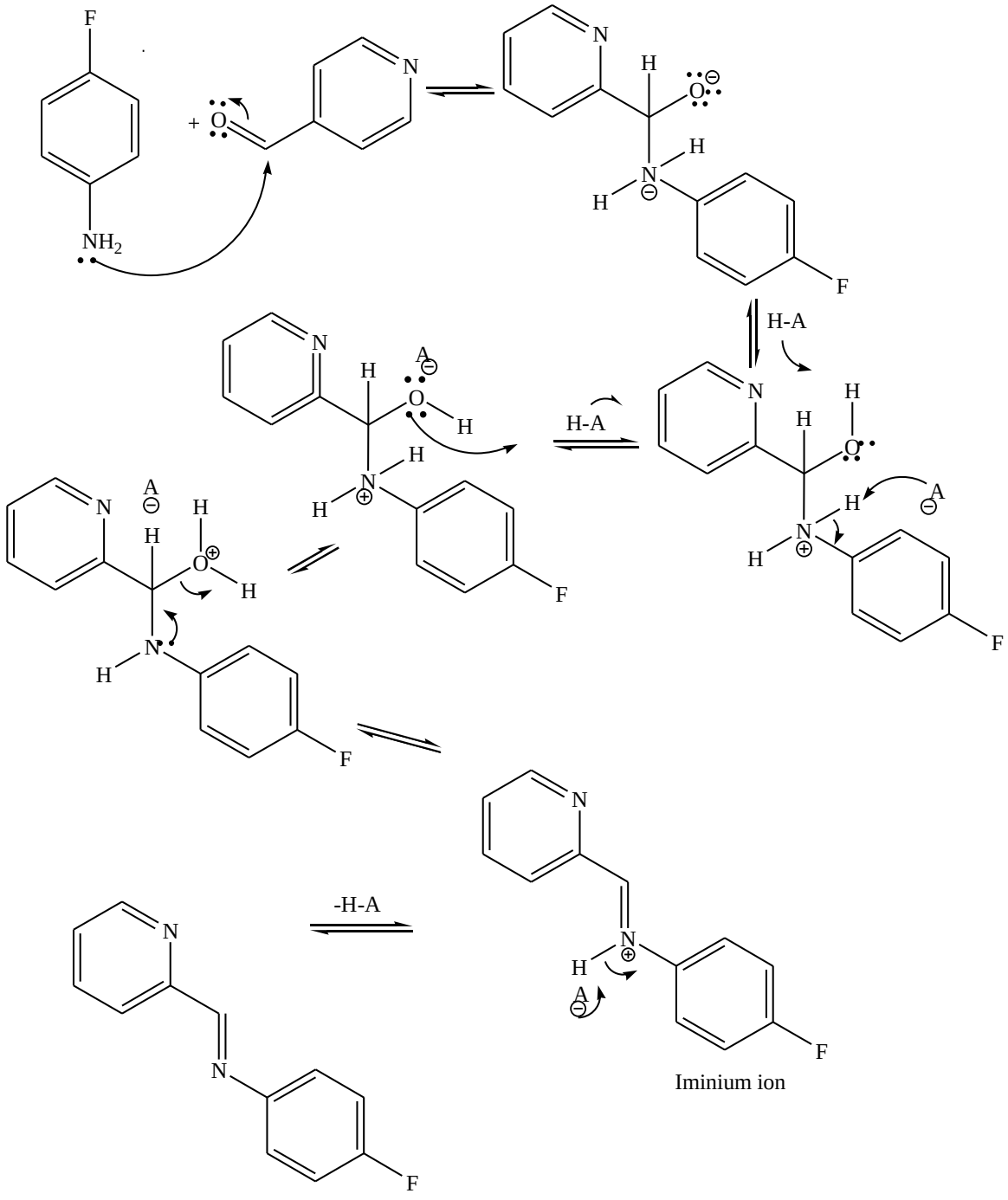

3.7 Synthesis of [(η^6-$C_6H_5CH_3$)RuCl(C_5H_4N-2-CH=N-X)] PF_6 complex [X = F]

This arene ruthenium(II) complex was synthesized according to the procedure in section 3.5.1 above, the ligand used was 4-fluoro-N-(2-pyridylmethylene)-aniline (**L4**).

In a 100 mL volumetric flask covered with an aluminium foil and purged with dry oxygen free nitrogen gas for 10 minutes was placed the precursor complex $[(\eta^6\text{-arene})Ru(\mu\text{-}Cl)Cl]_2$ (106 mg,0.20 mmol) dissolved in acetonitrile (10 ml).To this was added slightly excess(0.43 mmol ,86 mg) of the 4-fluoro-N-(2-pyridylmethylene)-aniline (0.43 mmol) dissolved in acetonitrile. The mixture was stirred for 3 h. The colour of the mixture lightened and maintained a reddish colouration. Volume reduction was done in vacuo to about 10 ml and an orange residue settled at the bottom of the volumetric flask. Excess ammonium hexafluorophosphate (70.09 mg, 0.43 mmol) was weighed, dissolved in 15 ml ethanol and added to the orange residue and the mixture cooled in an ice bath while stirring for 30 min. The formed orange residue was then filtered by vacuum filtration and washed twice with 10 ml portions of diethyl ether and dried in vacuo for 4 h. The solid was then dried under reduced pressure to give an orange powder. Yield :(94.3 mg, 89 %).

CHAPTER FOUR

RESULTS AND DISCUSSION

4.1 Introduction

The results of the characterization of the new complexes by FTIR, NMR, UV/Vis spectroscopy, melting points, elemental analyses, cyclic voltammetry as well as bioassays against the Gram-negative *Escherichia coli* and the Gram-positive *Staphylococcus aureus* are presented and discussed in the sections that follow.

4.2 Synthetic Studies

The bimetallic arene precursor $(\eta^6\text{-}C_6H_5CH_3)Ru(\mu\text{-}Cl)Cl]_2$ reacted with the N,N-bidentate ligands in dry acetonitrile as shown in Scheme 4.1 at ambient temperatures and gave the new mononuclear half-sandwich complexes $[(\eta^6\text{-}C_6H_5CH_3)RuCl(N,N)]PF_6$, **1-4.**

Scheme 4.1: Synthesis of $[(\eta^6\text{-arene})RuCl(N,N]PF_6$ complexes

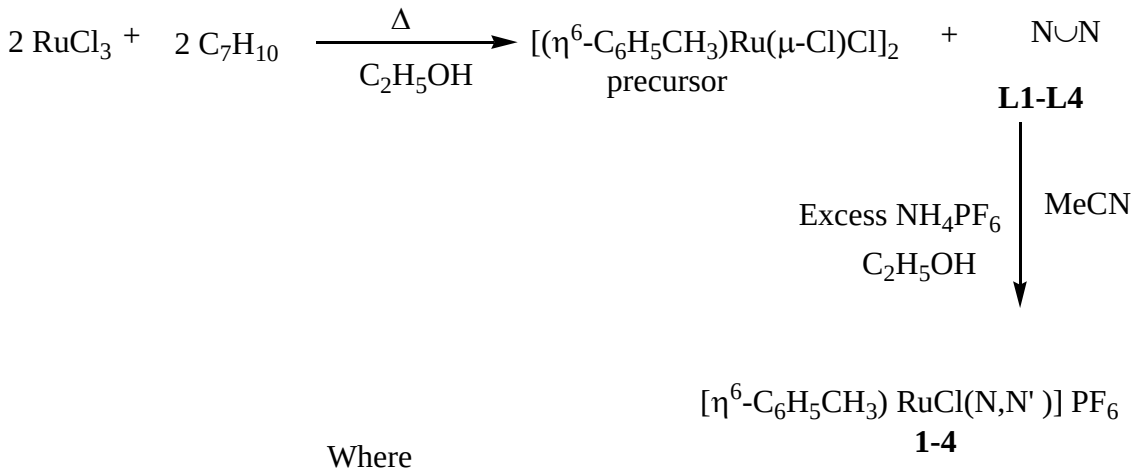

Where

N,N ' = 5,5'-dimethyl-2,2' bipyridine (**L1**)
= 4,4'-di-tert-butyl-2,2' bipyridine (**L2)**
= 2,2' bipyridine **(L3)**
= 4-fluoro-N-(2-pyridylmethylene)-aniline (**L4**)

Monometallic complexes ; $[\eta^6\text{-}C_6H_5CH_3)$ RuCl(N,N')] PF_6

1 = $[C_{19}H_{20}ClN_2Ru]$ PF_6
2 = $[C_{25}H_{32}ClN_2Ru]$ PF_6
3 = $[C_{17}H_{16}ClN_2Ru]$ PF_6
4 = $[C_{19}H_{17}ClN_2RuF]$ PF_6

The synthetic strategy for the production of the new half-sandwich N,N' bimetallic Ruthenium complexes was initially to synthesize precursor bimetallic arene sandwich complex $[(\eta^6\text{-}C_6H_5CH_3)Ru(\mu\text{-}Cl)Cl]_2$ capable of reacting with N,N' bidentate ligand (**L1-L4**) where N,N' = 5,5'-dimethyl-2,2'-bipyridine (**L1**) , 4,4'-di-tert-butyl-2,2'-bipyridine (**L2**), 2,2'-bipyridine (**L3**) and pyridine-imine Schiff base (X=fluoro);(**L4**) .The precursor bimetallic complex, reacted with the bidentate ligands in dry acetonitrile at ambient temperatures to give new half-sandwich mononuclear complexes $[(\eta^6\text{-}C_6H_5CH_3)RuCl(N,N)]PF_6$ (**1-4**).Synthetic steps are depicted in scheme 4.1 above. The complexes were formed in high yields of between 89-90 % based on the precursor complex $[(\eta^6\text{-}C_6H_5CH_3)Ru(\mu\text{-}Cl)Cl]_2$ as the limiting reagent.

4.3 Physical properties

This involved solubility tests and melting point determinations.

4.3.1 Solubility

The new half-sandwich monometallic complexes were obtained in good yields, they were air stable and readily soluble in polar solvents such as acetone, acetonitrile, DMSO and insoluble in non-polar organic solvents such as hexane and diethyl ether.

4.3.2 Melting point determinations

The melting points of the synthesized complexes are shown in Table 4.1, while the half-sandwich monometallic complexes were obtained in high yields as mainly yellow solids, their purity was also found to be good since the melting points of various samples of the same compounds were identical.

The melting points of the complexes were found to increase with increase in branching of the carbon chain of the ligands. It was observed that the complexes decomposed in the range of 193-228℃ and the decomposition temperature increased with increase in molecular weights of the complexes.

This may be due to the fact that going from branched to a highly branched makes a molecule to be compact in the solid phase hence need for more energy to weaken the intermolecular interactions (Dong and Hao, 2010).

Table 4.1: Melting points of ruthenium(II) complexes and ligands

	Ligand/Complex	M.W	Colour	Mpt/DCT (℃)	YIELD (%)
(a)	$C_{12}H_{12}N_2$ (**L1**)	184	White	116	-
(b)	$C_{18}H_{24}N_2$ (**L2**)	268	White	160	-
(c)	$C_{10}H_8N_2$ (**L3**)	156	White	72	-
(d)	$C_{12}H_9N_2F$ (**L4**)	200	Yellowish-grey	159	89
(e)	$[C_{19}H_{20}ClN_2Ru]PF_6$ (**1**)	557.5	Yellow	224	89
(f)	$[C_{25}H_{32}ClN_2Ru]PF_6$ (**2**)	642	Yellow	228	90
(g)	$[C_{17}H_{16}ClN_2Ru]PF_6$ (**3**)	529.97	Yellow	211	90
(h)	$[C_{19}H_{17}ClN_2RuF]PF_6$ (**4**)	573.97	Orange	193	89

4.4 Elemental analysis

The elemental analytical data of the new complexes are depicted in Table 4.2.It is evident that the experimental (found) and theoretical percentages of carbon, hydrogen and nitrogen (CHN) were in agreement and thus supported the molecular formulae of the new synthesized complexes.

The higher percentage of hydrogen found in some of the synthesized compounds may be due to the presence of water molecules trapped within the complex which were not removed completely during the drying stage. When water composition is factored in it shows that complex **2** and **3** may have one mole of H_2O within their crystal lattice.

Table 4.2: Elemental analysis data for synthesized complexes

COMPLEXES (M.F)	CALCULATED			FOUND		
	C	H	N	C	H	N
$[C_{19}H_{20}ClN_2Ru]PF_6$ (**1**)	40.93	3.59	5.02	40.91	3.61	5.02
$[C_{25}H_{32}ClN_2Ru]PF_6.H_2O$ (**2**)	45.49	5.15	4.24	44.83	5.19	4.24
$[C_{17}H_{16}ClN_2Ru]PF_6.H_2O$(**3**)	37.25	3.28	5.11	37.38	4.23	5.51
$[C_{19}H_{17}ClN_2RuF]PF_6$ (**4**)	39.76	2.96	4.88	38.96	2.99	5.28

4.5 Electro spray mass spectral analysis

The electro spray mass spectra of the complexes did not show the parent molecular ion (M^+) peak. However the most abundant ion peak in all the spectra was that of the fragment ion $[(\eta^6\text{-}C_6H_5CH_3)Ru(Cl)\ bpy]^+$ (Figure 4.1) which occur due to the loss of a PF_6 anion.

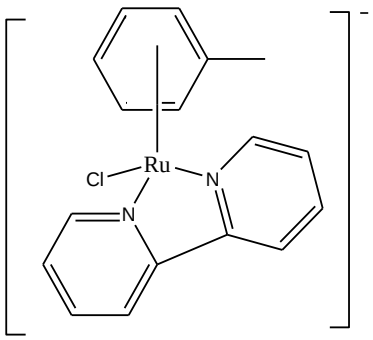

Figure 4.1: $[(\eta^6\text{-}C_6H_5CH_3)Ru(Cl)\ bpy]^+$ cation

A typical electrospray mass spectrum for the new complexes is shown for complex **3** in Figure 4.2. The most abundant peak occurs at m/z = 385 which is as a result of the complex losing PF_6^- counter ion.

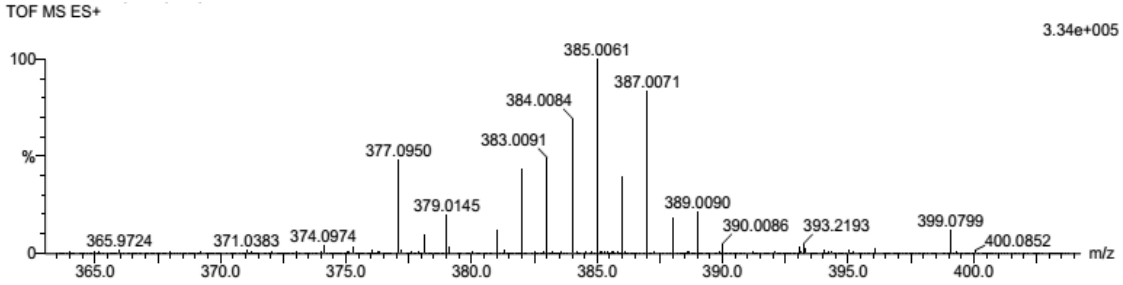

Figure 4.2: ES-MS spectrum showing the fragmentation pattern of $[C_{17}H_{16}N_2ClRu]\ PF_6$

The multiple peaks associated with the seven stable isotopes of ruthenium are clearly observed in each fragment .This is a clear proof that the yellow powder formed is the expected complex synthesized. The arene ($C_6H_5CH_3$) remained coordinated to the ruthenium metal in all the fragments. The formation of the complex **3** is further supported by induced fragmentation as shown in Figure 4.3 which shows that it is possible to induce some fragmentation in the source in order to gain some structural information about the sample.

By increasing the sample cone voltage in the source to a value of 55V the doubly charged ion was completely dissociated to give a number of fragment ions as shown in Figure 4.3.The peaks centered around m/z 385 are due to a charged fragment (charge state determined by the isotope separation) produced by the loss of the PF_6 counter ion. A further loss of a 2, 2'-bipyridine ligand from the ruthenium center gives the intense group of doubly charged ions centered around m/z 372.

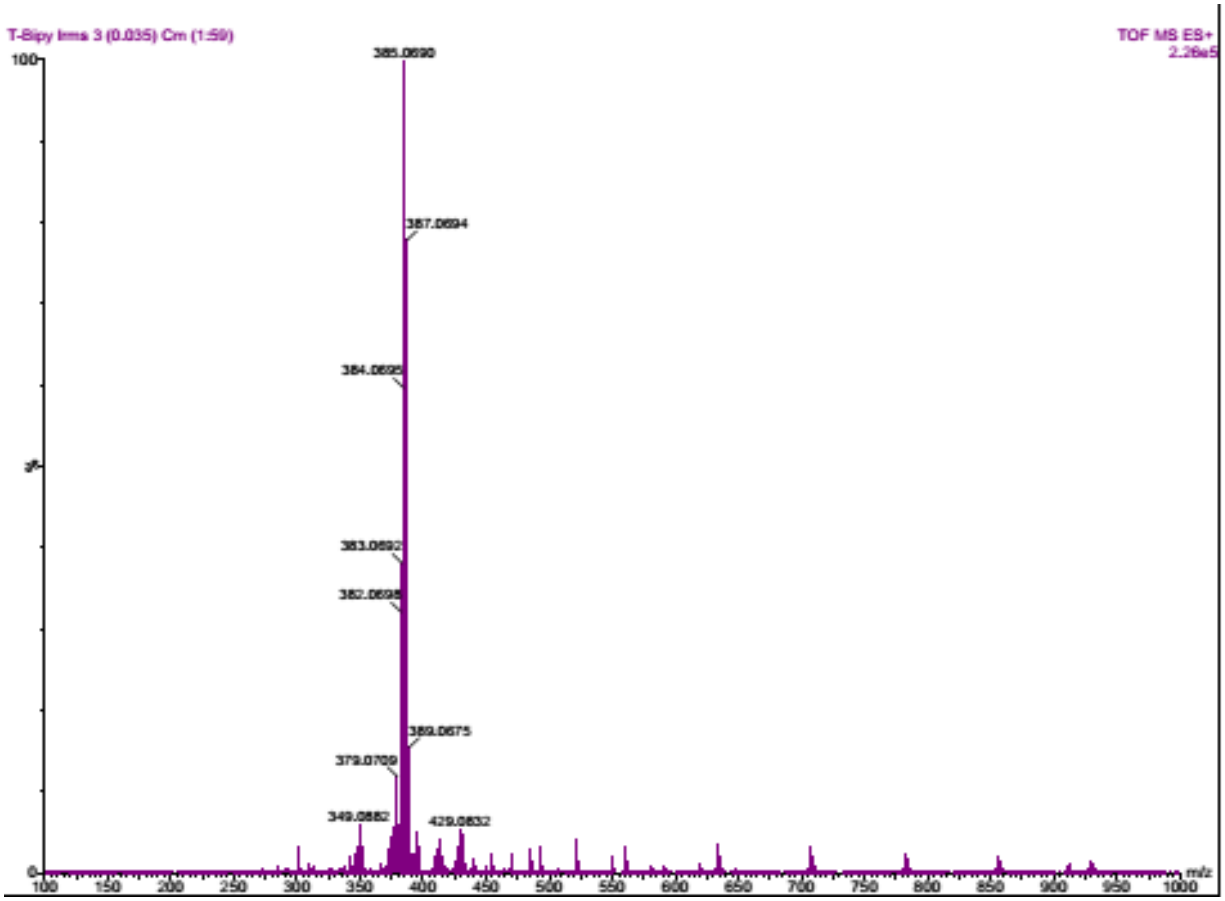

Figure 4.3: Induced fragmentation of $[C_{17}H_{16}ClN_2Ru]\ PF_6$ (**3**)

4.6 Spectral studies

This involved the UV/Vis and IR spectroscopy

4.6.1 UV/VIS spectral data

Electronic spectra of bipyridine and Schiff base ligands (**L1-L4**) was carried out in acetonitrile. They display bands of medium intensity at 317–344 nm and high intensity at

237–311 nm, as observed in Figure 4.4. The bands of medium and high intensity are assigned to the ligand centered π–π* and n–π* non -bonding electrons from the nitrogen. Transitions which are responsible for the colour of the complexes, respectively, are in agreement with observations on complexes with similar N,N′ bidentate ligands(Gichumbi *et al.*, 2017b). But they shift to low energy on coordination to the metal ion (Mc Crudden, 2008). The bands at 226 nm for *p*-Schiff base are an indication of intraligand transitions of π - π* character due to the presence of C=N chromophore. The bands appearing in the range of 220-280 nm associated with the characteristic of compounds containing aromatic structures has been reported (Sun *et al.*, 2016). In the literature the uncoordinated protonated bipyridine has been reported to signal intense absorption bands at 232 and 279 nm (Mc Crudden, 2008). Bands appearing between 322 nm can presumably be assigned to charge transfer transitions of n - π*. In general, the absorption maximum of Schiff base ligands is generally not sensitive to the length of polymethylene chain (Lutta and Kagwanja, 2000). The electronic spectra of *p*-Schiff base ligand and bipyridine ligands are summarized in Table 4.3.

When substitution occurs, the MLCT is shifted to a higher energy for all complexes as observed in Figure 4.5. This may be explained by the fact that the chlorine ligand through π bonding with the metal results in some back-bonding from metal to ligand. These π interactions have the effect of raising the energy levels of the metal dπ orbitals which reduces the separation between the highest occupied metal orbital (HOMO) of the metal and the lowest unoccupied molecular orbital (LUMO) of the ligand (Mc Crudden, 2008).

The bands at around 400 nm may be assigned to a metal–ligand charge-transfer transition (MLCT) (dπ–π* bands), as a result of the low-spin d^6 configuration of the Ru(II)complexes, which provide filled orbitals with correct symmetry that interact with the low-lying π* orbitals of the ligand. This data compare well with literature values for metal to ligand charge transfer of the ruthenium complex which occur at 389,467 and 561 nm for metal to ligand transfers in the visible region (Gichumbi *et al.*, 2016d) . Electronic spectra of the complex **4** Figure 4.7 obtained in acetonitrile showed absorption bands at 257 nm and 316 nm in the complexes. Some broad band was observed at 428 nm of low intensity was observed at Figure 4.6,which could be attributed to MLCT transition from the filled 4d orbital of the

metal to the empty π^* orbital of the ligand. These bands were not observed in the ligands thus confirming formation of complex **4**. This is in agreement with observation by other workers (Gichumbi *et al.*, 2016d).

Table 4.3: Electronic data for ligands and synthesized complexes

	λ (nm)	Absorbance	Transitions
5,5'-dimethyl-2,2'-bipyridine (**L1**)	244	0.7347	$\pi \rightarrow \pi*$
	288	0.9563	$\pi \rightarrow \pi*$
4,4'-di-*tert*-butyl-2,2'-bipyridine (**L2**)	240	0.8808	$\pi \rightarrow \pi*$
	286	0.9987	$\pi \rightarrow \pi*$
2,2'-bipyridine (**L3**)	238	0.5666	$\pi \rightarrow \pi*$
	283	0.7567	$\pi \rightarrow \pi*$
4-Fluoro-N-(2-pyridylmethylene)-aniline (**L4**)	226	0.5476	$\pi \rightarrow \pi*$
	281	0.6325	$\pi \rightarrow \pi*$
	315	0.4188	$n \rightarrow \pi*$
[$C_{19}H_{20}ClN_2Ru$] PF_6 (**1**)	237	0.6803	$\pi \rightarrow \pi*$
	263	0.7169	$\pi \rightarrow \pi*$
	359	0.201	$n \rightarrow \pi*$
	416	0.0333	MLCT
[$C_{25}H_{32}ClN_2Ru$] PF_6 (**2**)	290	0.7582	$\pi \rightarrow \pi*$
	348	0.6006	$n \rightarrow \pi*$
	410	0.0559	MLCT
[$C_{17}H_{16}ClN_2Ru$] PF_6 (**3**)	237	0.9599	$\pi \rightarrow \pi*$
	311	0.9217	$n \rightarrow \pi*$
	344	0.2365	$n \rightarrow \pi*$,
	416	0.0862	MLCT
[$C_{19}H_{17}ClN_2RuF$] PF_6 (**4**)	257	0.3008	$\pi \rightarrow \pi*$
	316	0.2919	$n \rightarrow \pi*$
	428	0.0938	MLCT

Replacement of chlorine with the ligand causes a bathochromic shift (red shift) of approximately 100 nm for complex all complexes as shown in Table 4.3 above.

Figure 4.4 shows the electronic spectra of precursor complex before complexation occurs.

Replacement of chlorine with the ligand causes a bathochromic shift (red shift) of approximately 100 nm for complex all complexes as shown in Table 4.3 above.

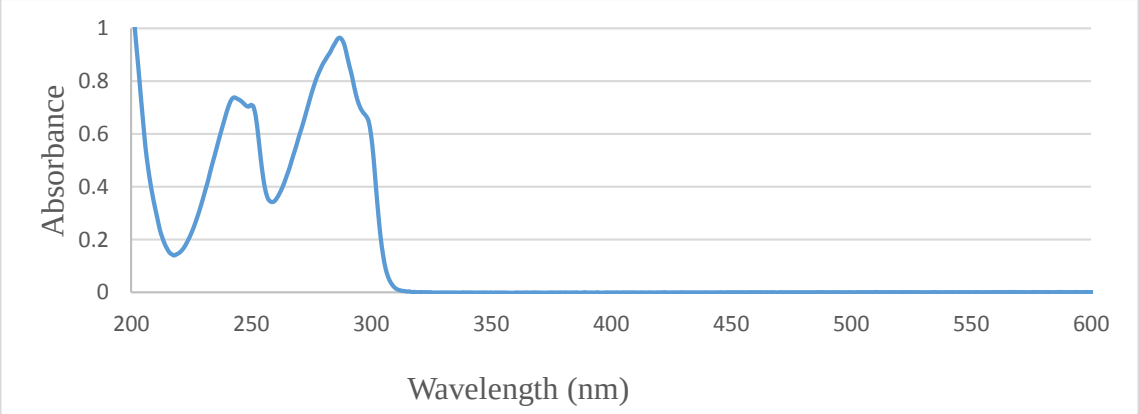

Figure 4.4: Electronic spectra of 5,5'-dimethyl-2,2'-bipyridine **(L1)**

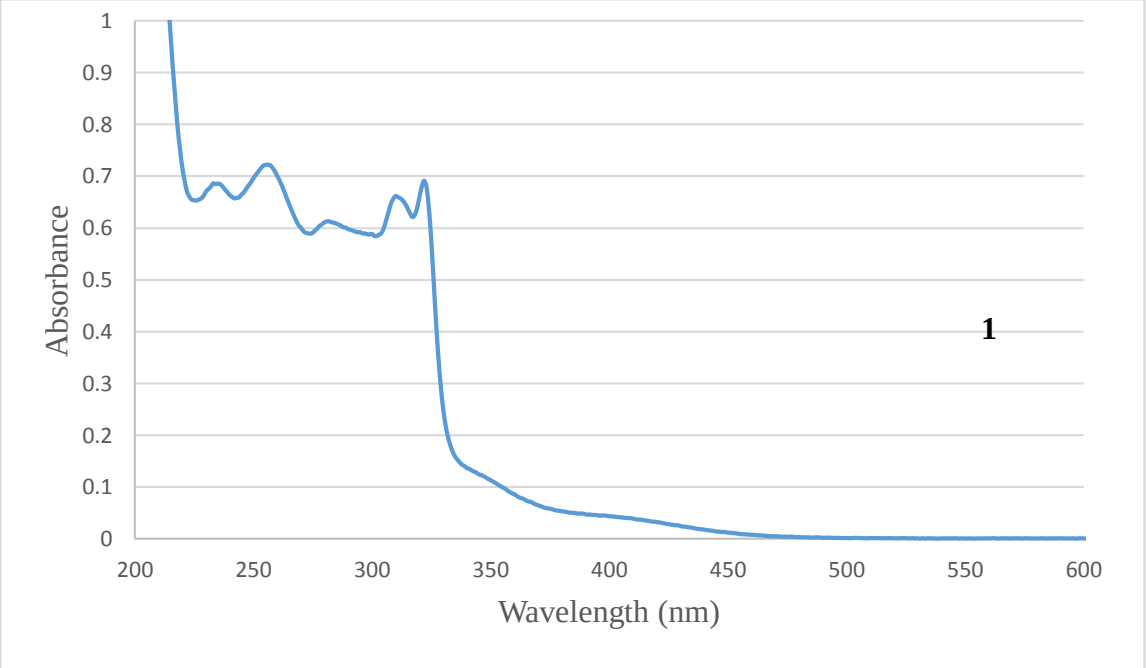

Figure 4.5: Electronic spectra of $[C_{19}H_{20}ClN_2Ru]\ PF_6$ **(1)**

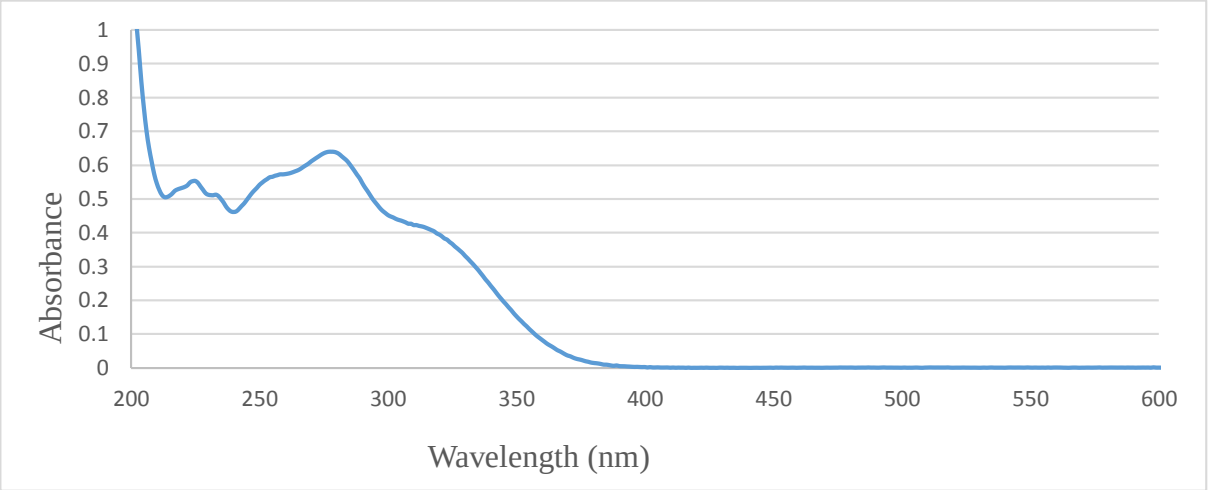

Figure 4.6: Electronic spectra of [$C_{12}H_9N_2F$] (**L4**)

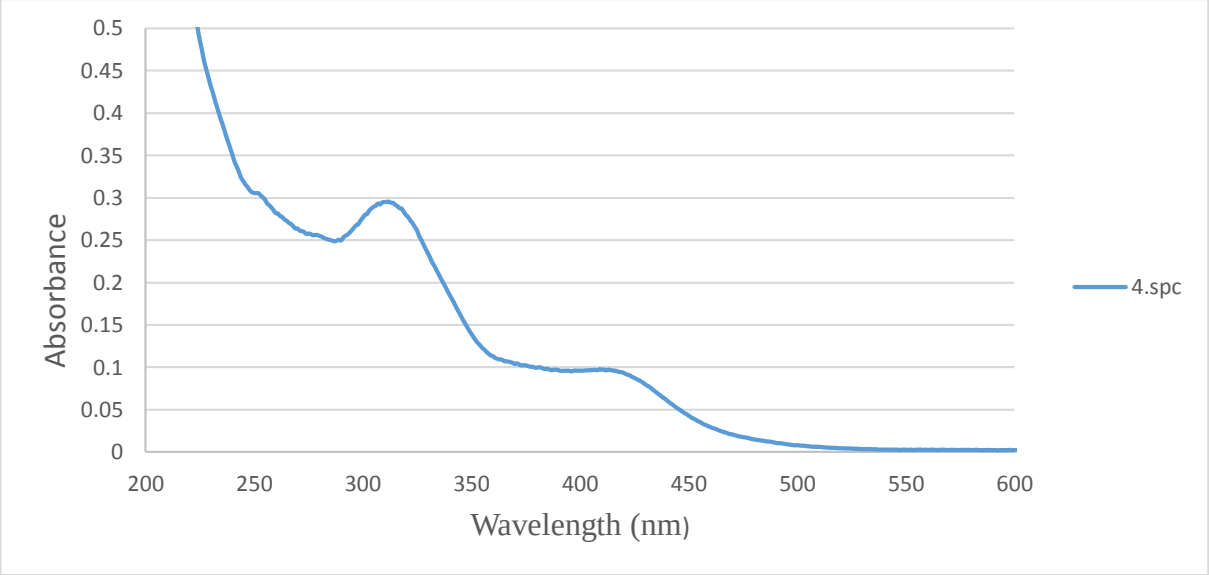

Figure 4.7: Electronic Spectra of [$C_{19}H_{17}ClN_2RuF$] PF_6 (**4**)

4.7 Infra-red Spectral studies

The infrared absorption spectra of the ligands (**L1-L3**) and their complexes [(η^6-$C_6H_5CH_3$)RuCl(N,N)]PF_6 show common characteristic features of a series of weak-to-moderate absorptions bands in the 3,150–3,009 cm^{-1} region, which are assigned to aromatic C–H stretch in the complexes. The vibrational bands at 2,927 and 2,938 cm^{-1} in ligand 2 and 3, respectively, show the presence of the aliphatic C–H stretching bonds of the methyl, methylene and/or the methine groups in the compounds (Adeloye *et al.*, 2012) there is a slight shift of the υ C-H_{str} of the ligands to higher frequency (~ 10-15 cm^{-1}) after complexation and this may be attributed to the spatial arrangement and/or substitution pattern of the alkyl groups in the [(η^6-$C_6H_5CH_3$)RuCl(N,N)]PF_6 complexes. The spectra of complexes **1-3** show absorption bands in the range of 1618 cm^{-1} to 1608 cm^{-1}, due to the symmetrical vibration of the C=N bond in the complexes, which shifted to lower wavenumbers than the equivalent band of the uncoordinated pyridine-imine ligands (1626–1600 cm^{-1}), indicating complex formation. The C=N in the N,N-donor bidentate ligands are observed in the 1592 cm^{-1} to 1527 cm^{-1} region. A Strong absorption band observed in the spectra for complex **1** at 821 cm^{-1} which is also present in the ligands although shifted to a lower frequency implies it is from the ligand. Strong absorption bands at 555 cm^{-1} observed for all complexes are attributed to the stretching frequency (P–F) of the PF_6 counter ion. Spectrum of bipyridine ligand (**L1**) and [(η^6-$C_6H_5CH_3$)RuCl(N,N)]PF_6 complex (**1**) are shown in Figure 4.8 and 4.9 respectively.

The IR spectrum of complex **4** shows an absorption band at 1617 cm^{-1} depicted in Figure 4.11, which can be assigned to the C=N stretching vibration. The position of the *v* (C=N) band shifted to lower wavenumbers (1617 cm^{-1}) in comparison to that of the free pyridine-imine ligand Figure 4.10

(1626 cm^{-1}). This is an indication that the ligand is coordinated to the arene moiety. This is consistent with the increase in the electron density on the ruthenium(II) centre caused by the coordination of the C=N- group, which resulted in increasing the back bonding to the nitrogen and hence a lower *v*(C=N) stretching vibration. Another strong peak in the region

555 cm^{-1} attributable to the PF_6 counter ion is also evident and is in agreement with other authors observations (Adeloye *et al.*, 2012).

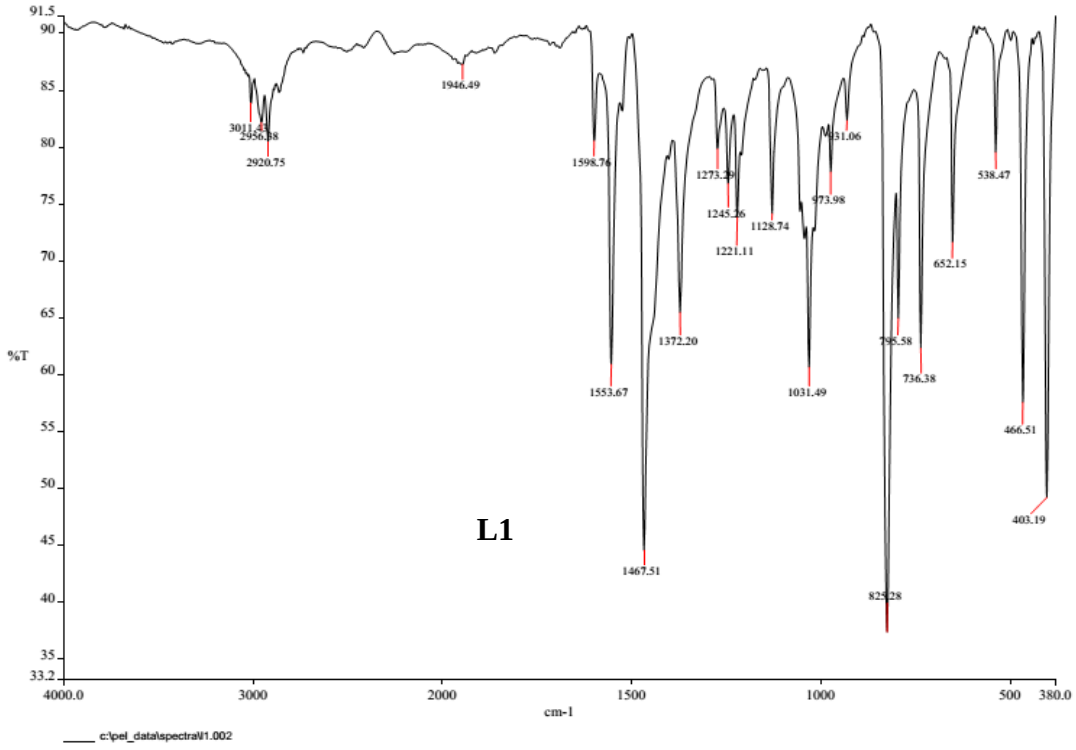

Figure 4.8: IR Spectra of $C_{12}H_{12}N_2$ (**L1**)

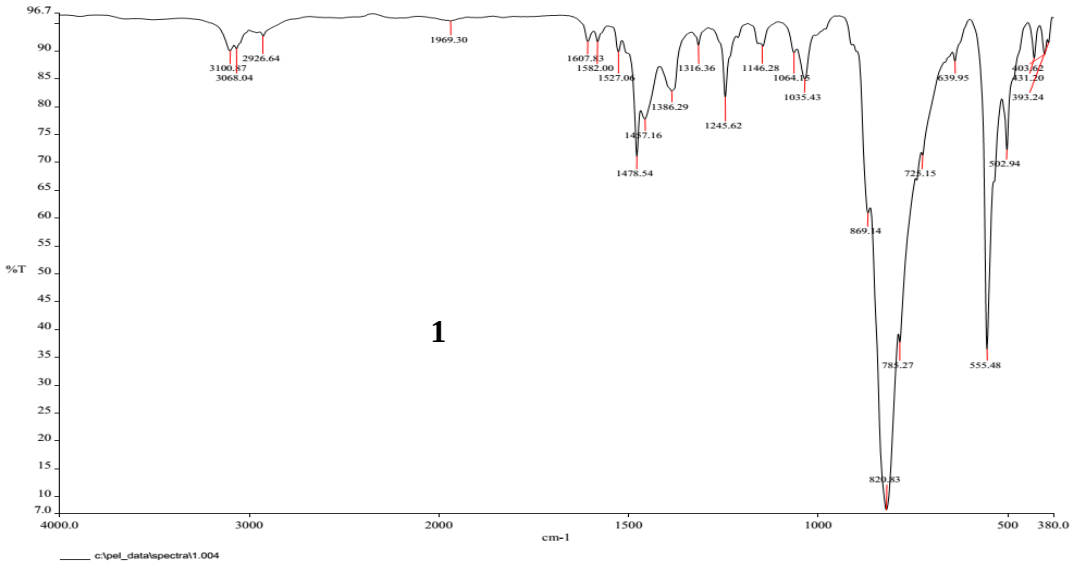

Figure 4.9: IR Spectra of $[C_{19}H_{20}ClN_2Ru]\ PF_6$ (**1**)

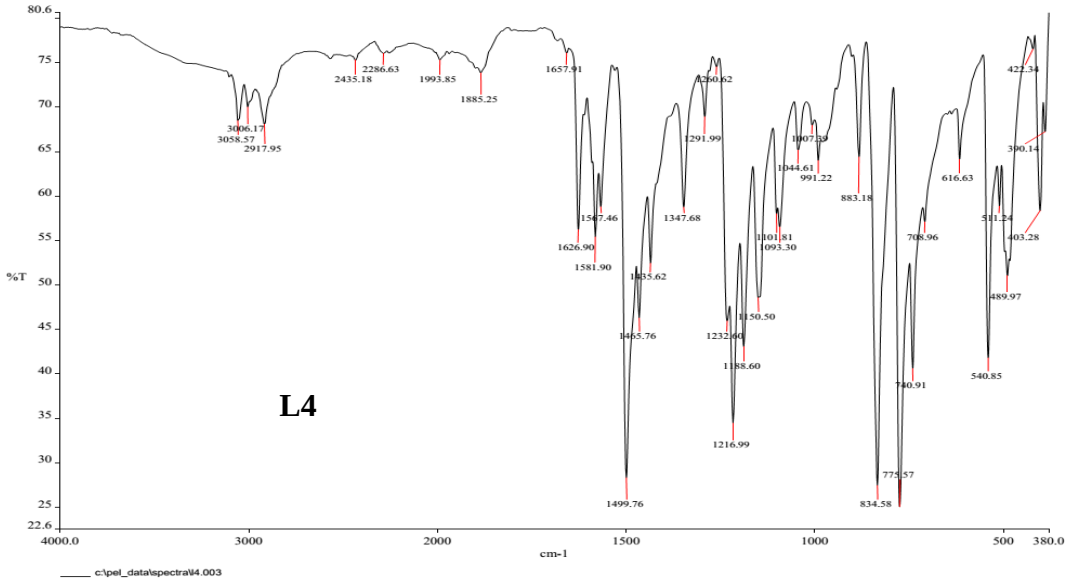

Figure 4.10: Infrared spectra of ligand $[C_{12}H_9N_2F]$ (**L4**)

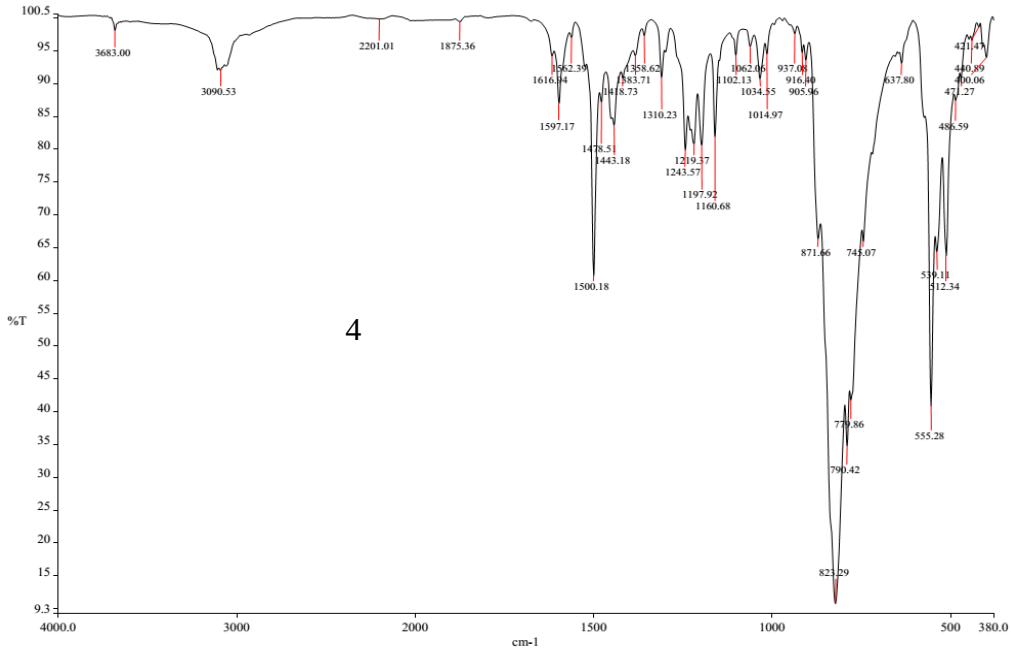

Figure 4.11: Infrared spectra of complex **4** $[C_{19}H_{17}ClN_2RuF]$ PF_6 in KBr

Selected C=C and C=N stretches of synthesized complexes (**1-4**) and ligands **L1-L4** are summarized in Table 4.4 below.

Table 4.4: IR Spectral data for ruthenium complexes and ligands

COMPOUND/	*v* (C=C) (cm^{-1})	*v* (C=N) (cm^{-1})
L 1	1553	1599
	1598	
L 2	1545	1583
	1582	
L 3	1568	1578
	1578	
L 4	1500	1627
	1567	
	1582	
1	1527	1608
	1582	
2	1524	1619
	1546	
3	1500	1608
	1527	
4	1500	1617
	1567	
	1597	

4.8 NMR spectroscopic analysis

Nuclear magnetic resonance (NMR) spectroscopy was used to elucidate the structure and confirm the purity of the synthesized compounds. The technique is especially useful for establishing the splitting pattern for the highly symmetrical 2, 2' bipyridine ligand in solution, their substituents and their ruthenium complexes.

4.8.1 ^{1}H NMR

^{1}H NMR was elucidated for the bipyridine ligands (**L1-L3**) and the pyridine-Imine Schiff base (L4) and their ruthenium complexes (**1-3**).

The^{1}H NMR data of ligand (**L1**) in deuterated DMSO showed four resonance signals, it exhibited a characteristic singlet peak at 2.34 ppm with an integral value of 6 assignable to 6H of the two identical methyl substituent groups, a doublet of doublet(dd) at 7.71 ppm with an integral value of 2 assignable to 2H (H_3,H_3'), doublet at 8.21 ppm with an integral value of 2, assignable to 2H (H_2,H_2') and doublet at 8.48 ppm with an integral value of 2, assignable to 2H (H_1,H_1'). The ^{1}H NMR of complex **1** shows eight resonance signals, a singlet at 9.37 ppm with an integral value of 2 is assignable to 2H (H_1'H_1'), a doublet at 8.44 ppm with an integral value of 2, assignable to 2H (H_3,H_3'), a doublet at 8.07 ppm with an integral value of 2, assignable to 2H (H_2,H_2'), a doublet at 6.32 ppm with an integral value of 2, assignable to 2H of arene (Ar), a doublet at 5.94 ppm with an integral value of 2, assignable to 2H (Ar).

A singlet at 5.78 ppm with an integral value of 1, assignable to 1H (Ar), a singlet at 2.51 ppm with an integral value of 6, assignable to 6H from the two methyl groups in the pyridine ring and a singlet at 2.23 ppm with an integral value of 3, assignable to 3H from the methyl group in the arene . Resonance patterns in the ^{1}H NMR spectra of the complexes confirms formation of complexes because there is a shift downfield of arene based protons upon the complexation with ligands. For instance when complex **1** is formed from ligand (**L1**), the chemical shifts of the arene ligands shifts downfield by approximately 0.5 ppm as shown in Figure 4.12 above and 4.13 below.

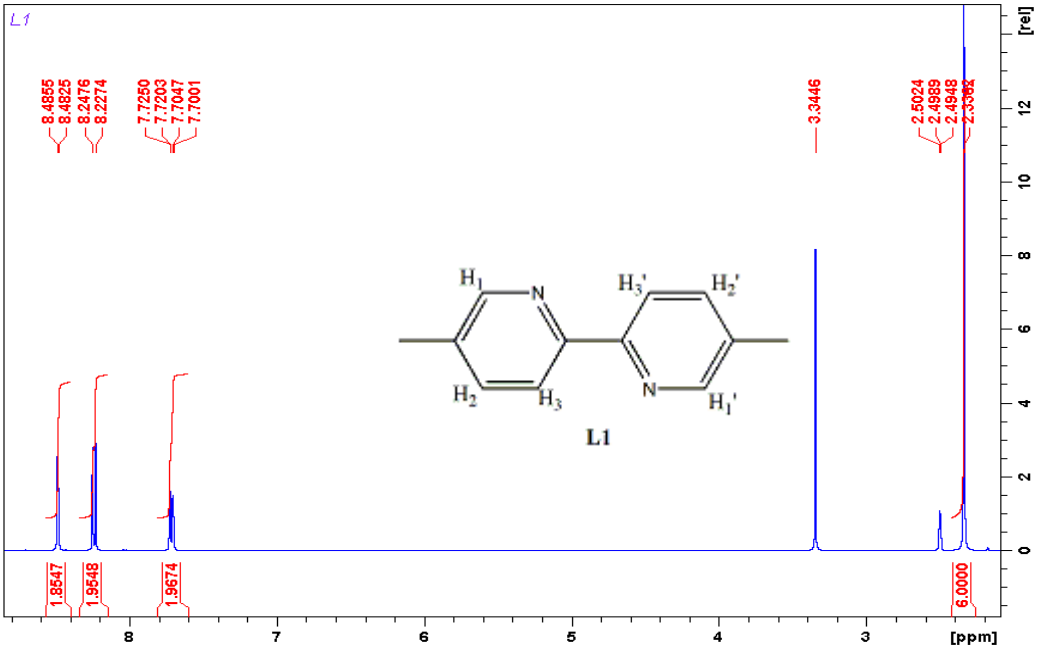

Figure 4.12: ^{1}H NMR of $C_{12}H_{12}N_2$ (**L1**)

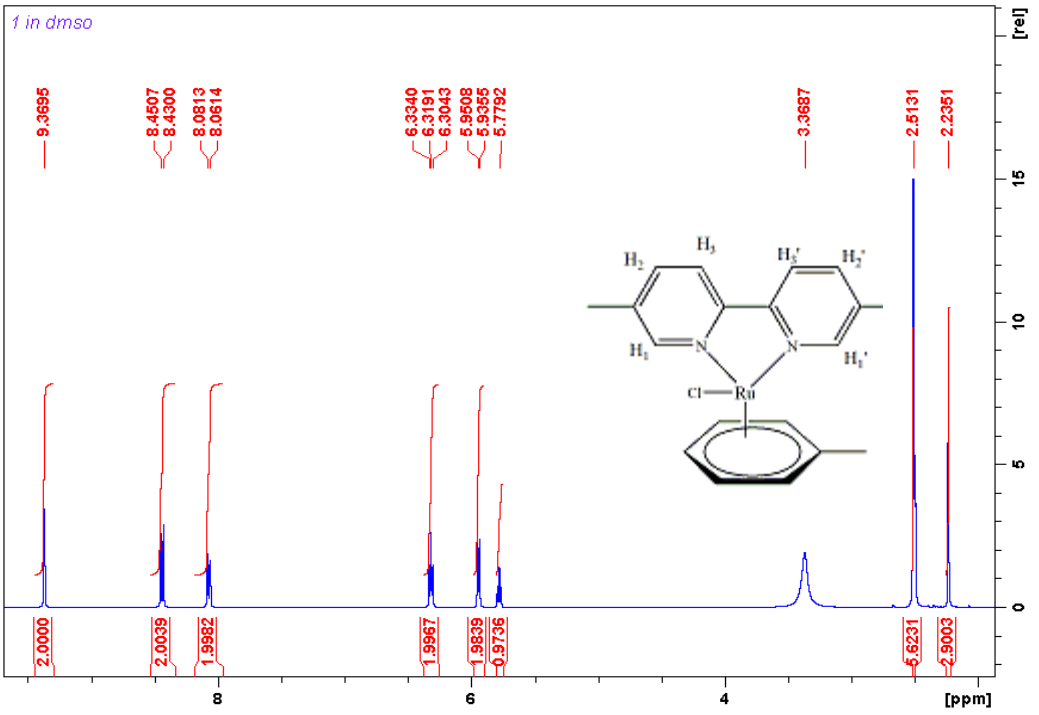

Figure 4.13: ^{1}H NMR of $[C_{19}H_{20}ClN_2Ru]$ PF_6 (**1**)

The ^{1}H NMR data of ligand (**L2**) shown in Figure 4.14 in deuterated DMSO showed four resonance signals, a doublet at 8.60 ppm with an integral value of 2 assignable to 2H (H_1,H_1'),a singlet at 8.39 ppm with an integral value of 2 assignable to 2H (H_3,$H_{3'}$),doublet of doublets at 7.47 ppm with an integral value of 2, assignable to 2H (H_2,H_2') and a singlet at 1.33 ppm with an integral value of 18, assignable to di-*tert*-butyl groups of the bipyridine. The ^{1}H NMR of complex **2** shows eight resonance signals , a doublet at 9.40 ppm with an integral value of 2 is assignable to 2H ($H_{1'}H_1$'),a doublet at 8.63 ppm with an integral value of 2, assignable to 2H (H_3,H_3'), a doublet of doublets at 7.70 ppm with an integral value of 2, assignable to 2H (H_2,H_2'), a doublet of doublets at 6.25 ppm with an integral value of 2, assignable to 2H of arene (Ar), a doublet at 5.92 ppm with an integral value of 2,assignable to 2H (Ar),a singlet at 5.78 ppm a with an integral value of 1,assignable to 1H (Ar),a singlet at 2.22 ppm with an integral value of 3,assignable to 3H from the methyl group in the arene and a singlet at 1.43 ppm a with an integral value of 18,assignable to 18H of the di-tert-butyl group in the bipyridine ring. Resonance patterns in the ^{1}H NMR spectra of ligand **L2** compared with the ^{1}H NMR spectra of the complex **2** shown in Figure 4.15 confirms complex formation because there is a shift downfield of arene based protons upon the complexation by approximately 0.5 ppm.

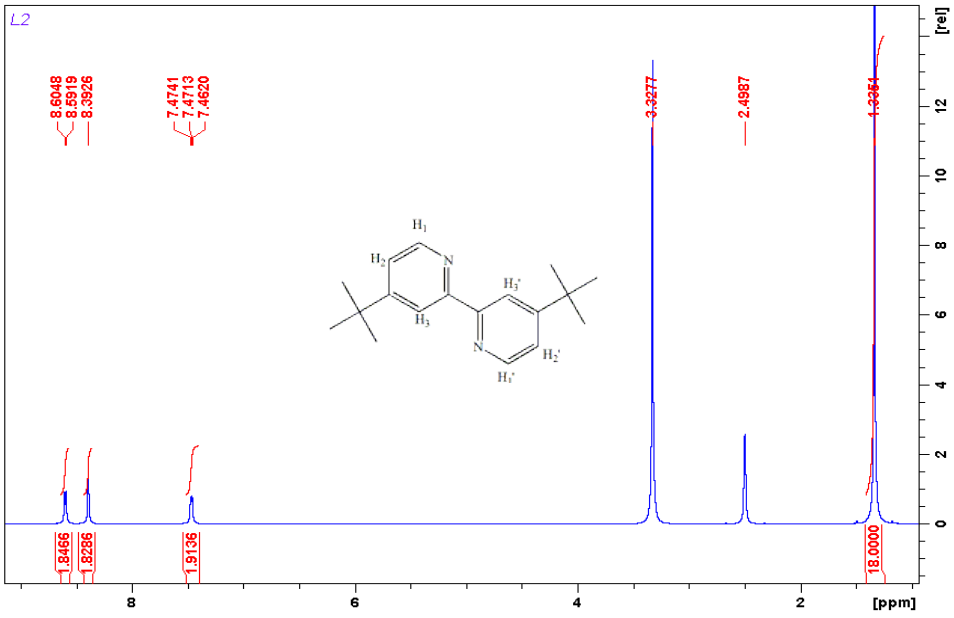

Figure 4.14: ^{1}H NMR of [$C_{18}H_{24}N_2$] (**L2**)

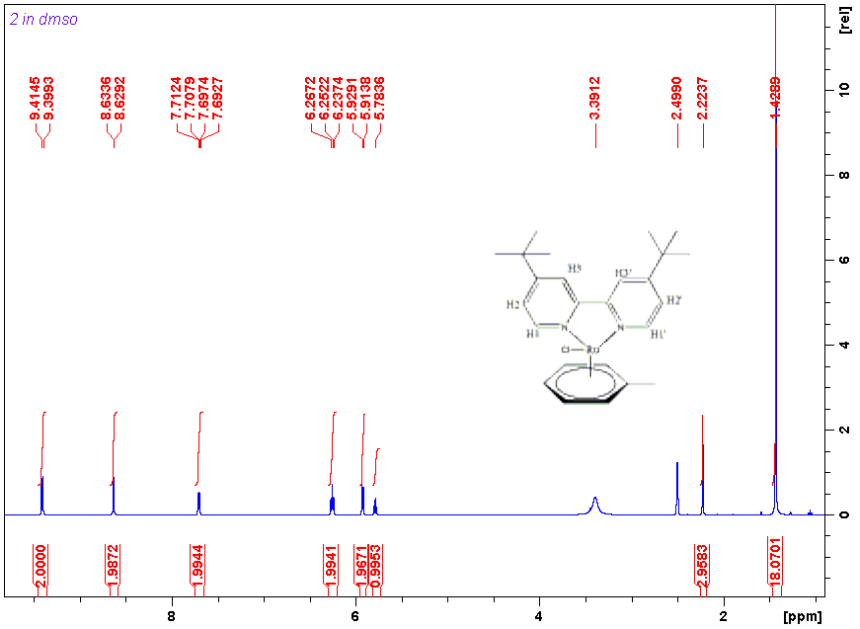

Figure 4.15: ^{1}H NMR of $[C_{25}H_{32}ClN_2Ru]$ PF_6 (**2**)

The^{1}H NMR data of ligand (**L3**) shown in Figure 4.16 in deuterated DMSO showed four resonance signals, a doublet at 8.67 ppm with an integral value of 2 assignable to 2H (H_1,H_1'),a doublet at 8.38 ppm with an integral value of 2 assignable to 2H (H_4,H_4'), doublet of doublets at 7.92 ppm with an integral value of 2, assignable to 2H (H_3,H_3') and doublet of doublets at 7.44 ppm with an integral value of 2, assignable to 2H (H_4,H_4'). The ^{1}H NMR of complex 3 formed from ligand **L3** shown in Figure 4.17 shows eight resonance signals , a doublet at 9.55 ppm with an integral value of 2 is assignable to 2H (H_1,H_1'),a doublet at 8.62 ppm with an integral value of 2, assignable to 2H (H_3,H_3'), a doublet at 8.27 ppm with an integral value of 2, assignable to 2H (H_2,H_2'),a singlet at 7.77 ppm with an integral value of 2 ,assignable to 2H (H_4,H_4'), a doublet of doublets at 6.30 ppm with an integral value of 2, assignable to 2H of arene (Ar), a doublet at 5.94 ppm with an integral value of 2,assignable to 2H (Ar),a singlet at 5.84 ppm a with an integral value of 1,assignable to 1H (Ar), a singlet at 2.23 ppm with an integral value of 3,assignable to 3H from the methyl group in the arene. Resonance patterns in the ^{1}H NMR spectra of ligand **L3** compared with the ^{1}H NMR spectra of the complex **3** shown in Figure 4.17confirms complex formation because there is a shift downfield of arene based protons upon the complexation by approximately 0.3 ppm.

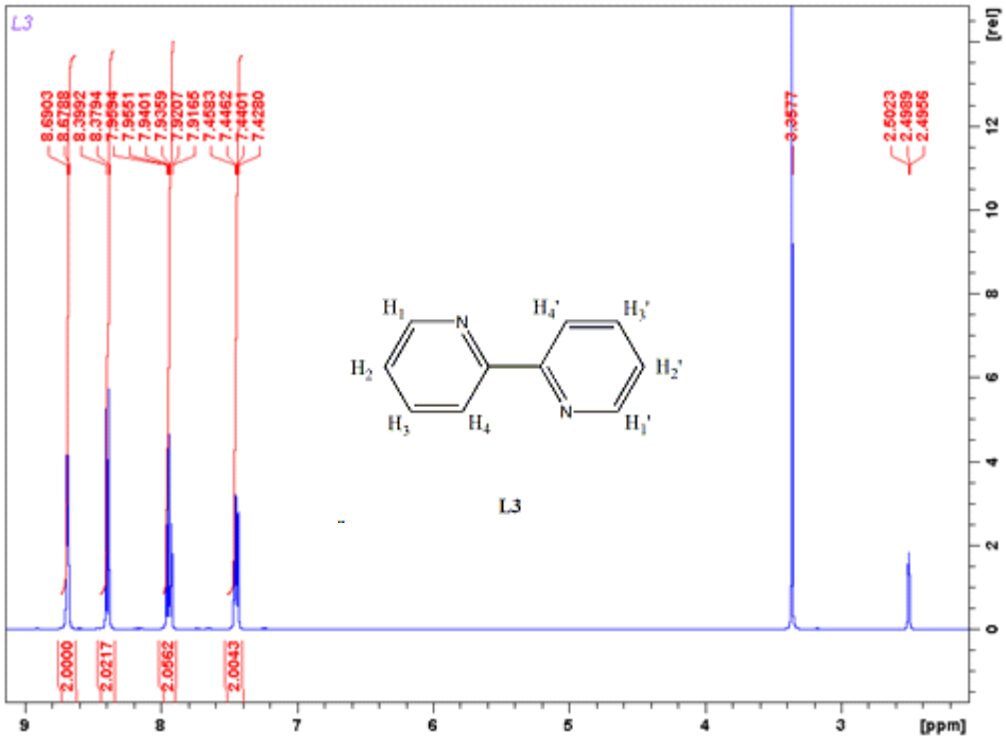

Figure 4.16: ^{1}H NMR of $[C_{10}H_8N_2]$ (**L3**)

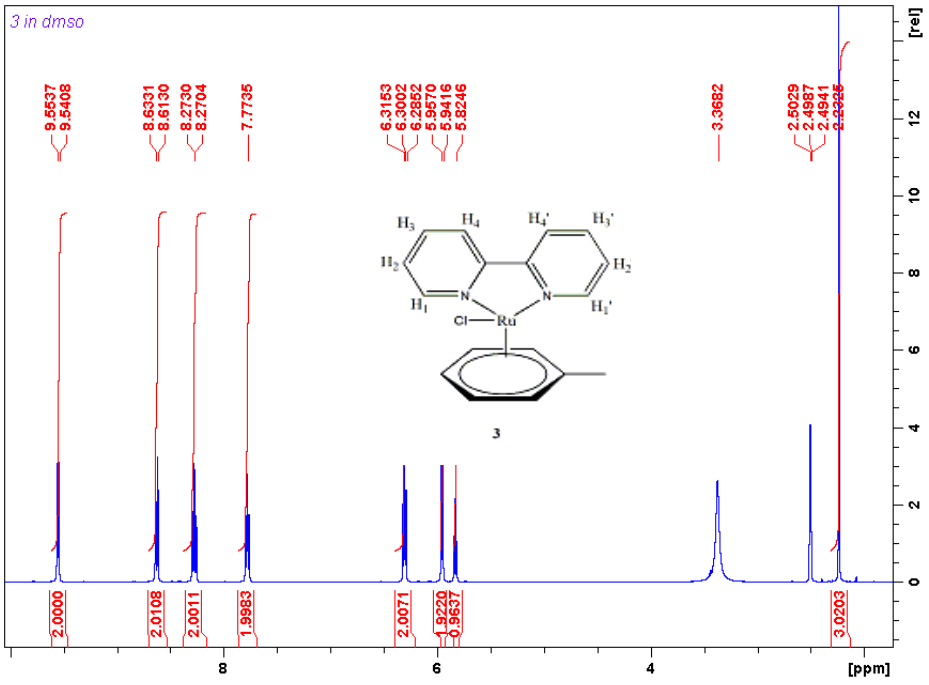

Figure 4.17: ^{1}H NMR of $[C_{17}H_{16}ClN_2Ru]$ PF_6 (**3**)

The ^{1}H NMR data of pyridine-imine Schiff base ligand **(L4)** shown in Figure 4.18, in DMSO-d_6 showed seven resonance signal peaks as follows, a doublet at 8.72 ppm with an integral value of 1 due to H_1, a doublet at 8.60 of integral value 1 assignable to H_4, a doublet of doublet at 7.97 ppm with an integral value of 1 assignable to H_3, doublet of doublets at 7.93 ppm with an integral value of 1 assignable to H_2, a singlet proton assignable to (H_5) at 7.50 ppm with an integral value of 1 due to azomethine proton (CH=N),doublet of doublets at 7.40 ppm with an integral value of 2 assignable to (H_6,H_6') ,doublet of doublets at 7.28 ppm with an integral value of 2 assignable to (H_7,H_7').The splitting pattern in this Schiff base is so complex because of lack of symmetry and the protons keeps splitting each other in multiple ways ,hence the reason this spectra not clear. The ^{1}H NMR of complex 4, Figure 4.19 showed nine resonance signals, a doublet at 9.55 ppm with an integral value of 1 assignable to H_1, singlet at 8.90 ppm assignable to H_5 with an integral value of 1 and is due to the azomethine proton, a doublet of doublet at 8.27 ppm with an integral value of 2.assignable to H_4.

Multiplet at 7.86 ppm with an integral value of 3 assignable to H_3, a doublet of doublets at 7.48 ppm with an integral value of 2 assignable to H_2, a doublet of doublets at 6.14 ppm with an integral value of 1, multiplet at 5.78 ppm with an integral value of 3, a doublet at 5.58 ppm with an integral value of 1 and a singlet at 2.12 ppm with an integral value of 3, assignable to the methyl group in the arene. Because of lack of symmetry there is a continuous overlap o splitting by various protons in this complex and hence the spectra is not clear. However resonance patterns in the ^{1}H NMR spectra of ligand **L4** compared with the ^{1}H NMR spectra of the complex **4** confirms formation of complex because there is a shift downfield of arene based protons upon the complexation by approximately 0.8 ppm.

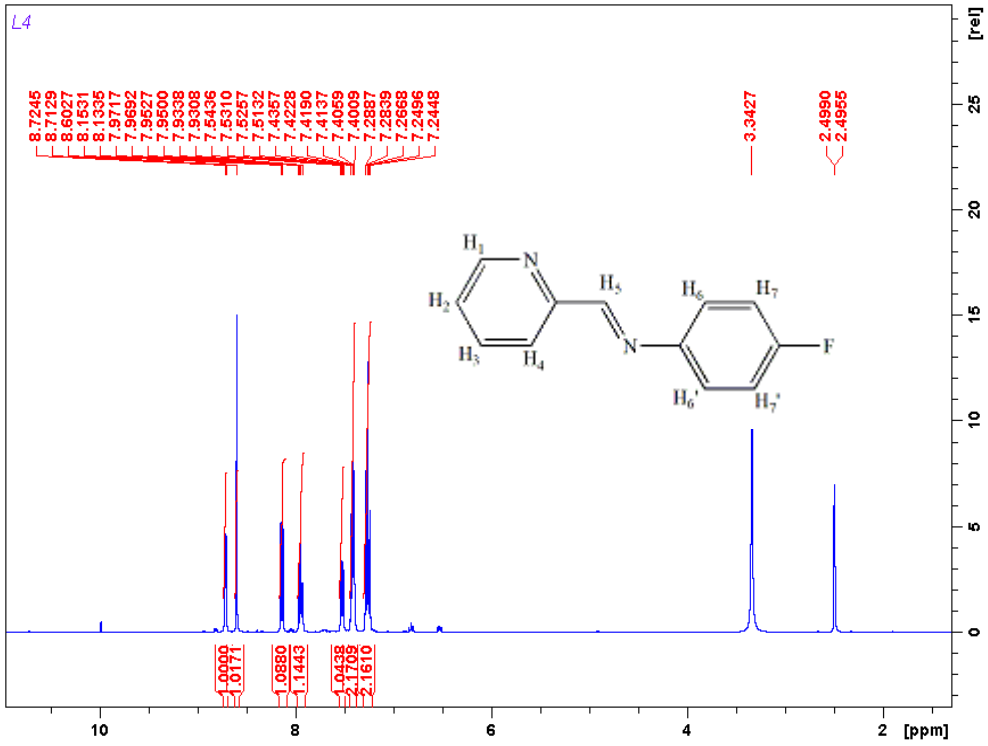

Figure 4.18: ^{1}H NMR of 4-fluoro-N-(2-pyridylmethylene)-aniline (**L4**)

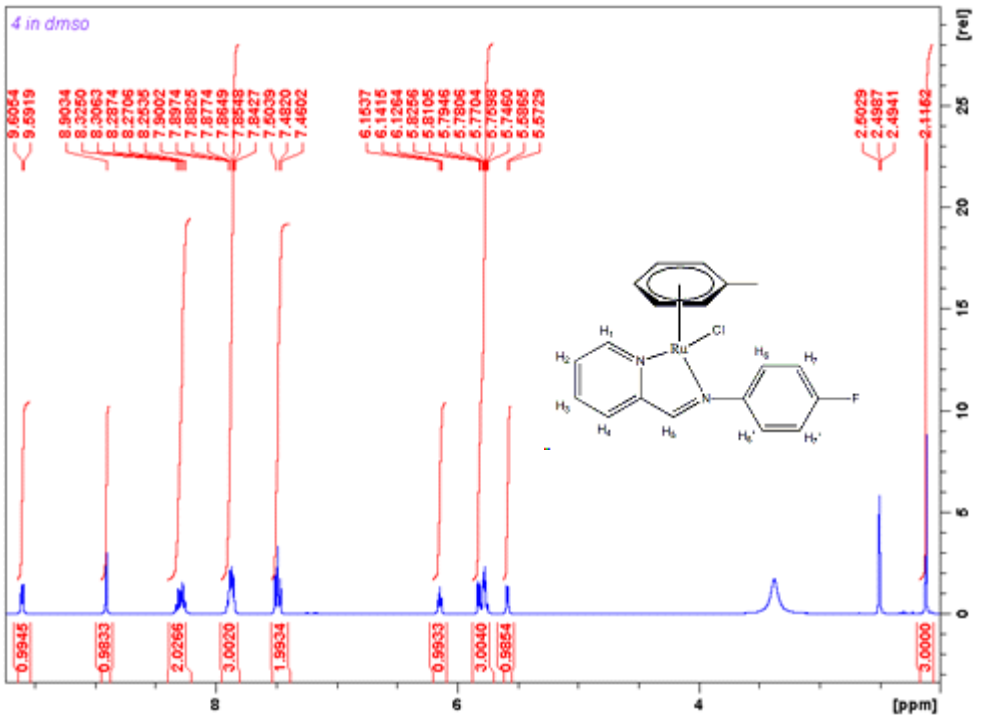

Figure 4.19:^{1}H NMR of $[C_{19}H_{17}ClN_2RuF]$ PF_6 (**4**)

4.8.2 ^{13}C NMR of $[C_{17}H_{16}ClN_2Ru]$ PF_6

Chemically equivalent carbons show a single signal. The ^{13}C NMR at 400 MHz in DMSO-d_6 was carried out for complex **3** whose structure is shown below Figure 4.20. It exhibits ten signal peaks.

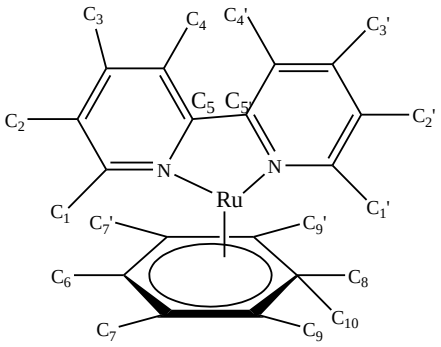

3

Figure 4.20: Chemical structure of $[C_{17}H_{16}ClN_2Ru]$ PF_6

The peaks are assignable to the arene ring carbon atoms in the complex were observed at 105.87, 90.53, 82.94, 79.73 and 18.75 ppm the methyl of the arene in the ^{13}C NMR spectra, respectively. The Carbon peaks for the bipyridine in the ruthenium complexes are shifted downfield than the peaks of the arene ring carbons. They are observed at 155.81, 154.53, 139.82, 127.35 and 123.65, as shown in Figure 4.21 below.

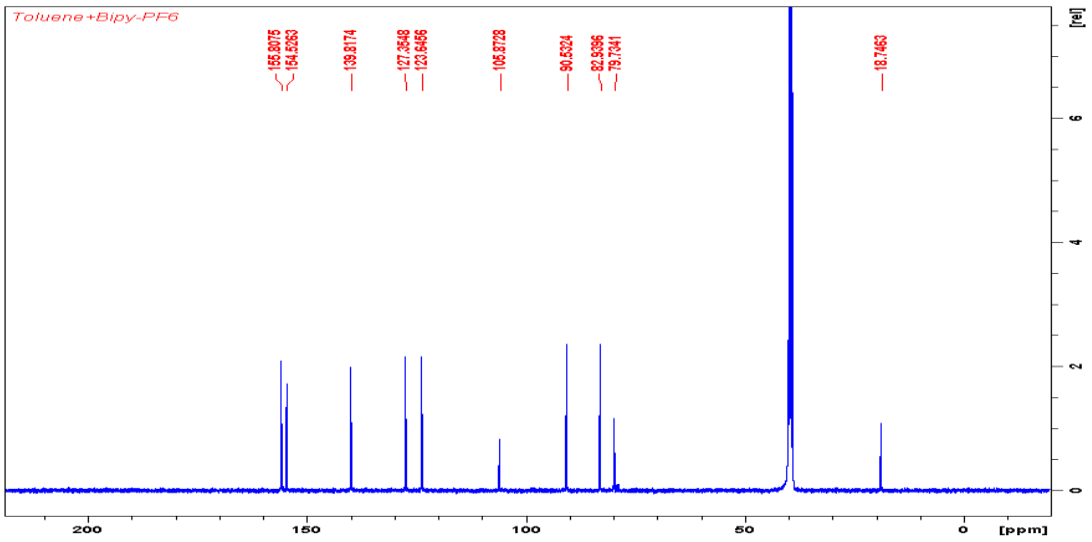

Figure 4.21: ^{13}C NMR for $[C_{17}H_{16}ClN_2Ru]$ PF_6

4.9 ^{31}P NMR spectroscopic analysis

The ^{31}P NMR of complex **1** Figure 4.22 was done to investigate the presence of PF_6 in the complex and it was observed to be present in the range of -131 to -151 ppm in agreement with the literature values for other hexafluorophosphate salts (Matsinha *et al.*, 2013; Gichumbi *et al.*, 2016b).

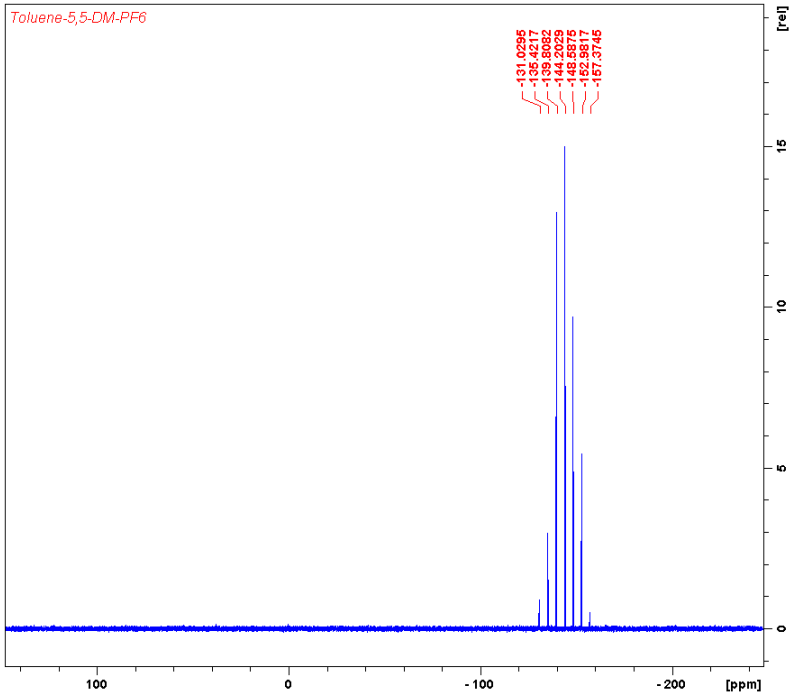

Figure 4.22: ^{31}P NMR spectra for $[C_{19}H_{20}ClN_2Ru]\ PF_6$

4.10 Electrochemical properties

The electrochemical properties of the synthesized complexes were investigated by cyclic voltammetry. Measurements were performed using BASi Epsilon E2 1177 model potentiostat, using a conventional three-electrode cell with platinum working electrode, platinum wire counter electrodes and a Ag/AgCl reference electrode using acetonitrile solvent. Scanning was done within the potential window of between – 2.0 to + 2.0 V. Sample solutions of 1 x 10^{-3} mol dm^{-3}were used while 0.06 M of [*n*-Bu_4N][PF_6] was used as the supporting electrolyte. Ferrocene was used as an internal standard even though potentials were recorded versus Ag/AgCl as reference electrode. Measurements were made at scan

rates of 200 mV/s, with a current range of 10 mA and 40 μA. Analysis was done under nitrogen blanket.

4.11 Cyclic voltammetry of $[(\eta^6\text{-}C_6H_5CH_3)RuCl(N,N]PF_6$

The cyclic voltammogram of complex **1** was scanned from 0.0 to + 1.0 V. Figure 4.23 shows cyclic voltammogram recorded at a platinum working electrode in acetonitrile solution $[(C_{19}H_{20}ClN_2Ru]\ PF_6$ at scan rate 200 mV/s . An anodic process, $Ru(II) \rightarrow Ru(III) + e^-$ occurs at +0.63 V and cathodic process $Ru(III) + e^- \rightarrow Ru(II)$ occurs at 0.54 V . Reversing the direction of the scan at + 1.0 V gives rise to a reversible peak + 0.587 V, [1/2(0.54 + 0.0.63)]. The peak potential separation between anodic and cathodic peaks ΔE being equal to 90 mV suggesting that the oxidation process of the Ru(II) centre in the complexes occur reversibly. The anodic and cathodic peak potentials observed are summarized in Table 4.5 below. Taking complex **1** as a typical example, the anodic current peak is 1.4234 μA and cathodic peak current is 1.0517 μA, the current ratio i_p^a/i_p^c equals to 1 confirming reversibility.

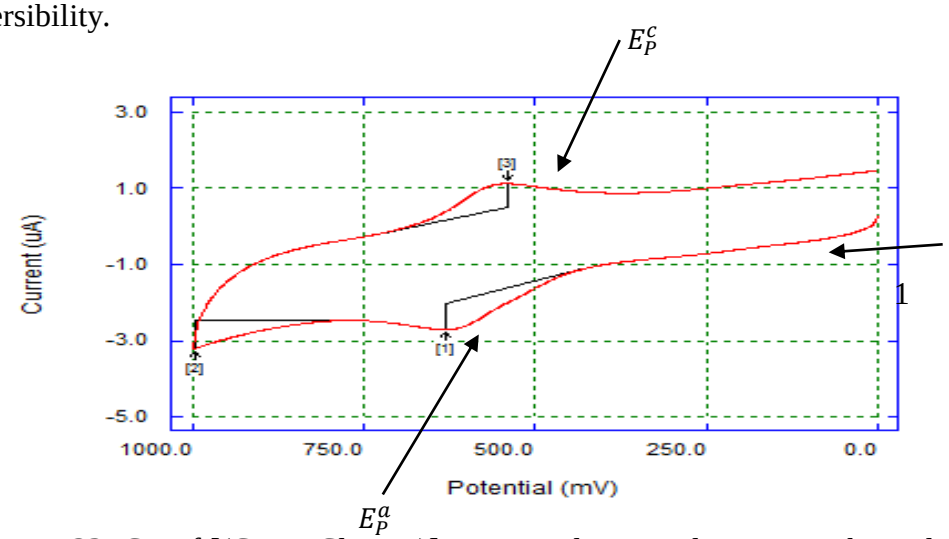

Figure 4.23: CV of $[(C_{19}H_{20}ClN_2Ru)]\ PF_6$ complex **1** at platinum working electrode in acetonitrile at a scan rate of 200 mV/s.

The Cyclic voltammogram of complex **2** was scanned from -0.5 to + 1.5 V. Figure 4.24 shows cyclic voltammogram recorded at a platinum working electrode in acetonitrile solution $[(C_{25}H_{32}ClN_2Ru]\ PF_6$ at scan rate 200 mV/s. Reversing the direction of the scan at + 1.5 V gives rise to an irreversible peak centered at 1.108 V and a reversible oxidation peak

at + 0.424 V, [1/2(0.471 + 0.376)] indicating that the ruthenium(II) centered complex oxidizes as Ru(II) → Ru(III) + e^- at + 0.424 V Vs Ag/Agcl. The irreversible oxidation peak at 1.108 V may be attributed to either Ru^{III} → Ru^{IV} oxidation or the oxidation process of the coordinated bipyridine ligands. Since the observed potential difference between the two observed successive oxidation processes (Ru^{II}/Ru^{III} and second irreversible oxidation process) in the complexes compares well with the reported Ru^{II}/Ru^{III}-Ru^{III}/Ru^{IV} potential in many ruthenium mononuclear complexes (Bhattacharyya *et al.*, 1999).

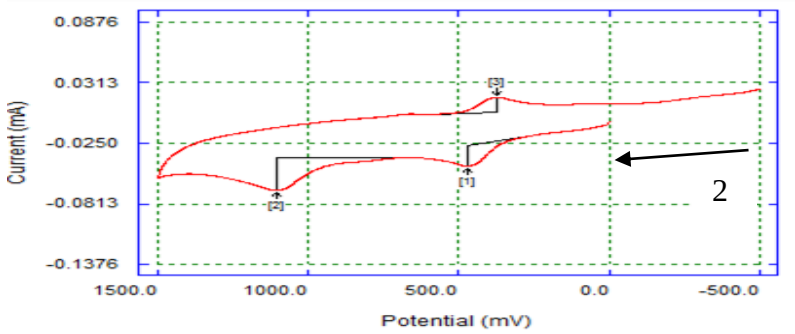

Figure 4.24: CV of [($C_{25}H_{32}ClN_2Ru$)] PF_6 complex **2** at platinum working electrode in acetonitrile at a scan rate of 200 mV/s

The Cyclic voltammogram of complex **3**, Figure 4.25 shows cyclic voltammogram recorded at a platinum working electrode in acetonitrile solution [($C_{17}H_{16}ClN_2Ru$] PF_6 and scan rate 200 mV/s . Reversing the direction of the scan at + 1.3 V give rise to a reversible oxidation peak at + 0.584 V, [1/2(0.642 + 0.525)] indicating that the ruthenium(II) centered complex oxidizes as Ru(II) → Ru(III) + e^- at + 0.584 V vs Ag/Agcl. The peak potential separation (ΔE) between cathodic and anodic peaks ΔE being equal to 125 mV suggests that the oxidation process of the Ru(II) centre in the complexes occur reversibly. The Cyclic voltammogram of complex **4** was scanned from – 0.5 V to + 1.5 V. Figure 4.26 shows cyclic voltammogram recorded at a platinum working electrode in acetonitrile solution [($C_{19}H_{17}ClN_2Ru$] PF_6 at scan rate 200 mV/s. Reversing the direction of the scan at + 1.5 V gives rise to an irreversible peak centered at 1.139 V and a reversible oxidation peak at + 0.513 V, [1/2(0.551 + 0.474)] indicating that the ruthenium(II) centered complex oxidizes as Ru(II) → Ru(III) + e^- at + 0.513 V, Vs Ag/Agcl. The irreversible oxidation peak at 1.139

V may be attributed to either Ru^{III} → Ru^{IV} oxidation or the oxidation process of the coordinated ligand. Since the observed potential difference between the two observed successive oxidation processes (Ru^{II}/Ru^{III} and second irreversible oxidation process) in the complexes compares well with the reported Ru^{II}/Ru^{III}-Ru^{III}/Ru^{IV} potential in many ruthenium mononuclear complexes (Bhattacharyya *et al.*, 1999).The peak potential separation between cathodic and anodic peaks ΔE was found to be 77 mV indicating a reversible reaction.The anodic peak current was 7.6997 μA and the cathodic peak current being 5.3437 μA gave a peak current ratio of approximately one confirming reversibility.

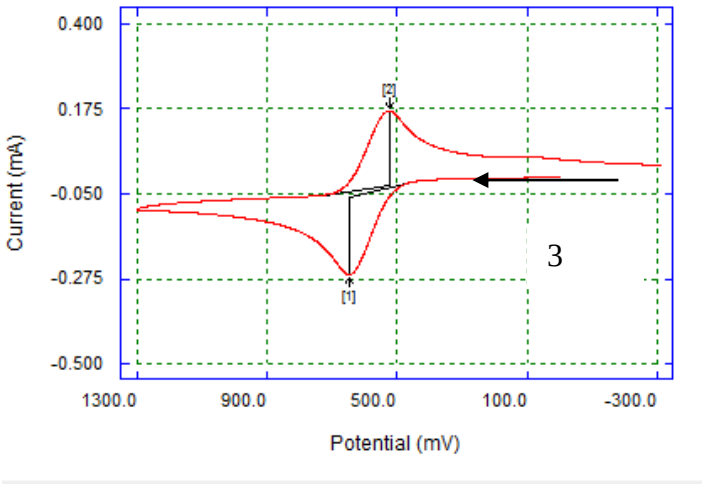

Figure 4.25: CV of $(C_{17}H_{16}ClN_2Ru]$ PF_6 complex **3** at platinum working electrode in acetonitrile at a scan rate of 200 mV/s

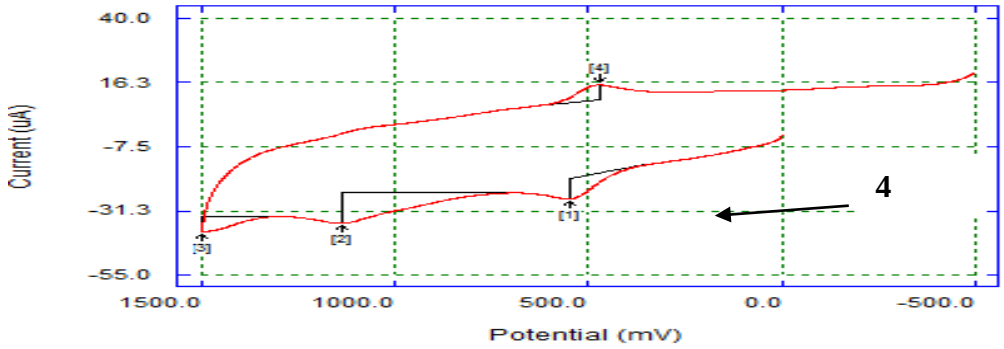

Figure 4.26: CV of $[(C_{19}H_{17}ClN_2RuF)]$ PF_6 complex **4** at platinum working electrode in acetonitrile at a scan rate of 200 mV/s

Table 4.5: Redox potentials for Ruthenium monometallic complexes in acetonitrile

COMPLEX	E_P^{ai} (Volts)	E_P^c (Volts)	E_P^{aii}(Volts)	$E_{1/2}$ (Volts)	Δ E (mV)
$[C_{19}H_{20}ClN_2Ru]\ PF_6$ (**1**)	0.54	0.63		0.587	90
$[C_{25}H_{32}ClN_2Ru]\ PF_6$ (**2**)	0.471	0.376	1.108	0.424	95
$[C_{17}H_{16}ClN_2Ru]\ PF_6$ (**3**)	0.642	0.525		0.584	125
$[C_{19}H_{17}ClN_2RuF]\ PF_6$ (**4**)	0.551	0.474	1.139	0.5125	77

Reduction potential (in volts) for the process $Ru^{3+} + e^- \rightarrow Ru^{2+}$ E^a= Anodic peak potential

Oxidation potential (in volts) for the process $Ru^{2+} \rightarrow Ru^{3+} + e^-$ E^c= cathodic peak potential

$$E_{1/2} = (E_{cathodic} + E_{anodic})/2$$

$$\Delta E = [\ E_{cathodic} - E_{anodic}] \text{ in mV}$$

The illustration in Figure 4.23,4.24 and 4.26 is the typical response for a one electron transfer of a ruthenium metal centre with a neutral ligand and an electronegative atoms indicating quasi-reversible oxidation (Mc Crudden, 2008).

The positive shift in redox potential resulting from substitution of the chloride by the bipyridine ligand is clearly demonstrated by comparison of the cyclic voltammograms in Figures 4.23, 4.24 and 4.26. Potential shifts due to ligand substitution have been attributed to effects of the electron density on the metal (Mc Crudden, 2008). Ligands such as chlorine which are strong σ donors result in lower oxidation potentials (Mc Crudden, 2008). For electron-withdrawing substituents, oxidation of the metal occurs at higher potentials and for electron-releasing substituents, it occurs at lower potentials (Thilagavathi *et al.*, 2010) (Mc Crudden, 2008). From the literature, cyclic voltammograms obtained from synthesized ruthenium complex displayed an irreversible oxidation wave corresponding to the Ru(II)/Ru(III) couple. This peak becomes less pronounced as scan rate is increased and

moves to 1.11V concurrently (Beckford *et al.*, 2016) (Moreno *et al.*, 2010). Another group synthesized ruthenium Schiff base tetradentate complexes and on studying cyclic voltammograms they found out that the observed oxidation state from ruthenium(III) to ruthenium(IV) was attributed to stability of coordinating ligands in the (Thilagavathi *et al.*, 2010).

4.12 Evaluation of antimicrobial activity by disc diffusion assay

The results of disc diffusion test indicated that the four synthesized complexes showed different inhibition growth, depending on bacterial strain and concentration of the test compound (Figure 4.27 to Figure 4.30). The numbers labelled on the test plates represent various concentrations into which the paper discs were soaked in 0.2 represents concentration of 0.2 mg/ml of solution and the disc at the centre of the plate is the positive control. Complexes **1-4** as well as their respective ligands were investigated for their antimicrobial activity against one Gram positive (*S. aureus*) and one Gram-negative (*E. coli*) bacteria. The activities of the complexes to inhibit these bacteria were compared to those of known antibacterial drug streptomycin (S-10).

4.13 Antibacterial activity of $[(\eta^6\text{-}C_6H_5CH_3)RuCl(C_{12}H_{12}N_2)]PF_6$

Complex **1** displayed in Figure 4.27 as well as its complexing ligand (**L1**) did not demonstrate any antimicrobial activity against both the Gram negative *E.coli* and Gram positive *S.aureus*, even at different concentrations.

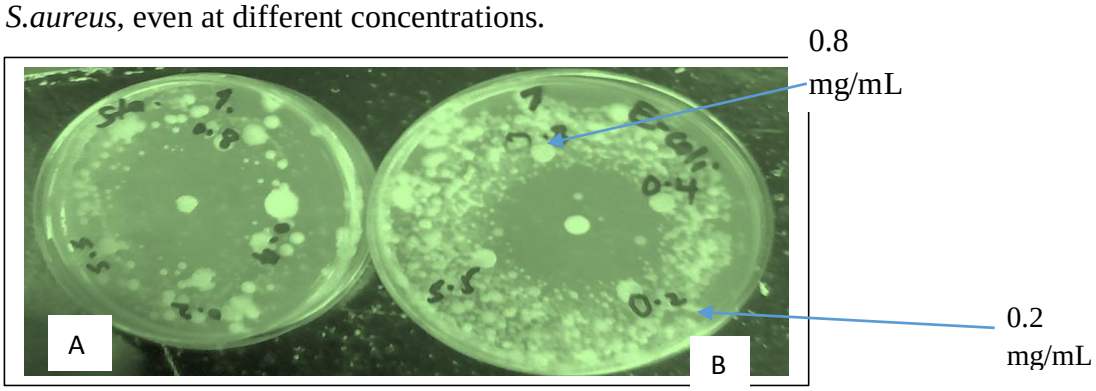

Figure 4.27: Complex; $[C_{19}H_{20}ClN_2Ru]\ PF_6$ (1)against (A) *S.aureus* and (B) *E.coli*

4.14 Antibacterial activity of $[(\eta^6\text{-}C_6H_5CH_3)RuCl(C_{18}H_{24}N_2)]PF_6$

Complex **2** was most effective against both the Gram-negative *E.coli* bacteria and Gram positive *S. aureus* following exposure to 0.2, 0.4 and 0.8 mg/L of synthesized complexes (**1-4**), dissolved in I mL DMSO. The highest activity of the complex was observed at the concentration of 0.2 mg/ml against *E.coli* ATCC 11775 which had a zone of inhibition of (30 mm), followed by concentration of 0.4 mg/ml. With *S. aureus* ATCC 12600, the highest activity was observed with zone of inhibition of (20 mm), at concentration of 0.2 mg/ml followed by concentration of 0.4 mg/ml with an inhibition zone of 16 mm as observed in Figure 4.28 the antibacterial activity of this test complex was also evident at low concentrations. However, the antibiotic Streptomycin (positive controls) was not more effective than the test complex with the diameter ranging 19 to 20 mm. The disc soaked with negative control DMSO did not show any activity. The activity of complex **2** is decreased with increased concentration. Its complexing ligand showed no activity.

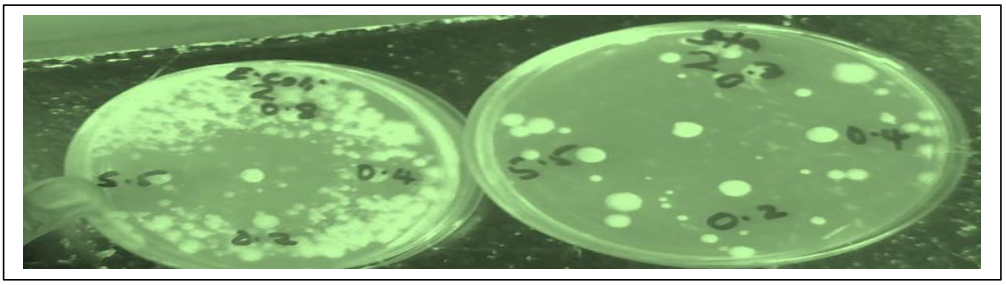

Figure 4.28: Antimicrobial plates $[C_{25}H_{32}ClN_2Ru]\ PF_6$ (**2**)

4.15 Antibacterial activity of $[(\eta^6\text{-}C_6H_5CH_3)RuCl(C_{10}H_8N_2)]PF_6$

Complex **3** Figure 4.29 did not show significant antibacterial activity against *S.aureus* even at high concentrations employed in this study. Maximum activity was observed at 0.4mg/mL against *E.coli*, much higher diameters of zones of inhibition of (27 mm) was observed. Summarized inhibition is recorded in Table 4.6. The inhibition of this complex was better than what is given by positive control Streptomycin S-10.

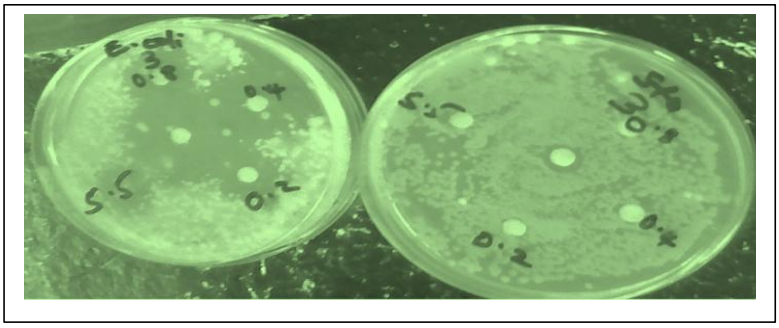

Figure 4.29: Antimicrobial plates $[C_{17}H_{16}ClN_2Ru]$ PF_6 (**3**)

4.16 Antibacterial activity of $[(\eta^6\text{-}C_6H_5CH_3)RuCl(C_5H_4N\text{-}2\text{-}CH{=}N\text{-}F)]PF_6$

The activity of Complex **4** shown in Figure 4.30 did not show significant antibacterial activity study against Gram positive *S. aureus*, even at high concentrations employed in this study. However activity was observed at all given concentrations equivalent to the activity of the positive control streptomycin S-10 with Gram negative *E. coli*.

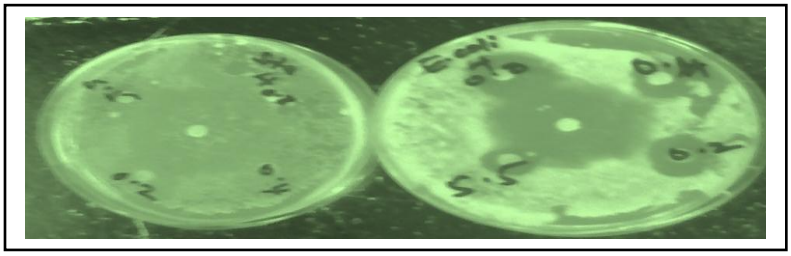

Figure 4.30: Antimicrobial plates $[C_{19}H_{17}ClN_2RuF]$ PF_6 (**4**)

The observed activity for this complex is shown Figure 4.30. Its complexing ligand is also active considering it is a Schiff base, with its activity better than the positive control streptomycin S-10. The activity of the complex was comparable to those reported for α,α′-diaminoalkane-bridged dicarbonyl(η5-cyclopentadienyl)ruthenium(II) complex salts, in their activity against resistant *E. faecalis* and methicillin-resistant *S. aureus* (Nyawade *et al.*, 2015a). The complexes reported in this study also show better activity than the ruthenium complexes with quinazoline and thiosemicarbazone ligands reported by Sathya and coworkers (Sathya *et al.*, 2009).and the ruthenium(III) complexes with bidentate N,N and N,O ligands reported by Govender and coworkers (Govender *et al.*, 2011).

Table 4.6: Antimicrobial Susceptibility tests results of ruthenium complexes with zones of inhibition to the nearest mm

	S.aureus			*E.coli*		
	ATCC 12600			ATCC 11775		
Compound						
Concentration (mg/mL)	0.2	0.4	0.8	0.2	0.4	0.8
5,5'-dimethyl-2,2'-bipyridine (**L1**)	0	0	0	0	0	0
	(R)	(R)	(R)	(R)	(R)	(R)
[$C_{19}H_{20}ClN_2Ru$] PF_6 (**1**)	0	0	0	0	0	0
	(R)	(R)	(R)	(R)	(R)	(R)
[$C_{25}H_{32}ClN_2Ru$] PF_6 (**2**)	20	16	0	30	25	20
	(S)	(S)	(R)	(S)	(S)	(S)
[$C_{17}H_{16}ClN_2Ru$] PF_6 (**3**)	0	0	0	20	27	18
	(R)	(R)	(R)	(S)	(S)	(S)
[$C_{19}H_{17}ClN_2RuF$] PF_6 (**4**)	0	0	0	20	20	20
	(R)	(R)	(R)	(S)	(S)	(S)
DMSO	0	0	0	0	0	0
	(R)	(R)	(R)	(R)	(R)	(R)
STREPTOMYCIN		24			19	
[10 µg/L]		(S)			(S)	

KEY:

R = Resistant $\leq$ **11**

S = Susceptible $\geq$ **15**

I = Intermediate **12-14**

CHAPTER FIVE

CONCLUSION AND RECOMMENDATION

The $[(\eta^6\text{-}C_6H_5CH_3)RuCl(N,N)]$ PF_6,$[(\eta^6C_6H_5CH_3)RuCl(C_5H_4N\text{-}2\text{-}CH{=}N\text{-}X]$ PF_6, mononuclear complexes (b) where N,N = 5,5'-dimethyl-2,2'-bipyridine , 4,4'-Di-*tert*-butyl-2,2'-bipyridine , 2,2'-bipyridine and X = *p*-fluorophenyl were successfully synthesized from the reactions of $[(\eta^6\text{-arene})Ru(\mu\text{-}Cl)Cl]_2$ dimers (where arene = $C_6H_5CH_3$) with the N,N-bidentate ligands. They were isolated and characterized using spectroscopic and analytical techniques.

The ligand **L1**-**L4** as well as their complexes **1– 4**, were investigated for their antimicrobial activity against selected Gram-positive and a Gram-negative bacteria. The observed activities indicates that an indication that a good number of the synthesized complexes are active. Of significance is complex **2** which is active against both *S.aureus* ATCC 12600 and *E. coli* ATCC 11775 whereas the complexes **2, 3, 4** are all active towards *E. coli* ATCC 11775 .Complex **1** is not active towards either of the bacterial strains.

5.1 Conclusion

The half-sandwich η^6-arene ruthenium(II) complexes containing fluoro substituted pyridine-imine Schiff base ligand complex **4**, was successfully synthesized and obtained in good yields (89 %). The coordination of the ligand towards the metal precursor occurred via the azomethine nitrogen of the lone pair present and the coordination behavior was determined using FTIR, UV/VIS, elemental analyses and ^{1}H NMR. The successful coordination of the neutral mononuclear Ru(II) complex were confirmed by a shift to a lower frequency of the C=N moiety absorption band to around 1616 cm^{-1} in the FTIR spectra. The coordination was further confirmed by the downfield shift of the azomethine proton signal to around 8.90 ppm in the ^{1}H NMR in comparison to the ligand signal at 8.60 ppm. The electrochemical properties was investigated and an irreversible oxidation peak was observed at 1.139 V and a reversible peak at 0.515 V indicating that the ruthenium(II) centered complex oxidizes as Ru(II) $\rightarrow$ Ru(III) + e^-. The irreversible oxidation peak at 1.139 V may be attributed to either $Ru^{III} \rightarrow Ru^{IV}$ oxidation or the oxidation process of the coordinated ligand. The half-sandwich η^6-arene ruthenium(II) complexes containing bipyridine substituted ligands,

complexes **1-3**, were successfully synthesized and obtained in good yields (89-90 %). The coordination of the ligand towards the metal precursor occurred via the nitrogen of the pyridine ring present and the coordination behavior was determined using FTIR, UV/VIS, elemental analyses and ^{1}H NMR. The successful coordination of the neutral mononuclear Ru(II) complex were confirmed by a shift to a higher frequency of the C=N moiety absorption band to around (1608-1619) cm^{-1} in the FTIR spectra in comparison to the bipyridine ligands absorption bands between (1578-1598) cm^{-1}. The coordination was further confirmed by the downfield shift of the arene based protons upon complexation by about 0.3-0.5 ppm. The electrochemical properties was investigated and an reversible oxidation peak was observed indicating that the ruthenium(II) centered complex oxidizes as Ru(II) $\rightarrow$ Ru(III) + e^{-}. Bioactivities evaluated against selected Gram negative *E-coli* ATCC 11775 and Gram positive *S aureus* ATCC 12600 with streptomycin S-10 as the positive control and Dimethyl sulfoxide as the negative control and most of the complexes were found to have good activities with some complexes showing even better activity than the positive control.

5.2 Recommendations

The synthesized complexes are stable and since they have shown activities in some bacterias further studies with different ligands complexed to the metal can be done to establish their mode of action.

The synthesized complexes can also be subjected to catalytic studies to determine their catalytic activity.

REFERENCES

Adeloye Adewale O, Olomola Temitope O, Adebayo Akinbulu I and Ajibade Peter A. (2012). A high molar extinction coefficient bisterpyridyl homoleptic Ru (II) complex with trans-2-methyl-2-butenoic acid functionality: Potential dye for dye-sensitized solar cells. *International journal of molecular sciences,* **13**: 3511-3526.

Al-Amiery Ahmed A, Al-Majedy Yasmien K, Ibrahim Heba H and Al-Tamimi Ali A. (2012). Antioxidant, antimicrobial, and theoretical studies of the thiosemicarbazone derivative Schiff base 2-(2-imino-1-methylimidazolidin-4-ylidene) hydrazinecarbothioamide (IMHC). *Organic and medicinal chemistry letters,* **2**: 4.

Allardyce Claire S and Dyson Paul J. (2001). Ruthenium in medicine: current clinical uses and future prospects. *Platinum Metals Review,* **45**: 62-69.

Ang Wee Han, Casini Angela, Sava Gianni and Dyson Paul J. (2011). Organometallic ruthenium-based antitumor compounds with novel modes of action. *Journal of Organometallic Chemistry,* **696**: 989-998.

Beckford Floyd A, Stott Alyssa, Mbarushimana P Canisius, LeBlanc Marc-Andre, Hall Kinsey, Smith Samantha, Bullock Jimmie L, Houghton Dennis J, Holder Alvin A and Gerasimchuk Nikolay. (2016). Anticancer, biophysical and computational investigations of half-sandwich ruthenium (II) thiosemicarbazone complexes: The effect of arene versus thiacrown face-cap. *Interdiscip J Chem,* **1**: 1-15.

Bennett MA, Huang T- N, Matheson TW, Smith AK, Ittel Steven and Nickerson William. (1982). 16.(η6- Hexamethylbenzene) Ruthenium Complexes. *Inorganic Syntheses,* **21**: 74-78.

Bennett Martin A and Smith Anthony K. (1974). Arene ruthenium (II) complexes formed by dehydrogenation of cyclohexadienes with ruthenium (III) trichloride. *Journal of the Chemical Society, Dalton Transactions*: 233-241.

Bhattacharyya Debadeep, Chakraborty Soma, Munshi Pradip and Lahiri Goutam Kumar. (1999). Ruthenium (ii/iii) bipyridine complexes incorporating thiol-based imine functions: Synthesis, spectroscopic and redox properties. *Polyhedron,* **18**: 2951-2959.

Canivet Jérôme, Karmazin-Brelot Lydia and Süss-Fink Georg. (2005). Cationic arene ruthenium complexes containing chelating 1, 10-phenanthroline ligands. *Journal of Organometallic Chemistry*, **690**: 3202-3211.

Clarke Michael J. (2003). Ruthenium metallopharmaceuticals. *Coordination Chemistry Reviews*, **236**: 209-233.

Cotton FA, Wilkinson G, Murillo CA and Bochmann M. (1980). Advanced chemistry: Wiley.

Cotton SA. (1997). Ruthenium and osmium. In *Chemistry of Precious Metals* (pp. 1-77): Springer.

Crutchley Robert J. (1994). Intervalence charge transfer and electron exchange studies of dinuclear ruthenium complexes. *Advances in inorganic chemistry,* **41**: 273-325.

da Silva Cleiton M, da Silva Daniel L, Modolo Luzia V, Alves Rosemeire B, de Resende Maria A, Martins Cleide VB and de Fátima Ângelo. (2011). Schiff bases: A short review of their antimicrobial activities. *Journal of Advanced research,* **2**: 1-8.

Daul Claude, Schläpfer Carl Wilhelm and von Zelewsky Alexander. (1979). The electronic structure of cobalt (II) complexes with schiff bases and related ligands. In *Inorganic Chemistry and Spectroscopy* (pp. 129-171): Springer.

Davies David L, Fawcett John, Krafczyk Roland and Russell David R. (1997). Arene ruthenium complexes with chiral Schiff bases derived from pyridine-2-carboxaldehyde or 2-acetylpyridine. *Journal of Organometallic Chemistry,* **545**: 581-585.

Dayan Osman, Demirmen Selin and Özdemir Namık. (2015). Heteroleptic ruthenium (II) complexes of 2-(2-pyridyl) benzimidazoles: a study of catalytic efficiency towards transfer hydrogenation of acetophenone. *Polyhedron,* **85**: 926-932.

De Sudipta, Zhang Jiaguang, Luque Rafael and Yan Ning. (2016). Ni-based bimetallic heterogeneous catalysts for energy and environmental applications. *Energy & Environmental Science*, **9**: 3314-3347.

Dehghanpour Saeed and Mahmoudi Ali. (2007). Synthesis, structure, and redox properties of copper (I) complexes with phenylpyridin-2-ylmethyleneamine derivatives. *Main Group Chemistry*, **6**: 121-130.

Dickert H, Machka K and Braveny I. (1981). The uses and limitations of disc diffusion in the antibiotic sensitivity testing of bacteria. *Infection,* **9**: 18-24.

Dong Renhao and Hao Jingcheng. (2010). Complex fluids of poly (oxyethylene) monoalkyl ether nonionic surfactants. *Chemical reviews,* **110**: 4978-5022.

El-Aziz Dina M Abd, Etaiw Safaa Eldin H and Ali Elham A. (2013). Synthesis, spectroscopic, cytotoxic aspects and computational study of N-(pyridine-2-ylmethylene) benzo [d] thiazol-2-amine Schiff base and some of its transition metal complexes. *Journal of Molecular Structure,* **1048**: 487-499.

Elschenbroich Ch. (2006). Organometallics, Third Completely Revised and Extended Edition: Wiley-VCH, Weinheim.

Fadeeva VI, Shekhovtsova TN and Ivanov VM. (2001). Osnovy analiticheskoi khimii. Prakticheskoe rukovodstvo (Fundamentals of Analytical Chemistry. A Practical Guide): Moscow Vysshaya Shkola.

Florea Ana-Maria and Büsselberg Dietrich. (2011). Cisplatin as an anti-tumor drug: cellular mechanisms of activity, drug resistance and induced side effects. *Cancers,* **3**: 1351-1371.

Gichumbi Joel M, Friedrich Holger B and Omondi Bernard. (2016a). Application of arene ruthenium (II) complexes with pyridine-2-carboxaldimine ligands in the transfer hydrogenation of ketones. *Journal of Molecular Catalysis A: Chemical,* **416**: 29-38.

Gichumbi Joel M, Friedrich Holger B and Omondi Bernard. (2016b). Solvato-polymorph of [(η 6-C 6 H 6) RuCl (L)] PF 6 (L=(2, 6-dimethyl-phenyl-pyridin-2-yl methylene amine). *Journal of Molecular Structure,* **1113**: 55-59.

Gichumbi Joel M, Friedrich Holger B and Omondi Bernard. (2016c). Synthesis and characterization of half-sandwich ruthenium (II) complexes with N-alkyl pyridyl-imine ligands and their application in transfer hydrogenation of ketones. *Transition Metal Chemistry,* **41**: 867-877.

Gichumbi Joel M, Friedrich Holger B and Omondi Bernard. (2016d). Synthesis and characterization of piano-stool ruthenium complexes with N, N′-pyridine imine bidentate ligands and their application in styrene oxidation. *Journal of Organometallic Chemistry,* **808**: 87-96.

Gichumbi Joel M, Friedrich Holger B and Omondi Bernard. (2017a). Synthesis and characterization of some new half-sandwich ruthenium (II) complexes with bidentate N, N′-ligands and their application in alcohol oxidation. *Inorganica Chimica Acta,* **456**: 55-63.

Gichumbi Joel M, Friedrich Holger B, Omondi Bernard, Singh Moganavelli, Naicker Kovashnee and Chenia Hafizah Y. (2016e). Synthesis, characterization, and cytotoxic and antimicrobial activities of ruthenium (II) arene complexes with N, N-bidentate ligands. *Journal of Coordination Chemistry,* **69**: 3531-3544.

Gichumbi Joel M, Omondi Bernard and Friedrich Holger B. (2017b). Half- Sandwich Osmium (II) Complexes with Bidentate N, N- Chelating Ligands and Their Use in the Transfer Hydrogenation of Ketones. *European journal of inorganic chemistry,* **2017**: 915-924.

Govender Preshendren, Renfrew Anna K, Clavel Catherine M, Dyson Paul J, Therrien Bruno and Smith Gregory S. (2011). Antiproliferative activity of chelating N, O-and N, N-ruthenium (II) arene functionalised poly (propyleneimine) dendrimer scaffolds. *Dalton Transactions,* **40**: 1158-1167.

Grubbs Robert H. (2006). Olefin- metathesis catalysts for the preparation of molecules and materials (Nobel lecture). *Angewandte Chemie International Edition,* **45**: 3760-3765.

Günnaz Salih, Özdemir Namık, Dayan Serkan, Dayan Osman and Çetinkaya Bekir. (2011). Synthesis of Ruthenium (II) Complexes Containing Tridentate Triamine (′ N ℕ ℕ′) and Bidentate Diamine Ligands (N ℕ′): as Catalysts for Transfer Hydrogenation of Ketones. *Organometallics,* **30**: 4165-4173.

Holm RH, Everett GW and Chakravorty A. (1966). Metal complexes of Schiff bases and β-ketoamines. *Progress in Inorganic Chemistry, Volume 7*: 83-214.

Horn Sabine and Albrecht Martin. (2011). Transfer hydrogenation of unfunctionalised alkenes using N-heterocyclic carbeneruthenium catalyst precursors. *Chemical Communications,* **47**: 8802-8804.

Ikariya Takao and Blacker A John. (2007). Asymmetric transfer hydrogenation of ketones with bifunctional transition metal-based molecular catalysts. *Accounts of chemical research,* **40**: 1300-1308.

Johnson T and Case C. (1995). Chemical Methods of Control," adapted from Laboratory Experiments in Microbiology, Brief Edition, Redwood City: CA: Benjamin/Cummings Publishing Co.

Kumar K Naresh, Venkatachalam G, Ramesh R and Liu Y. (2008). Half-sandwich para-cymene ruthenium (II) naphthylazophenolato complexes: Synthesis, molecular structure, light emission, redox behavior and catalytic oxidation properties. *Polyhedron*, **27**: 157-166.

Kumar Prashant, Gupta Rakesh Kumar and Pandey Daya Shankar. (2014). Half-sandwich arene ruthenium complexes: synthetic strategies and relevance in catalysis. *Chemical Society Reviews*, **43**: 707-733.

Kumar Prashant, Singh Ashish Kumar, Pandey Rampal, Li Pei-Zhou, Singh Sanjay Kumar, Xu Qiang and Pandey Daya Shankar. (2010). Synthesis, characterization and reactivity of arene ruthenium compounds based on 2, 2′-dipyridylamine and di-2-pyridylbenzylamine and their applications in catalytic hydrogen transfer of ketones. *Journal of Organometallic Chemistry*, **695**: 2205-2212.

Li Fangfei, Collins J Grant and Keene F Richard. (2015). Ruthenium complexes as antimicrobial agents. *Chemical Society Reviews*, **44**: 2529-2542.

Linares Fátima, Galindo Miguel A, Galli Simona, Romero M Angustias, Navarro Jorge AR and Barea Elisa. (2009). Tetranuclear coordination assemblies based on half-sandwich ruthenium (II) complexes: noncovalent binding to DNA and cytotoxicity. *Inorganic chemistry*, **48**: 7413-7420.

Lutta Samwel T and Kagwanja Stanley M. (2000). Synthesis and electrochemical studies of heterobinuclear complexes containing copper and molybdenum nitrosyl groups linked by Schiff base ligands. *Transition Metal Chemistry*, **25**: 415-420.

Marchetti Fabio, Pettinari Claudio, Pettinari Riccardo, Cerquetella Adele, Di Nicola Corrado, Macchioni Alceo, Zuccaccia Daniele, Monari Magda and Piccinelli Fabio. (2008). Synthesis and intramolecular and interionic structural characterization of half-sandwich (arene) ruthenium (II) derivatives of bis (pyrazolyl) alkanes. *Inorganic chemistry*, **47**: 11593-11603.

Martin CR, Foss CA, Kissinger PT and Heineman WR. (1996). Laboratory Techniques in Electroanalytical Chemistry: Kissinger, PT, Heineman, WR, Eds.

Matsinha Leah C, Malatji Peter, Hutton Alan T, Venter Gerhard A, Mapolie Selwyn F and Smith Gregory S. (2013). Water- Soluble Half- Sandwich RuII–Arene Complexes: Synthesis, Structure, Electrochemistry, DFT Studies, and Aqueous Phase Hydroformylation of 1- Octene. *European journal of inorganic chemistry,* **2013**: 4318-4328.

Mc Crudden Denis. (2008). Synthesis and characterisation of some osmium and ruthenium complexes and the application of Os (bpy) 2-(pyridine-4-COOH)-CI in an electrochemical DNA biosensor.

McCleverty Jon A and Meyer Thomas J. (2004). *Comprehensive coordination chemistry II*: Elsevier Ltd.

Mohan Nanjan, Subarkhan Mohamed Kasim Mohamed and Ramesh Rengan. (2018). Synthesis, antiproliferative activity and apoptosis-promoting effects of arene ruthenium (II) complexes with N, O chelating ligands. *Journal of Organometallic Chemistry*, **859**: 124-131.

Moreno Virtudes, Lorenzo Julia, Aviles Francesc X, Garcia M Helena, Ribeiro Joao P, Morais Tânia S, Florindo Pedro and Robalo M Paula. (2010). Studies of the antiproliferative activity of ruthenium (II) cyclopentadienyl-derived complexes with nitrogen coordinated ligands. *Bioinorganic chemistry and applications,* **2010**.

Morris Robert E, Aird Rhona E, del Socorro Murdoch Piedad, Chen Haimei, Cummings Jeff, Hughes Nathan D, Parsons Simon, Parkin Andrew, Boyd Gary and Jodrell Duncan I. (2001). Inhibition of cancer cell growth by ruthenium (II) arene complexes. *Journal of medicinal chemistry*, **44**: 3616-3621.

Nieto Ismael, Livings Michelle S, Sacci III John B, Reuther Lauren E, Zeller Matthias and Papish Elizabeth T. (2011). Transfer Hydrogenation in Water via a Ruthenium Catalyst with OH Groups near the Metal Center on a bipy Scaffold. *Organometallics,* **30**: 6339-6342.

Nurkkala Lasse. (2007). *Design, Synthesis and Properties of Bipyridine-capped Oligothiophenes for Directed Energy and Electron Transfer in Molecular Electronic Applications.* Institutionen för biologi och kemiteknik.

Nyawade Eunice A, Friedrich Holger B, Omondi Bernard, Chenia Hafizah Y, Singh Moganavelli and Gorle Sridevi. (2015a). Synthesis and characterization of new α, α′-diaminoalkane-bridged dicarbonyl (η 5-cyclopentadienyl) ruthenium (II) complex salts: antibacterial activity tests of η 5-cyclopentadienyl dicarbonyl ruthenium (II) amine complexes. *Journal of Organometallic Chemistry*, **799**: 138-146.

Nyawade Eunice A, Friedrich Holger B, Omondi Bernard and Mpungose Philani. (2015b). Synthesis and characterization of new (η5-cyclopentadienyl) dicarbonylruthenium (II) amine complexes: their application as homogeneous catalysts in styrene oxidation. *Organometallics,* **34**: 4922-4931.

Prabhu Padmavathi P, Pande Sushant and Shastry CS. (2011). Synthesis and biological evaluation of schiff's bases of some new benzothiazole derivatives as antimicrobial agents. *Int. J. Chem. Tech. Res,* **3**: 185-191.

Prakash Om, Sharma Kamal Nayan, Joshi Hemant, Gupta Pancham Lal and Singh Ajai K. (2013). Half sandwich complexes of chalcogenated pyridine based bi-(N, S/Se) and terdentate (N, S/Se, N) ligands with (η 6-benzene) ruthenium (ii): synthesis, structure and catalysis of transfer hydrogenation of ketones and oxidation of alcohols. *Dalton Transactions,* **42**: 8736-8747.

Raja Mathiyazhagan Ulaganatha, Raja Nandhagopal and Ramesh Rengan. (2010). Transfer Hydrogenation of Ketones Using Recyclable (η6-Arene) Ruthenium (II) Naphthylazo-p-Methyl Phenolate Complex. *The Open Catalysis Journal,* **3**: 30-33.

Rhyoo Hae Yoon, Park Hee-Jung and Chung Young Keun. (2001). The first Ru (II)-catalysed asymmetric hydrogen transfer reduction of aromatic ketones in aqueous media. *Chemical Communications*: 2064-2065.

Rhyoo Hae Yoon, Park Hee-Jung, Suh Won Hyuk and Chung Young Keun. (2002). Use of surfactants in water-soluble ruthenium (II) complex-catalyzed asymmetric hydrogen-transfer reduction of aromatic ketones. *Tetrahedron letters,* **43**: 269-272.

Romain Charles, Gaillard Sylvain, Elmkaddem Mohammed K, Toupet Loïc, Fischmeister Cédric, Thomas Christophe M and Renaud Jean-Luc. (2010). New dipyridylamine ruthenium complexes for transfer hydrogenation of aryl ketones in water. *Organometallics,* **29**: 1992-1995.

Saleem Fariha, Rao Gyandshwar Kumar, Kumar Arun, Mukherjee Goutam and Singh Ajai K. (2013). Half-sandwich ruthenium (II) complexes of click generated 1, 2, 3-triazole based organosulfur/-selenium ligands: structural and donor site dependent catalytic oxidation and transfer hydrogenation aspects. *Organometallics,* **32**: 3595-3603.

Sathya N, Muthusamy P, Padmapriya N, Raja G, Deivasigamani K and Jayabalakrishnan C. (2009). Spectrometric, catalytic, and antimicrobial studies of mononuclear Ru (III) Schiff-base complexes. *Journal of Coordination Chemistry,* **62**: 3532-3543.

Schutz RW. (1996). Ruthenium enhanced titanium alloys. *Platinum Metals Review,* **40**: 54-61.

Shafi Syed, Alam Mohammad Mahboob, Mulakayala Naveen, Mulakayala Chaitanya, Vanaja G, Kalle Arunasree M, Pallu Reddanna and Alam MS. (2012). Synthesis of novel 2-mercapto benzothiazole and 1, 2, 3-triazole based bis-heterocycles: their anti-inflammatory and anti-nociceptive activities. *European journal of medicinal chemistry,* **49**: 324-333.

Sharma Alpesh K, Joshi Hemant, Sharma Kamal Nayan, Gupta Pancham L and Singh Ajai K. (2014). 2-Propanol vs Glycerol as Hydrogen Source in Catalytic Activation of Transfer Hydrogenation with (η6-Benzene) ruthenium (II) Complexes of Unsymmetrical Bidentate Chalcogen Ligands. *Organometallics,* **33**: 3629-3639.

Shavaleev Nail M, Bell Zöe R, Easun Timothy L, Rutkaite Ramune, Swanson Linda and Ward Michael D. (2004). Complexes of substituted derivatives of 2-(2-pyridyl) benzimidazole with Re (I), Ru (II) and Pt (II): structures, redox and luminescence properties. *Dalton Transactions*: 3678-3688.

Singh Ashish Kumar, Yadav Mahendra, Pandey Rampal, Kumar Prashant and Pandey Daya Shankar. (2010). Half-sandwich ruthenium, rhodium and iridium complexes containing dipyridyl amine based ligands. *Journal of Organometallic Chemistry,* **695**: 1932-1939.

Singh Pradhumn and Singh Ajai K. (2010). Transfer hydrogenation of ketones and catalytic oxidation of alcohols with half-sandwich complexes of ruthenium (II) designed using benzene and tridentate (S, N, E) type ligands (E= S, Se, Te). *Organometallics*, **29**: 6433-6442.

Singh Taruna, Kishan Ram, Nethaji Munirathinam and Thirupathi Natesan. (2011). Synthesis, Reactivity Studies, Structural Aspects, and Solution Behavior of Half Sandwich Ruthenium (II) N, N′, N ″-Triarylguanidinate Complexes. *Inorganic chemistry*, **51**: 157-169.

Sun Ying, Dai Yuan-Chen, Wang Xue, Cheng Jia-Ming and Jia Wei-Guo. (2016). Preparation, crystal structures and properties of half-sandwich ruthenium complexes containing salicylbenzoxazole ligands. *Journal of Coordination Chemistry*, **69**: 48-56.

Swartz Leoni Destine. (2015). *Synthesis and Characterization of pyridyl/quinolyl imine ruthenium (II) and palladium (II) complexes in catalysis.* University of the Western Cape.

Syamal A and Maurya MR. (1989). Coordination chemistry of Schiff base complexes of molybdenum. *Coordination Chemistry Reviews*, **95**: 183-238.

Thilagavathi N, Manimaran A and Jayabalakrishnan C. (2010). Synthesis, characterization, electrochemistry, catalytic, and antimicrobial studies of ruthenium (III) complexes containing ONO donor ligands. *Journal of Coordination Chemistry*, **63**: 1252-1262.

Türkmen Hayati, Kani İbrahim and Çetinkaya Bekir. (2012). Transfer Hydrogenation of Aryl Ketones with Half- Sandwich RuII Complexes That Contain Chelating Diamines. *European journal of inorganic chemistry*, **2012**: 4494-4499.

Wilkins Tracy D and Thiel Teresa. (1973). Modified broth-disk method for testing the antibiotic susceptibility of anaerobic bacteria. *Antimicrobial agents and chemotherapy*, **3**: 350-356.

Zheng Zhanjiang, Elmkaddem Mohammed Kamal, Fischmeister Cédric, Roisnel Thierry, Thomas Christophe M, Carpentier Jean-François and Renaud Jean-Luc. (2008). Synthesis of new dipyridinylamine and dipyridinylmethane ligands and their coordination chemistry with Mg (II) and Zn (II). *New Journal of Chemistry*, **32**: 2150-2158.

APPENDICES

Appendix 1 : Electronic spectra of ligand (L2)

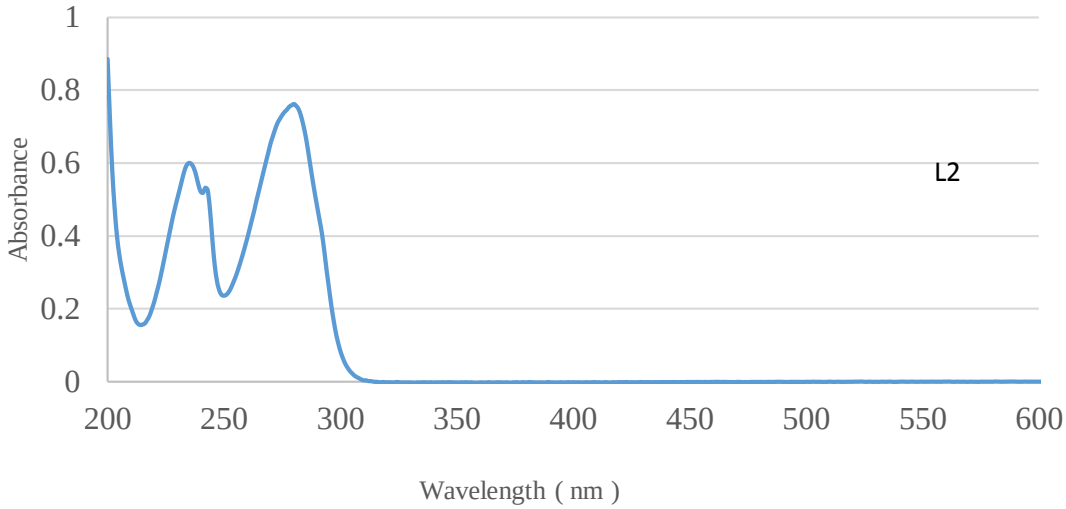

Appendix 2 : Electronic spectra of ligand (L3)

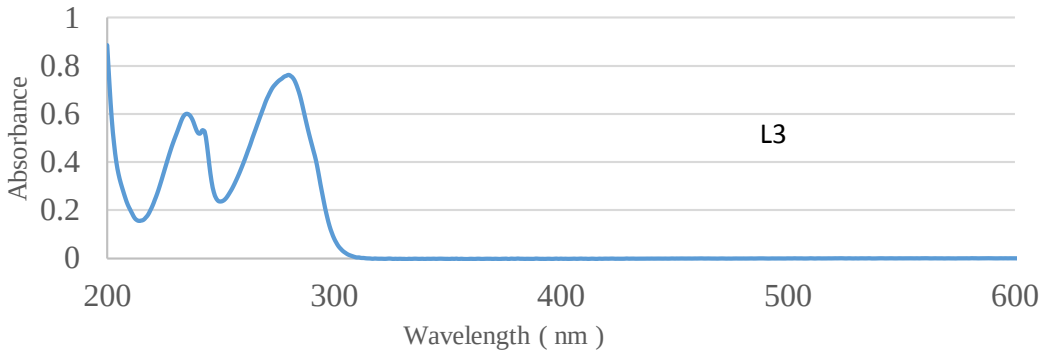

Appendix 3 : Electronic spectra of precursor molecule $[(\eta^6\text{-}C_6H_5CH_3)Ru(\mu\text{-}Cl)Cl]_2$

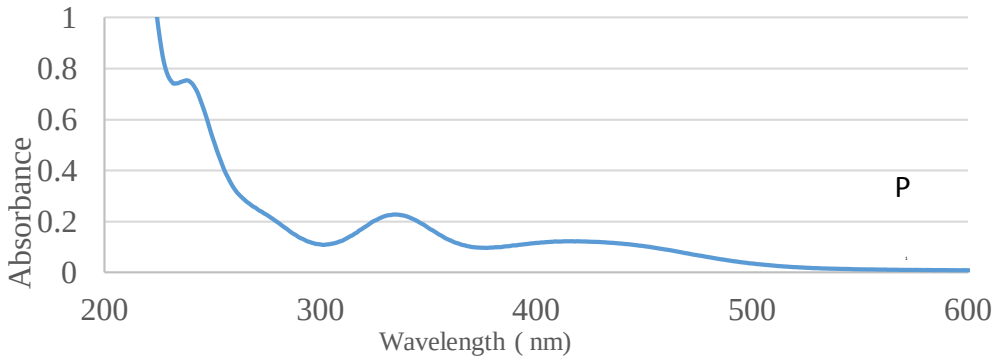

Appendix 4 : Electronic Spectra of Complex (2)

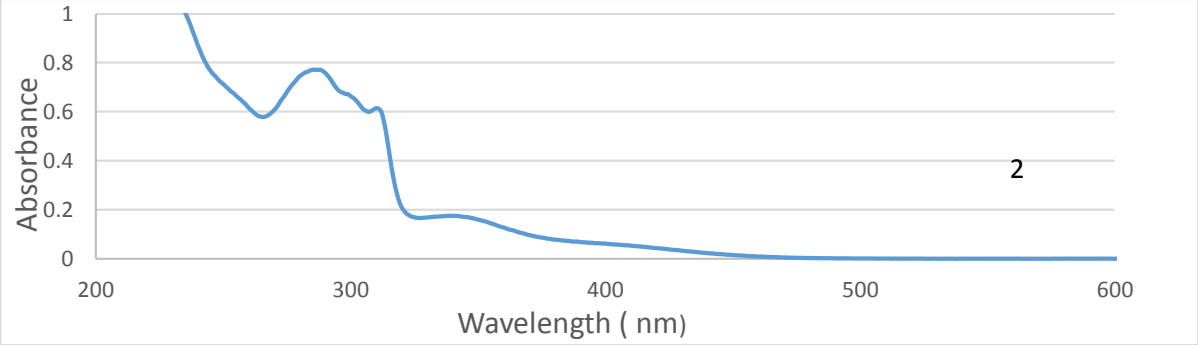

Appendix 5 : Electronic spectra of complex 3

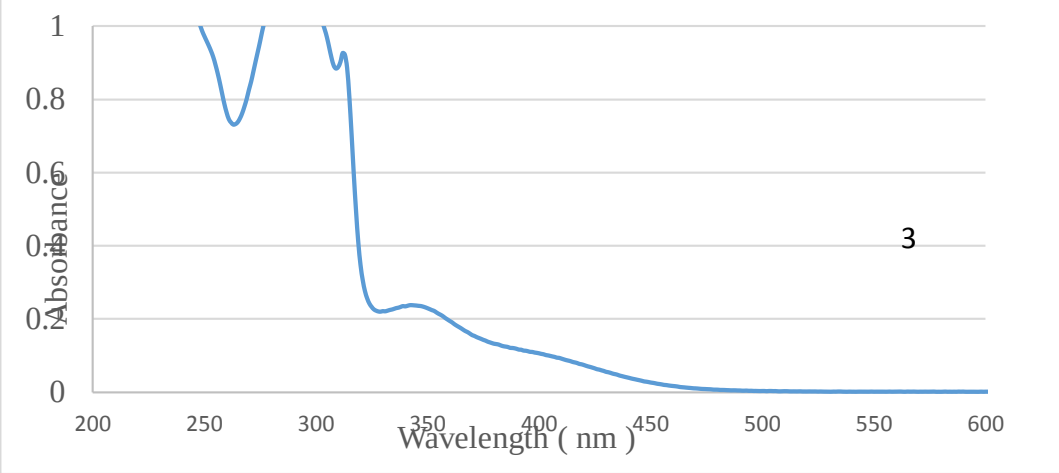

Appendix 6 : IR spectra of ligand (L2)

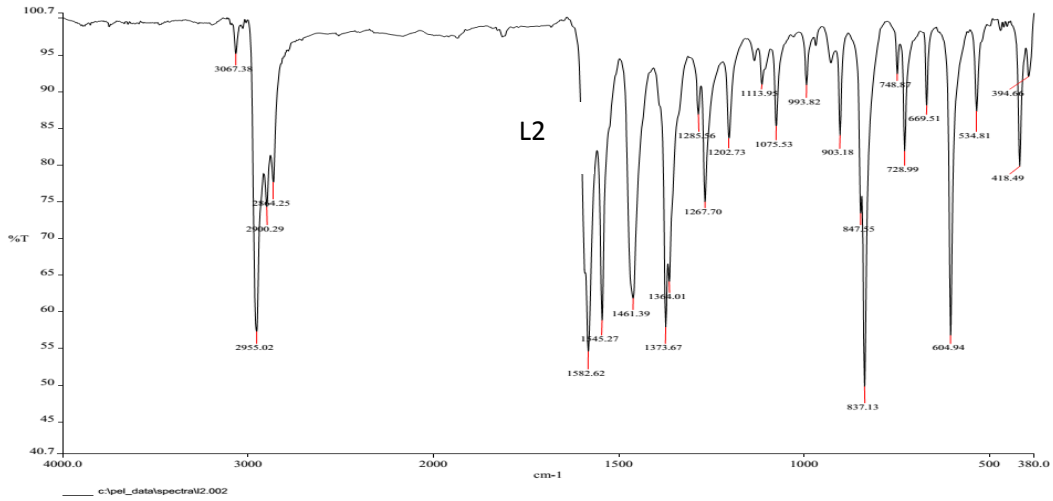

Appendix 7: IR spectra of complex (2)

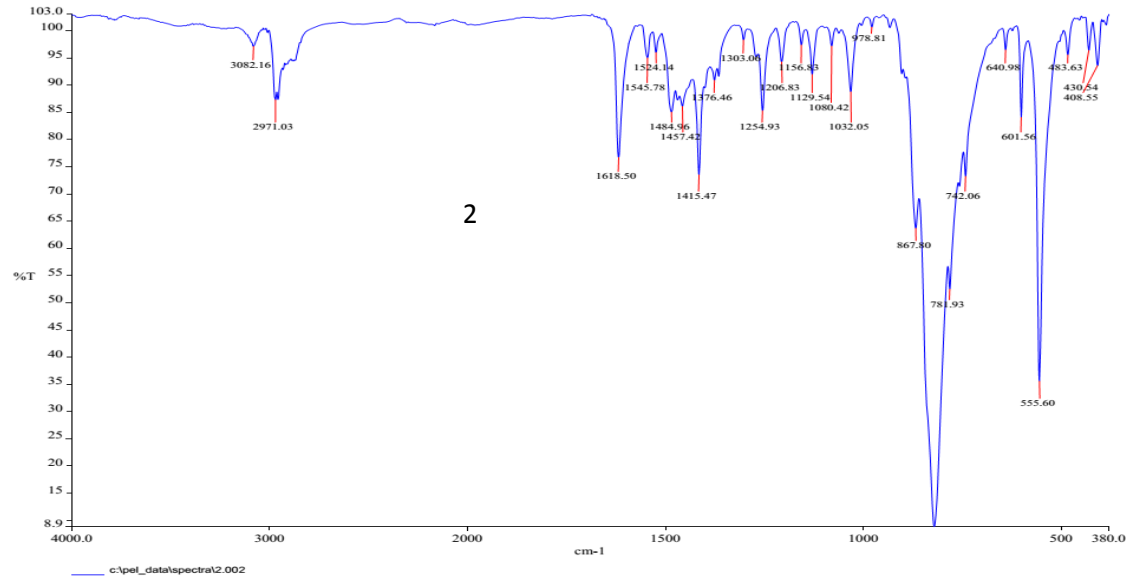

Appendix 8 : IR spectra of ligand 3

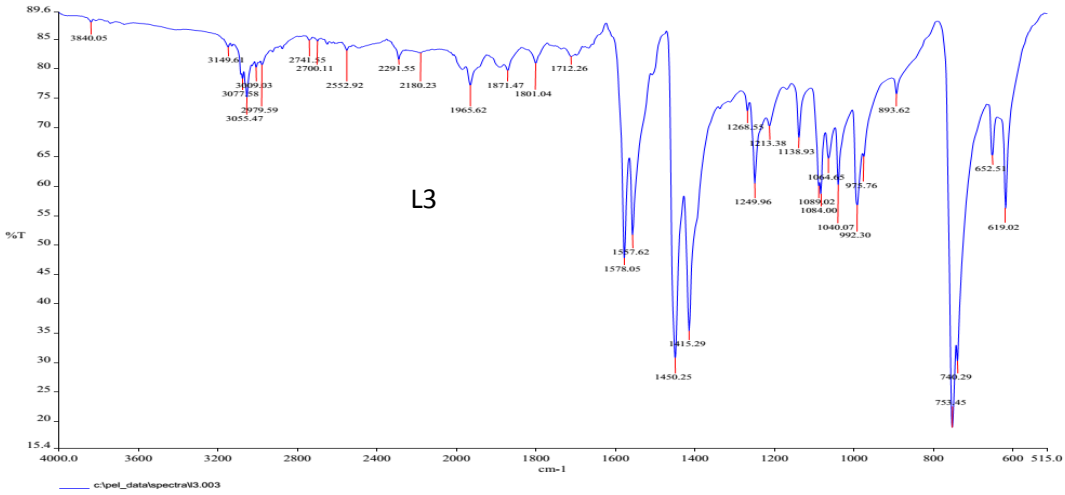

Appendix 9 : IR spectra of complex 3

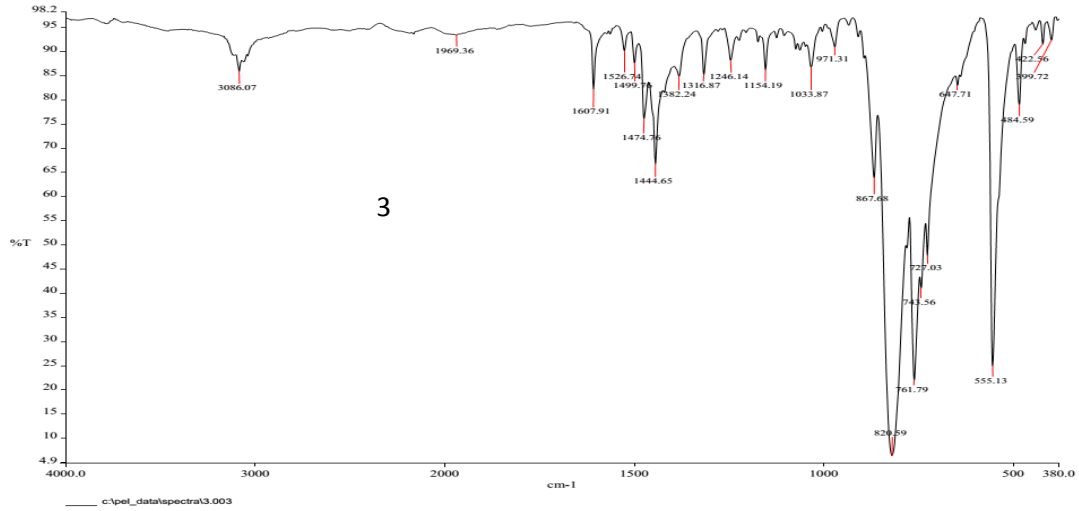

Appendix 10 : ^{1}H NMR of precursor molecule

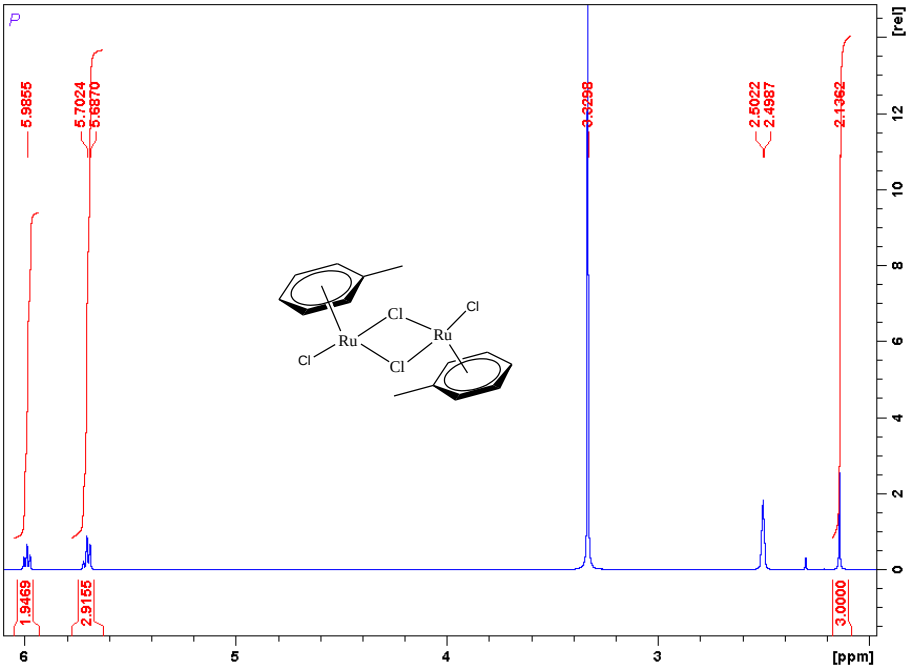

Appendix 11 : Antimicrobial test of 4-fluoro-N-(2-pyridylmethylene)-aniline

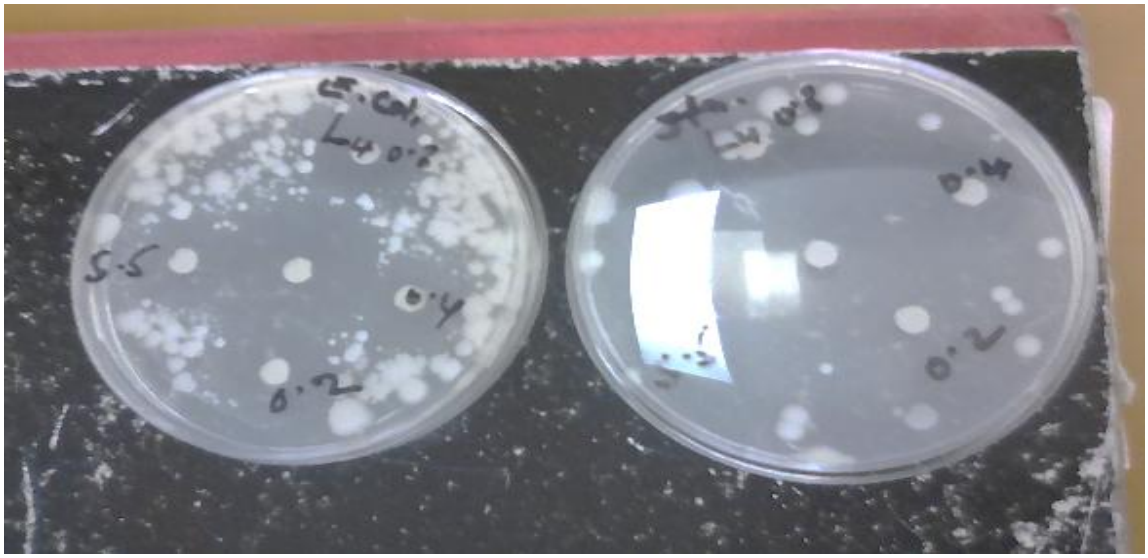

Appendix 12: Potentiostat (BASi Epsilon)

Appendix 13: Vario EL III Elemental analyser

Appendix 14: Synthetic ruthenium complexes reaction, laboratory set up

Appendix 15: ^{31}P NMR spectra $[C_{17}H_{16}N_2ClRu]\ PF_6$

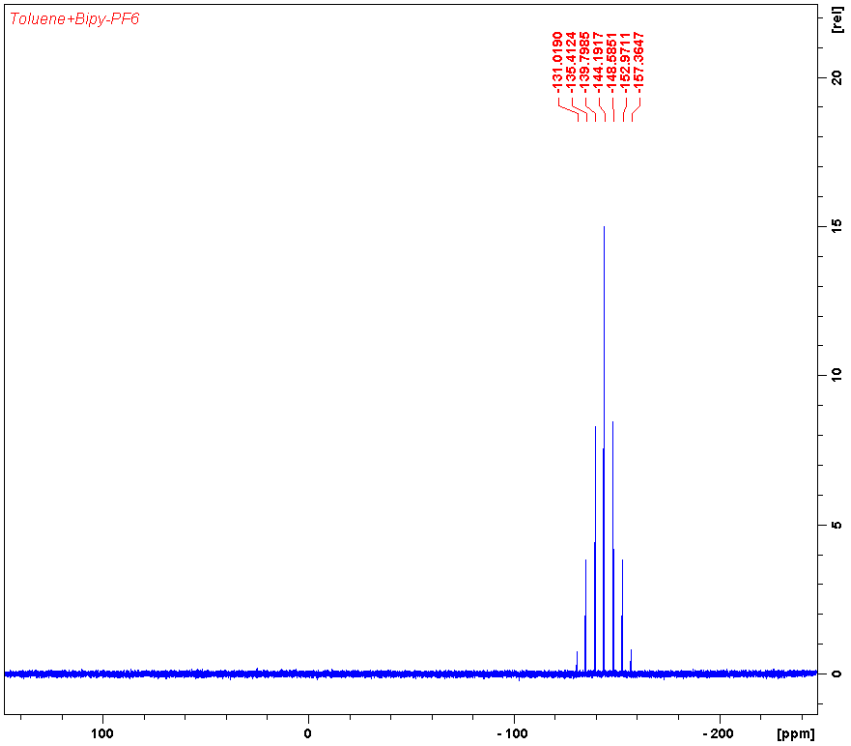

Appendix 16: Research Permit

THIS IS TO CERTIFY THAT:
MS. KOSKE MARGARET CHEPKEMOI
of EGERTON UNIVERSITY, 0-20115
Egerton,has been permitted to conduct research in *Nairobi, Nakuru , Tharaka-Nithi Counties*

on the topic: *SYNTHESIS, CHARACTERIZATION, ELECTROCHEMISTRY AND ANTIMICROBIAL STUDIES OF HALF SANDWICH N, N-BIDENTATE RUTHENIUM COMPLEXES*

for the period ending:
3rd November,2018

.....
Applicant's Signature

Permit No : NACOSTI/P/17/93489/19638
Date Of Issue : 7th November,2017
Fee Recieved :Ksh 1000

.....
Director General
National Commission for Science, Technology & Innovation

CONDITIONS

1. **The License is valid for the proposed research, research site specified period.**
2. **Both the Licence and any rights thereunder are non-transferable.**
3. **Upon request of the Commission, the Licensee shall submit a progress report.**
4. **The Licensee shall report to the County Director of Education and County Governor in the area of research before commencement of the research.**
5. **Excavation, filming and collection of specimens are subject to further permissions from relevant Government agencies.**
6. **This Licence does not give authority to transfer research materials.**
7. **The Licensee shall submit two (2) hard copies and upload a soft copy of their final report.**
8. **The Commission reserves the right to modify the conditions of this Licence including its cancellation without prior notice.**

REPUBLIC OF KENYA

NACOSTI

National Commission for Science, Technology and Innovation

RESEARCH CLEARANCE PERMIT

Serial No.A 16384

CONDITIONS: see back page